MASTER EN INGENIERÍA INDUSTRIAL

TRABAJO FIN DE MASTER

POWER-TO-X SIMULATION AND EVALUATION OF MEMBRANE REACTORS FOR THE PRODUCTION OF RENEWABLE METHANOL

Autor: Carlos Ignacio Laiz Quereda

Director: Vincent Dieterich

Madrid

Declaro, bajo mi responsabilidad, que el Proyecto presentado con el título

Power-to-X Simulation and Evaluation of Membrane Reactors for the Production of Renewable Methanol

en la ETS de Ingeniería - ICAI de la Universidad Pontificia Comillas en el

curso académico 2020/21 es de mi autoría, original e inédito y

no ha sido presentado con anterioridad a otros efectos.

El Proyecto no es plagio de otro, ni total ni parcialmente y la información que ha sido

tomada de otros documentos está debidamente referenciada.

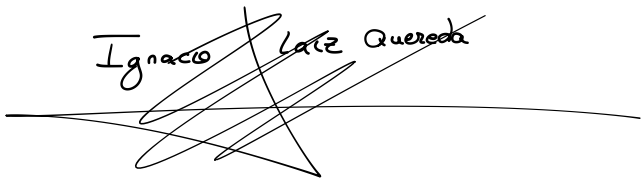

Fdo.: Carlos Ignacio Laiz Quereda Fecha: 31/08/ 2021

Autorizada la entrega del proyecto

EL DIRECTOR DEL PROYECTO

Fdo.: Vincent Dieterich Fecha: 31/08/ 2021

COMILLAS
UNIVERSIDAD PONTIFICIA
ICAI

MASTER EN INGENIERÍA INDUSTRIAL

TRABAJO FIN DE MASTER

POWER-TO-X SIMULATION AND EVALUATION OF MEMBRANE REACTORS FOR THE PRODUCTION OF RENEWABLE METHANOL

Autor: Carlos Ignacio Laiz Quereda

Director: Vincent Dieterich

Madrid

Acknowledgements

First, I would like to thank **Technical University of Munich** (TUM), especially to my supervisor **Vincent Dieterich** for his interest, help and attachment to me and my thesis. Without you, this project would have never been possible. Moreover, I would like to thank the **Fraunhofer Institute for Ceramic Technologies and Systems IKTS** and especially to **Dr.-Ing. Jörg Richter** and **Dr. Benjamin Jäger** for their hints, input, and help during my project.

I would also like to thank to my home University **Universidad Pontificia de Comillas ICAI-ICADE** for its education and values. Without any doubt, these years have been the best of my life and somehow it has been because of the opportunity to develop myself personally and academically in an atmosphere as the one of ICAI School of Engineering. Finally, I would like to thank to **Prof José Ignacio Linares Hurtado** for his support and supervision of my thesis.

This work is dedicated to all my loved ones, especially to my mother Pilar, my uncles Jesús, Francisco and Chuli, my grandmother María, my friends and my father who rests in heaven. Thanks for who I am.

POWER-TO-X SIMULATION AND EVALUATION OF MEMBRANES REACTORS FOR THE PRODUCTION OF RENEWABLE METHANOL

Autor: Laiz Quereda, Carlos Ignacio.
Director: Dieterich, Vincent.
Entidad Colaboradora: Technical University of Munich (TUM)

RESUMEN DEL PROYECTO

El metanol renovable parece ser uno de los productos Power-2-X más prometedores, ya que puede utilizarse en el sector del transporte como combustible, en la industria química como materia prima y en el sector energético a través de las pilas de combustible. El e-Metanol puede obtenerse combinando hidrógeno, producido por electrólisis (a través de H_2O y excedentes de energías renovables), con CO_2 procedente de procesos de captura de carbono. Sin embargo, uno de los mayores retos de la síntesis del metanol es la limitación de la conversión del metanol debido al equilibrio químico: en la mayoría de los casos, sólo se puede conseguir una conversión inferior al 25% en una sola pasada del reactor. Una posible solución podría ser el uso de reactores de membrana, que permiten una separación in situ de los productos formados durante la reacción, sorteando así la limitación del equilibrio. En este sentido, el objetivo de esta tesis es apoyar esta investigación dentro del proyecto E2Fuels de la Universidad Técnica de Múnich (TUM), evaluando, analizando y simulando el rendimiento y el aumento de la producción de la síntesis de metanol renovable utilizando reactores de membrana y, a continuación, confirmar la viabilidad y eficacia de esta posible solución. Según los resultados de la simulación, la separación in situ tanto del metanol como del agua parece ser el enfoque más prometedor para aumentar tanto la conversión como las tasas de producción del metanol. Si el 90% del metanol y el agua producidos se pudieran separar in situ a través de la membrana, la conversión del metanol podría aumentar hasta un 73,91%, y se podría obtener una tasa de producción máxima de 36,96 mol/s.

Palabras clave: Síntesis de metanol, reactores de membrana, e-Methanol, Power-2-X, descabornización del sector del transporte, descabornización del sector energético.

1. Introducción

Los combustibles sintéticos representan un enfoque prometedor para aumentar la penetración de la energía renovable en el sector del transporte, y así reducir antes las emisiones de gases de efecto invernadero. Los combustibles sintéticos como el e-Metanol

pueden utilizarse en motores de combustión interna con pocas modificaciones [1]. Además, los e-combustibles podrían permitir el uso de los excedentes de energía fotovoltaica y eólica en el sector del transporte [2,3]. Además, debido a sus bajas pérdidas por almacenamiento y transporte, también pueden utilizarse como opción complementaria de almacenamiento de electricidad a largo plazo [4].

El e-Metanol, parece ser uno de los productos Power-to-Liquids (PtL) más prometedores, ya que puede utilizarse en el sector del transporte como combustible [5], en la industria química, y como medio de almacenamiento en el sector energético [6,7].

Sin embargo, uno de los mayores retos en la síntesis de metanol es la limitación del rendimiento de metanol debido al equilibrio químico: en la mayoría de los casos, sólo se puede obtener un 25% de conversión de metanol en una sola pasada del reactor. Una posible solución podría ser el uso de reactores de membrana, que permiten separar in situ los productos que se forman durante la reacción del metanol, y así, sortear la limitación del equilibrio.

En este sentido, el objetivo de esta tesis es modelar un reactor de membrana y realizar una simulación en estado estacionario para evaluar los efectos de la separación in situ de los productos (agua y/o metanol) en la conversión y en las tasas de producción del metanol. Para más información sobre la introducción y motivación de esta tesis, se remite al lector a la lectura del Capítulo 1.

2. Definición del proyecto

Hasta donde sabemos, faltan investigaciones que comparen los efectos de la separación de los diferentes productos formados en la síntesis del metanol (agua y/o metanol). Por lo tanto, esta tesis pretende cubrir este vacío de investigación analizando los efectos de la separación in situ del agua y/o metanol mediante simulaciones en estado estacionario. Por último, se comparará el rendimiento de los reactores de membrana con separación in situ con la síntesis del metanol convencional en cuanto a conversión y tasas de producción de metanol. En el Capítulo 1 se presenta más información sobre los objetivos de investigación de esta tesis.

3. Descripción del modelo/sistema/herramienta

Se ha modelado un reactor de membrana basándose en las recomendaciones del trabajo de investigación de Terreni et al. [8]. Según estos autores y Galucci et al. [9], se puede utilizar un modelo cinético para simular el comportamiento de un reactor de membrana siempre que

se conozca el valor de permeabilidad. En esta tesis se explora la separación in situ de agua y/o metanol. El principio de funcionamiento del modelo se presenta en la Ilustración a.1. En el Capítulo 3 se ofrece más información sobre el modelo.

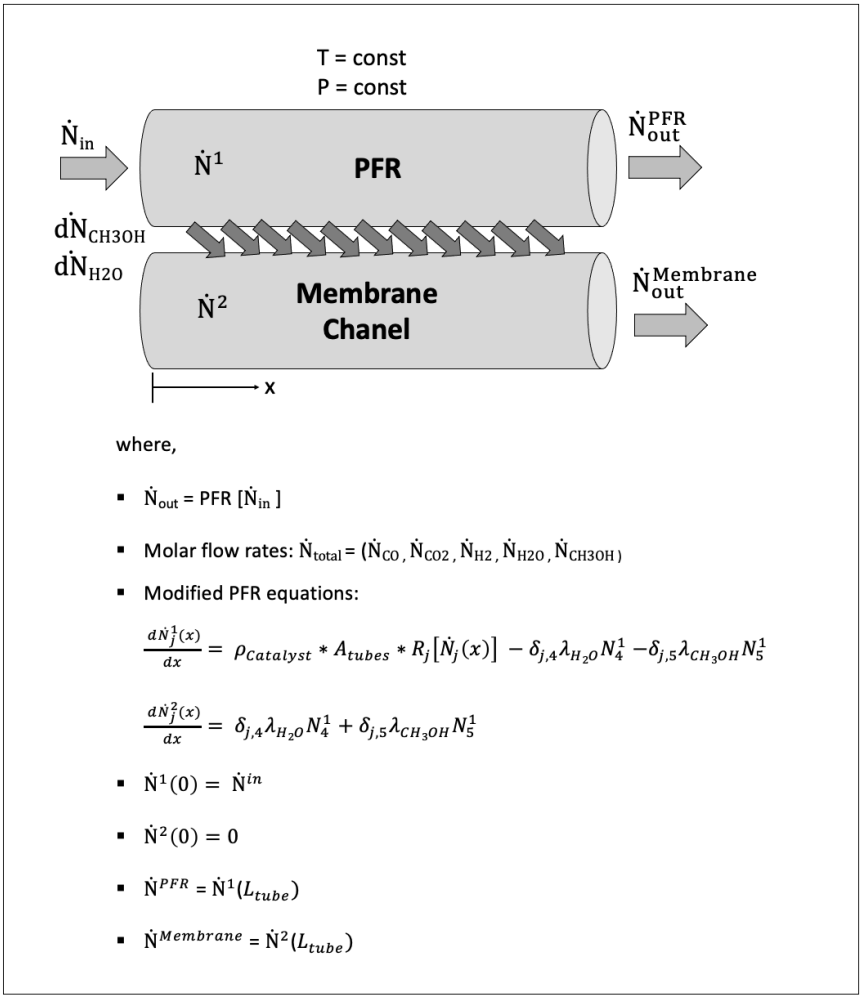

Ilustración a.1 - Esquema computacional del reactor de membrana tipo "plug flow reactor (PFR)". Nótese la presencia de un canal paralelo que representa la "membrana". Por este canal sólo pueden fluir selectivamente el metanol y/o el agua producidos durante la reacción. El símbolo $\delta_{j,k}$ es el termino "Kronecker delta". Definición de la función PFR y de las ecuaciones diferenciales, que relacionan los caudales molares de los componentes de entrada y salida. Adaptado de "A simplified simulation of catalytic reactors for CO_2 reduction" [8].

4. Resultado

Los resultados de la simulación sugieren que la máxima conversión y tasa de producción del metanol se obtienen para el caso de la separación simultánea in-situ de metanol y agua. Si el 90% del metanol y el agua producidos se pueden separar a través de la membrana, la

conversión del metanol podría aumentar hasta el 73,91% y obtener una tasa de producción máxima de 36,96 mol/s. Un reactor convencional, en las mismas condiciones de operación de presión, relación molar H_2/CO_2 y temperatura óptima, alcanzaría en cambio una conversión del metanol del 24,63% y una tasa de producción de 12,42 mol/s. Los resultados se presentan en el Capítulo 4 y se discuten en el Capítulo 5.

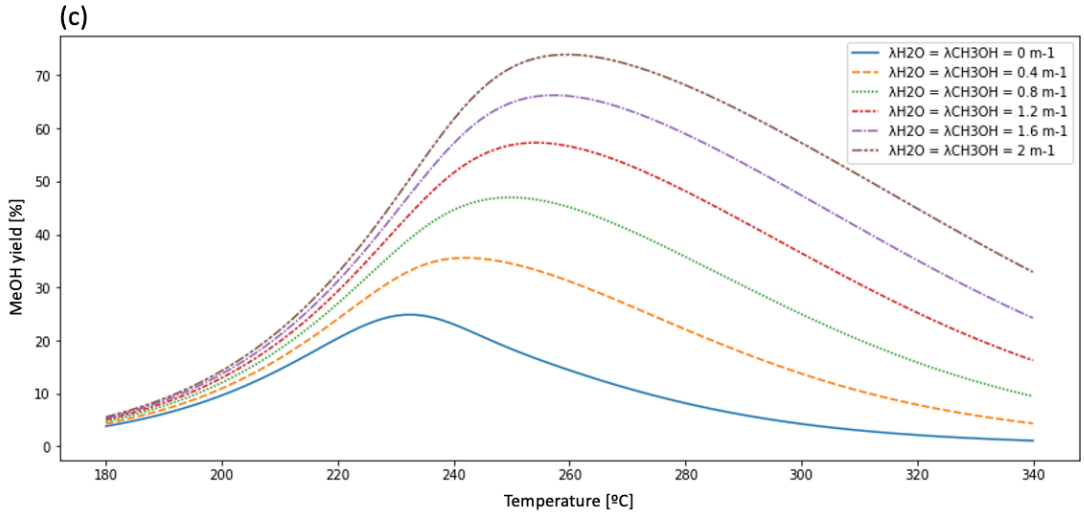

Ilustración b.1. Conversión del MeOH [%] en el reactor de flujo de membrana (MPFR). Condiciones de funcionamiento: P = 60 bar, $\lambda_{CH3OH}, \lambda_{H2O}$ dadas, y H_2/CO_2 = 4.

5. Conclusiones

Las simulaciones confirman la hipótesis de que los reactores de membrana pueden superar el equilibrio termodinámico y lograr un mayor rendimiento y tasas de producción de metanol. Las membranas de carbón y de zeolita inorgánica se han identificado como las dos membranas más prometedoras para la producción de metanol, ya que pueden soportar las altas temperaturas que implica la síntesis de este producto. Para el reactor convencional se obtiene una conversión máxima del 24,63% y una tasa de producción de 12,42 mol/s para 60 bar, y una relación molar H_2/CO_2 de 4. La separación in situ tanto del metanol como del agua parece especialmente prometedora. La eliminación del 90% de ambos productos (agua y metanol) aumentaría el rendimiento de metanol hasta el 73,91% y la tasa de producción hasta 36,96 mol/s. La eliminación in situ del agua también podría ser interesante. Para otras relaciones de permeabilidad más realistas, las simulaciones muestran mejoras menores en la conversión del metanol y en las tasas de producción. Esto se discute más en detalle en el Capitulo 4.

6. Referencias

[1] I. Ridjan, B. V. Mathiesen, D. Connolly, and N. Duić, "The feasibility of synthetic fuels in renewable energy systems," *Energy*, vol. 57, pp. 76–84, 2013, doi: 10.1016/j.energy.2013.01.046.

[2] H. Lund and E. Münster, "Integrated transportation and energy sector CO2 emission control strategies," *Transp. Policy*, vol. 13, no. 5, pp. 426–433, 2006, doi: 10.1016/j.tranpol.2006.03.003.

[3] E. Pursiheimo, H. Holttinen, and T. Koljonen, "Inter-sectoral effects of high renewable energy share in global energy system," *Renew. Energy*, pp. 1119–1129, 2019, doi: 10.1016/j.renene.2018.09.082.

[4] M. Moser *et al.*, "Synthetic Liquid Hydrocarbons from Renewable Energy – Results of the Helmholtz Energy Alliance," *Chemie-Ingenieur-Technik*, vol. 89, no. 3, pp. 274–288, 2017, doi: 10.1002/cite.201500154.

[5] A. Santasalo-Aarnio *et al.*, "Application of Synthetic Renewable Methanol to Power the Future Propulsion," *SAE Tech. Pap. Ser.*, vol. 1, Sep. 2020, doi: 10.4271/2020-01-2151.

[6] K. Räuchle, L. Plass, H. J. Wernicke, and M. Bertau, "Methanol for Renewable Energy Storage and Utilization," *Energy Technol.*, vol. 4, no. 1, pp. 193–200, 2016, doi: 10.1002/ente.201500322.

[7] E. Moioli, R. Mutschler, and A. Züttel, "Renewable energy storage via CO2 and H2 conversion to methane and methanol: Assessment for small scale applications," *Renew. Sustain. Energy Rev.*, vol. 107, no. March, pp. 497–506, 2019, doi: 10.1016/j.rser.2019.03.022.

[8] J. Terreni, A. Borgschulte, M. Hillestad, and B. D. Patterson, "Understanding catalysis—a simplified simulation of catalytic reactors for CO2 reduction," *ChemEngineering*, vol. 4, no. 4, pp. 1–16, 2020, doi: 10.3390/chemengineering4040062.

[9] F. Gallucci, *Inorganic Membrane Reactors for Methanol Synthesis*. Elsevier B.V., 2018.

POWER-TO-X SIMULATION AND EVALUATION OF MEMBRANE REACTORS FOR THE PRODUCTION OF RENEWABLE METHANOL

Author: Laiz Quereda, Carlos Ignacio.
Supervisor: Dieterich, Vincent.
Collaborating Entity: Technical University of Munich (TUM)

ABSTRACT

Renewable Methanol seems to be one of the most promising Power-2-X products, since it can be used in the transport sector as a fuel, in the chemistry industry as a feedstock and in the energy sector via fuel cells. e-Methanol can be obtained by combining hydrogen produced by electrolysis (trough H_2O and surplus of renewable energies) with CO_2 from carbon capture processes. However, one of the biggest challenges in methanol synthesis is the limitation of the methanol yield due to the chemical equilibrium: in most cases, only less than 25% methanol yield can be achieved in one reactor run. One possible solution could be the use of membrane reactors, which enable an in-situ separation of water formed during the reaction of methanol, and thus could circumvent the equilibrium limitation. In this sense, the aim of this thesis is to support this research within the E2Fuel project at Technical University of Munich (TUM), by evaluating, analyzing, and simulating the yield and production increase of renewable methanol synthesis using membrane reactors and then, confirm the viability and effectivity of this possible solution. According to the simulation results, the in-situ removal of both methanol and water seems to be the most promising approach to increase both the methanol yield and production rates. The methanol yield could be increased up to 73.91%, and a maximum production rate of 36.96 mol/s can be obtained, if 90% of the produced methanol and water could be removed through the membrane.

Keywords: Methanol Synthesis, Membrane Reactors, e-Methanol, Power-2-X, Decabornization of Transport Sector, Decabornization of Power Sector.

1. Introduction

e-fuels represent a promising approach to increase the share of renewable energy in the transport sector and reduce the GHG emissions sooner, since they can be used in internal combustion engines with relatively few modifications [1]. Moreover, e-fuels could enable the use of photovoltaic and wind energy surpluses in the transport sector [2,3]. Additionally,

due to their low storage and transport losses, they can also be used as complementary long-term electricity storage option [4].

e-Methanol, seems to be one of the most promising Power-to-Liquids (PtL) products, since it can be used in the transport sector as a fuel [5], in the chemistry industry, and as a storage medium in the energy sector [6,7].

However, one of the biggest challenges in the methanol synthesis is the limitation of the methanol yield due to chemical equilibrium: in most cases, only 25% methanol yield can be obtained in one reactor run. One possible solution could be the use of membrane reactors, which enable an in-situ separation of water formed during the reaction of methanol, and thus, to circumvent the equilibrium limitation.

In this sense, the goal of this thesis is to model a membrane reactor and perform a steady-state simulation to evaluate the effects of in-situ product removal on methanol yield and production rates. For more information about the introduction and motivation of this thesis, the reader is referred to read Chapter 1.

2. Project Definition

To the best of our knowledge, there is a lack of research comparing the effects of removing the different products formed in the methanol synthesis (water and/or methanol). Therefore, this thesis aims to cover this research gap by investigating the effects of in-situ water and/or methanol removal via model steady-state simulations. Finally, the performance of membrane reactors with in-situ product removal will be compared to the conventional methanol synthesis against methanol yield and methanol production rates. More information about the research objectives of this thesis is presented in Chapter 1.

3. Model Description

A membrane reactor has been modelled based on the recommendations of the research work of Terreni et al. [8]. According to these authors and Galucci et al. [9], a kinetic model can be used to simulate the behavior of a membrane reactor providing that the permeation value is known. In this thesis, the in-situ removal of water and /or methanol is explored. The working principle of the model is presented in Figure a.2. More information about the modelling approach is provided in Chapter 3.

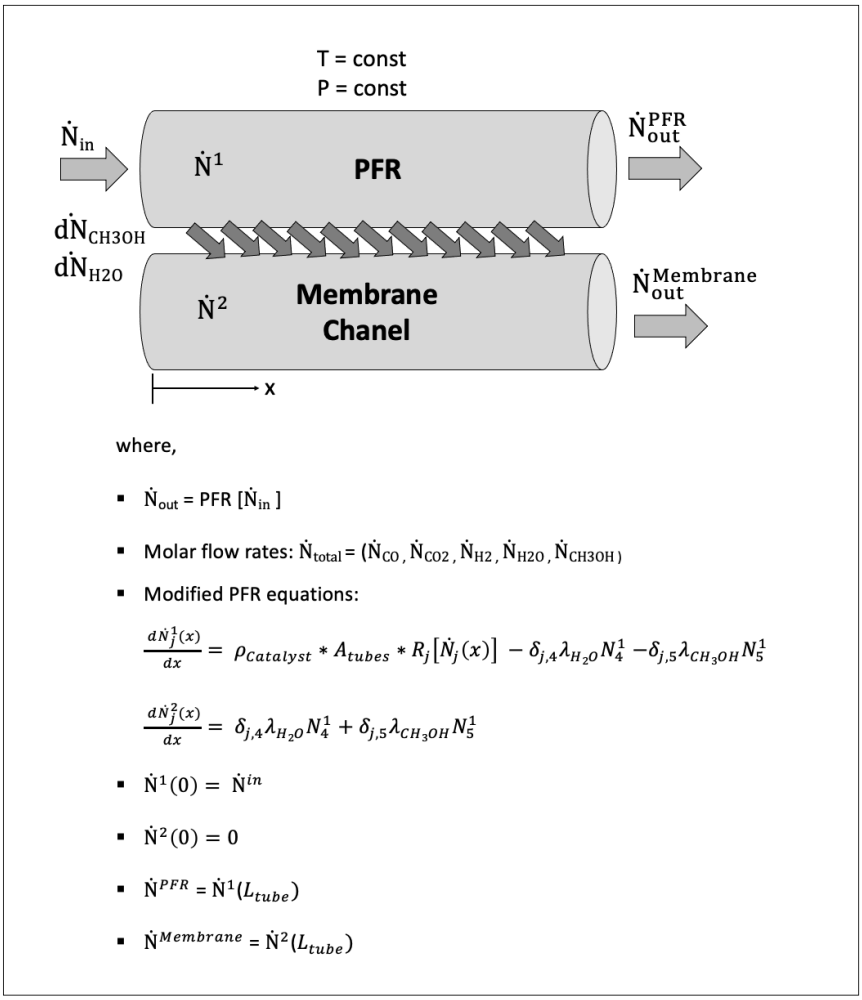

Figure a.2 - Computational scheme of the membrane plug flow reactor. Note the presence of a parallel channel representing the "membrane". Through this channel only methanol and water can selectively flow. The symbol $\delta_{j,k}$ is the "Kronecker delta". Definition of the PFR function and differential equations, which relates the input and output component molar flow rates. Adapted from "A simplified simulation of catalytic reactors for CO_2 reduction" [8].

4. Results

The simulation results suggest that the maximum methanol yield and production rates are obtained for the case of simultaneous in-situ removal of both methanol and water. The methanol yield could be increased up to 73.91%, and a maximum production rate of 36.96 mol/s can be obtained, if 90% of the produced methanol and water could be removed through the membrane. A conventional reactor at the same operation conditions of pressure, H_2/CO_2 molar ratio and optimal temperature, would in contrast achieve a methanol yield of 24.63% and a production rate of 12.42 mol/s. The results are presented in Chapter 4 and discussed in Chapter 5.

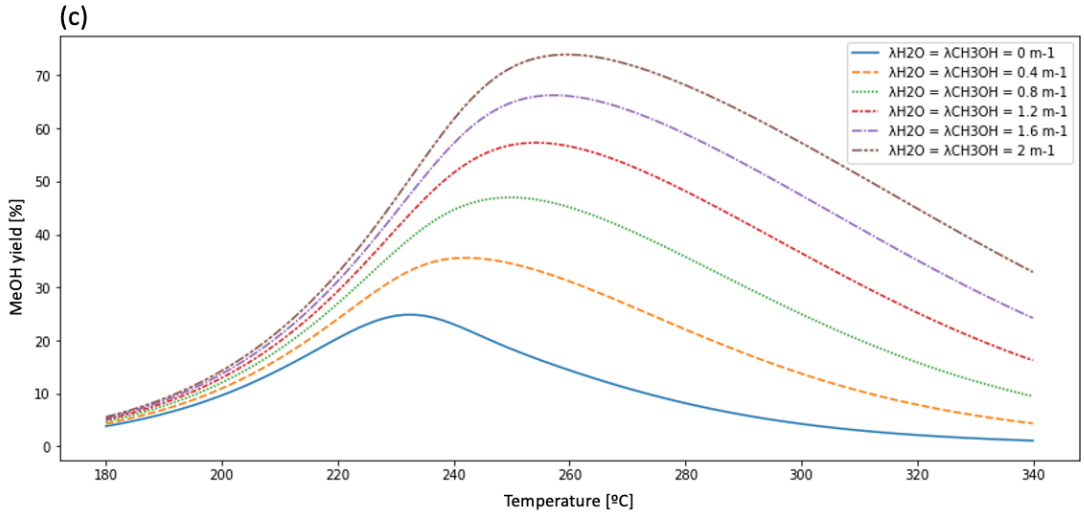

Figure b.2 - MeOH yield [%] in the membrane plug flow reactor (MPFR). Operation conditions: P = 60 bar, given $\lambda_{CH3OH}, \lambda_{H2O}$, and $H_2/CO_2 = 4$.

5. Conclusions

The simulations confirm the idea that membrane reactors can circumvent the thermodynamic equilibrium and achieve higher methanol yield and production rates. Carbon and inorganic zeolite membranes have been identified as the two most promising membranes for methanol production, since they can stand the high temperatures involved in the methanol synthesis. For the conventional reactor a maximum methanol yield of 24.63% and a production rate of 12.42 mol/s are obtained for 60 bar, and a H_2/CO_2 molar ratio of 4. The in-situ removal of both methanol and water seems especially promising. The removal of 90% of these products (water and methanol) would increase the methanol yield up to 73.91% and the production rate up to 36.96 mol/s. The in-situ removal of water could also be interesting. For other more realistic permeation ratios, the simulations show smaller improvements on methanol yield and production rates.

6. References

[1] I. Ridjan, B. V. Mathiesen, D. Connolly, and N. Duić, "The feasibility of synthetic fuels in renewable energy systems," *Energy*, vol. 57, pp. 76–84, 2013, doi: 10.1016/j.energy.2013.01.046.

[2] H. Lund and E. Münster, "Integrated transportation and energy sector CO2 emission control strategies," *Transp. Policy*, vol. 13, no. 5, pp. 426–433, 2006, doi: 10.1016/j.tranpol.2006.03.003.

[3] E. Pursiheimo, H. Holttinen, and T. Koljonen, “Inter-sectoral effects of high renewable energy share in global energy system,” *Renew. Energy*, pp. 1119–1129, 2019, doi: 10.1016/j.renene.2018.09.082.

[4] M. Moser *et al.*, “Synthetic Liquid Hydrocarbons from Renewable Energy – Results of the Helmholtz Energy Alliance,” *Chemie-Ingenieur-Technik*, vol. 89, no. 3, pp. 274–288, 2017, doi: 10.1002/cite.201500154.

[5] A. Santasalo-Aarnio *et al.*, “Application of Synthetic Renewable Methanol to Power the Future Propulsion,” *SAE Tech. Pap. Ser.*, vol. 1, Sep. 2020, doi: 10.4271/2020-01-2151.

[6] K. Räuchle, L. Plass, H. J. Wernicke, and M. Bertau, “Methanol for Renewable Energy Storage and Utilization,” *Energy Technol.*, vol. 4, no. 1, pp. 193–200, 2016, doi: 10.1002/ente.201500322.

[7] E. Moioli, R. Mutschler, and A. Züttel, “Renewable energy storage via CO2 and H2 conversion to methane and methanol: Assessment for small scale applications,” *Renew. Sustain. Energy Rev.*, vol. 107, no. March, pp. 497–506, 2019, doi: 10.1016/j.rser.2019.03.022.

[8] J. Terreni, A. Borgschulte, M. Hillestad, and B. D. Patterson, “Understanding catalysis—a simplified simulation of catalytic reactors for CO2 reduction,” *ChemEngineering*, vol. 4, no. 4, pp. 1–16, 2020, doi: 10.3390/chemengineering4040062.

[9] F. Gallucci, *Inorganic Membrane Reactors for Methanol Synthesis*. Elsevier B.V., 2018.

Index

LIST OF FIGURES

LIST OF TABLES

LIST OF ABBREVIATIONS

Abbreviation	Meaning
GHG	Greenhouse Gas
IMO	International Marine Organization
KPIs	Key Performance Indicators
LNG	Liquified Natural Gas
LPG	Liquified Petroleum Gas
MPFR	Membrane Plug Flow Reactor
PFR	Plug Flow Reactor
PtL	Power-to-Liquids
PtX	Power-to-X
RES	Renewable Energy Sources
SAF	Sustainable Aviation Fuels
SDGs	Sustainable Development Goals
TUM	Technical University of Munich

Chapter 1. INTRODUCTION

1.1 MOTIVATION

Despite the Paris agreement and the sustainability goals for 2030, global emissions of CO_2, the most important greenhouse gas (GHG), continue to increase. In 2021 the global energy-related CO_2 emissions are projected to rebound and grow by 4.8% reaching again 33 Gt after the corona crisis [1].

While significant progress has been made in the global electricity generation over the last two decades, the greenhouse gas emissions in other sectors have stagnated or even increased. According to Siemens Energy, in 2019 40% of the world´s emissions came from electricity production (see Figure 1). Similarly, the industry and transport sectors are together responsible for 45% of the global CO_2 emissions, whereas renewable energy sources cover only 8% of the total energy consumption in these sectors [2].

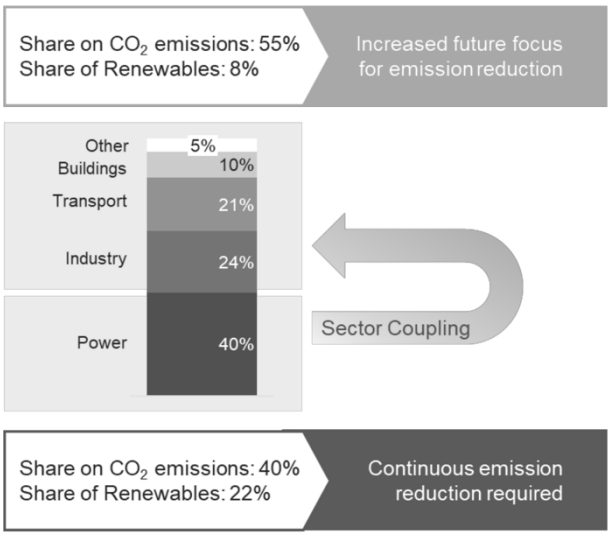

Figure 1: Energy related global CO_2 emissions and their shares by sectors, taken from W.Paper "A universal green fuel" [2].

This trend occurs both in Europe and Germany. According to the Federal Environmental Agency and the Shell energy scenarios, the transportation and electric power generation sectors account for more than three fifths of the Germany energy-related CO_2 emissions [3].

Decarbonizing the mobility sector is more complex and costly compared to the power sector, and thus, it will most likely come from a combination of sector coupling and the use of carbon-neutral e-fuels like e-Methanol and "green" Hydrogen [2].

Because of this, and with the aim to reduce the GHG emissions in the transport sector, the Technical university of Munich (TUM) joined forces with key industrial and research institutional partners under the E2Fuels Project, which is funded by the German Federal Ministry for Economic Affairs and Energy (BMWi) under the funding code 03EIV011G as part of the research initiative "Energiewende im Verkehr" [4].

According to the German Energy Agency, e-fuels (also commonly known as synthetic fuels) can be defined as gaseous and liquid fuels such as hydrogen, methane, methanol, synthetic petrol, and diesel fuels generated from renewable electricity [5]. These fuels are synthesized with electricity from renewable energy sources and using CO_2 from capture technologies, biomass, or from exhaust industrial waste (see Figure 2) [6,7].

e-fuels represent a promising approach to increase the share of renewable energy in the transport sector and reduce the GHG emissions sooner, since they can be used in internal combustion engines with relatively few modifications [8]. These fuels seems especially promising to decarbonize the aviation, marine and heavy road transport, since liquid hydrocarbons have a high energy and power density [9,10].

Synthetic fuels produced by Power-to-X are ready for instant use. They can be blended gradually with fossil fuels until they fully replace fossil fuels as a primary energy source. Another advantage with respect to other solutions is that existing infrastructure such as gas pipelines, gas stations, or storage facilities can be continued to be used [11].

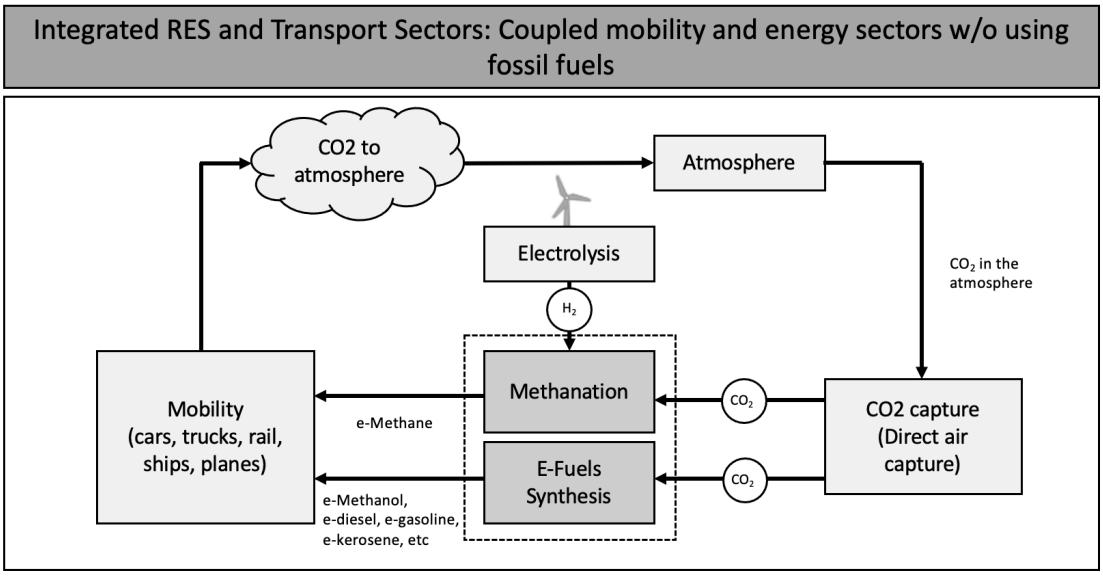

Figure 2. Integrated RES and Transport Sector: Coupled mobility and energy sectors w/o using fossil fuels. Adapted from W.Paper "A universal green fuel" [2]

The aviation industry introduced their own category of CO_2-neutral fuels known as Sustainable Aviation Fuels (SAF), which can be produced from biomass, waste, or using renewable energy to produce e-fuels. Here, e-Gasoline and e-Kerosene are projected to be the best option for RES integration in the aviation industry. However, these fuels are still considered as a long term solution and not usable for instantaneous application [12,13].

The International Marine Organization (IMO) has also set an ambitious target to reduce emissions by 50% in 2050 relative to 2008 [14]. The most promising alternatives to today´s heavy fuel oils are liquified natural gas (LNG), methanol, hydrogen, and ammonia. E-methanol seems especially interesting for large passenger ships like ferries and cruise ships [15].

Moreover, e-fuels can be used both in stationary and mobile applications. In this way, they could enable the use of photovoltaic and wind energy surpluses in the transport sector [16 ,17]. Additionally, due to their low storage and transport losses, they can also be used as complementary long-term electricity storage option [18].

Similarly, synthetic fuels can contribute to the flexibilization and integration of fluctuating renewable energies in the power sector (demand side management) and simultaneously increase the market value of renewable energy sources (RES) [19]. Furthermore, modern gas turbines can be operated with a mix of hydrogen and natural gas, with an hydrogen share of 5 to 100% [11].

However, these fundamental advantages are offset by the fact that synthetic fuels are not yet economically viable compared to fossil fuels due to the high energy losses during the process and high productions costs, meaning that further technological innovations are needed in both production and application [20].

The task of the Chair of Energy Systems at TUM is to model the production of synthetic fuels and to integrate it optimally in the energy system. This research is mainly focused on modelling the entire path of e-Hydrogen, e-Methane and e-Methanol [4].

Renewable methanol, also known as e-Methanol, seems to be one of the most promising Power-to-Liquids (PtL) products, since it can be used in the transport sector as a fuel [21], in the chemistry industry, and as a storage medium in the energy sector [22,23]. Some authors suggest that renewable methanol can then become an all-around substitute for petroleum, since it can be used both in the mobility sector and chemical industry [24,25].

According to Siemens Energy, e-Methanol could be a good alternative and/or supplementary technology with respect to fuel cell and battery vehicle technologies, since it provides a high energy density and range. Furthermore, e-Methanol allows simultaneously the use of existing infrastructure (fuelling station and car fleet) and a no-increase in the refuelling time with respect fossil fuels (see Figure 3) [2].

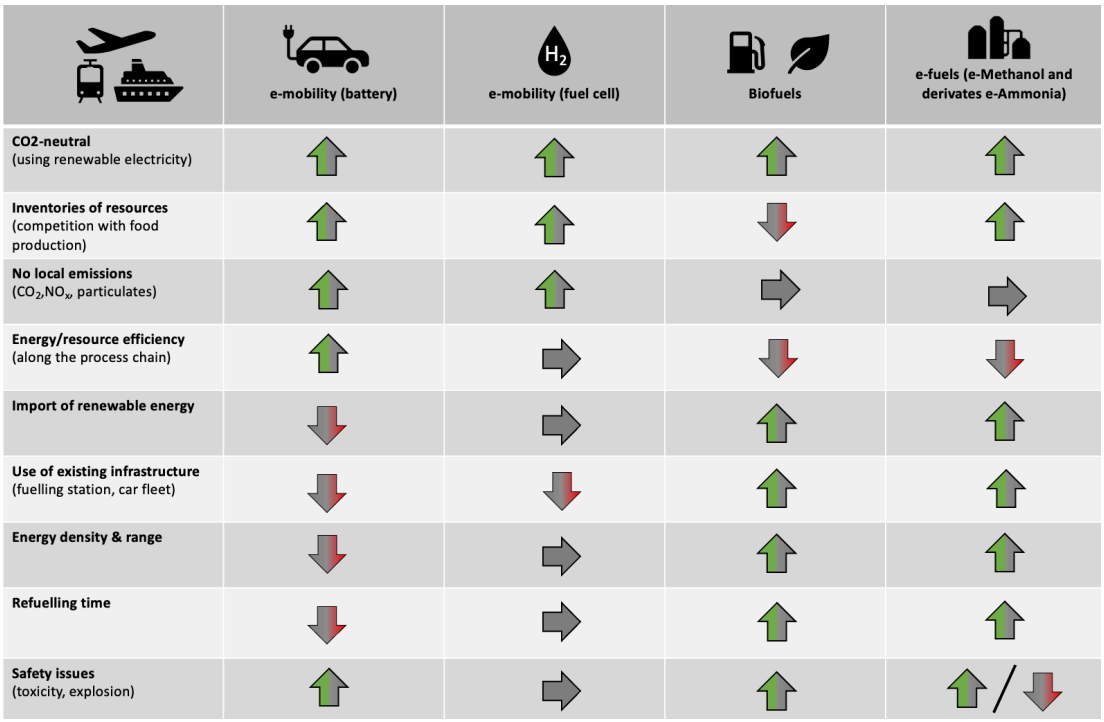

Figure 3. Comparison of possibilities for decarbonizing the transport sector, taken from W.Paper "A universal green fuel" [2]. Green arrows represent advantages, red arrows disadvantages and grey arrows mean in average over the other technologies.

Methanol is considered a carbon-neutral fuel, and its CO_2 footprint is on the order of 10 g CO_2/MJ_{th} compared to 80-90 g CO_2/MJ_{th} for fossil-sourced methanol [2].

e-Methanol can be obtained by combining hydrogen produced by electrolysis with CO_2 from carbon capture processes (Figure 4). By doing so, methanol production can be CO_2-neutral. Note that methanol becomes sustainable or "green" only if it is produced from green-hydrogen of either biological or electrochemical origin and CO_2 (what is commonly known as renewable methanol synthesis) [26].

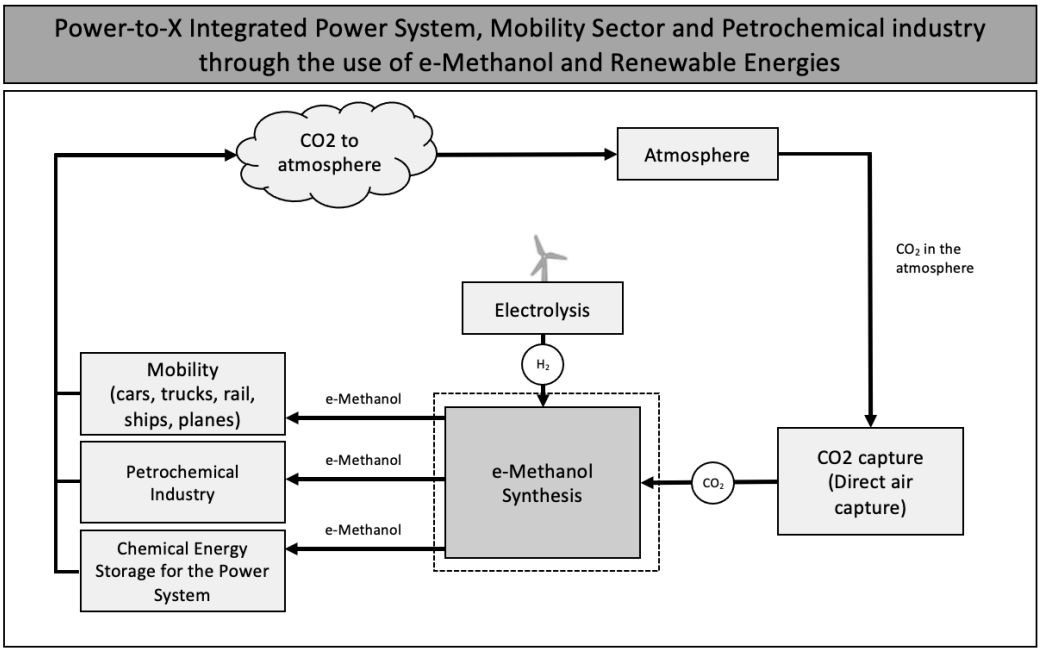

Figure 4. Power-to-X Integrated Power System, Mobility Sector and Petrochemical Industry using e-Methanol and Renewable Energies (own creation).

However, one of the biggest challenges in the methanol synthesis is the limitation of the methanol yield due to chemical equilibrium: in most cases, only 25% methanol yield can be obtained in one reactor run. One possible solution could be the use of membrane reactors, which enable an in-situ separation of water formed during the reaction of methanol, and thus, to circumvent the equilibrium limitation.

In this sense, the aim of this thesis is to support the research within the E2Fuel project, by evaluating, analysing, and simulating the yield and efficiency increase of renewable methanol synthesis using membrane reactors and then, to confirm the viability and effectivity of this possible solution.

1.2 RESEARCH OBJECTIVES AND TASK DEFINITION

The research objectives of this project are the following:

1. Conduct literature research on membrane reactors and identify the most promising membrane types to produce renewable methanol.
2. Model a membrane reactor to simulate and explore the effects of in-situ product removal on methanol yield and production rates.
3. Development of steady-state simulation of the renewable methanol synthesis with the novel membrane reactor concept.
4. Determination of the import key performance indicators (KPIs) and comparison with conventional methanol synthesis.
5. Evaluate the viability and performance of the technology.

This project is also aligned to some Sustainable Development Goals (SDGs). The production of e-Methanol together with Power-to-X technologies can reduce the GHG emissions of the power, transport and industrial sectors.

Thus, this thesis is aligned to the following Sustainable Development Goals (SDGs): *3. Good Health and Well-being, 7. Affordable and clean energy, 9. Industry, Innovation and Infrastructure, 11. Sustainable Cities and Communities, 12. Responsible Consumption and Production and 13. Climate Action* [27].

e-Methanol could decarbonize the transport system in a fast and affordable way. Therefore, this thesis is aligned to the sustainable development goals “Affordable and clean Energy” and “Sustainable Cities and Communities”.

Similarly, the aim of this thesis is to prove the use of membrane reactors to increase the yield and efficiency of the renewable methanol synthesis. Thus, this research is also aligned to the sustainable development goals “Industry, Innovation and Infrastructure”, “Responsible Consumption and Production” and “Climate Action”.

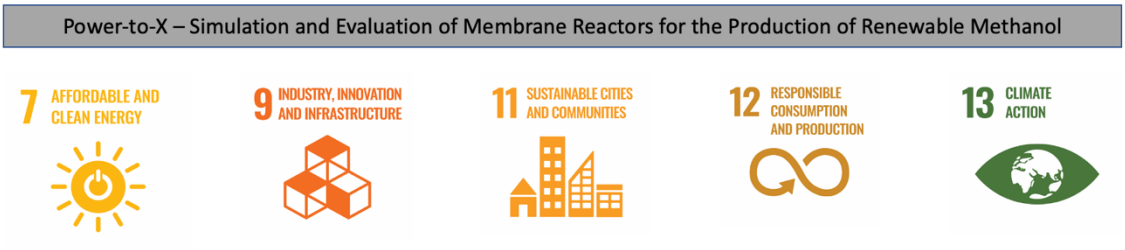

Figure 5. Alignment of the thesis with the Sustainable Development Goals (SDGs), own creation based on the Sustainable Development Goals (SDGs) taken from [27].

More information about the SDGs and the position of Comillas Univeristy with respect the fulfillment of these goals is presented in Appendix E.

1.3 THESIS STRUCTURE

The goal of this thesis is to answer the following research questions:

- What are the most promising membranes for the production of renewable methanol?
- What improvements can membrane reactors bring to the process compared to the conventional methanol synthesis?
- What scope do these improvements have?

With the aim of answering these research questions, the thesis is structured as follows:

The Chapter 1 presented a brief motivation for the thesis. Chapter 2 provides the reader with an overview of the current state of the art in membrane reactors for methanol production. Moreover, this chapter gives insight into the methanol synthesis process and its evolution through history.

Thereafter, Chapter 3 presents the methodology used to model both conventional and membrane reactors. Chapter 4 contains the simulation results and a comparative analysis. Chapter 5 discusses the results, the methodology and the model limitations. Finally, Chapter 6 offers an overview of the thesis by summarizing the conclusions and suggest future research gaps to cover with future research works.

Chapter 2. STATE OF THE ART

This chapter presents a brief overview of Power-to-X and sector coupling solutions. Moreover, the term "methanol economy" is explained. Finally, the methanol synthesis process and the current state of the art in membrane reactors for methanol production are presented in detail. The most important research projects and works in this respect are summarized and described.

2.1 POWER-TO-X AND SECTOR COUPLING

Power-to-X describes methods for converting electrical energy into liquid or gaseous chemical energy sources through electrolysis and further synthesis processes (see Figure 6) [11]. The increasing global dependence of the power generation sector on renewable energies is posing challenges to the electricity infrastructures and require flexible solutions to balance the power generation and demand [28].

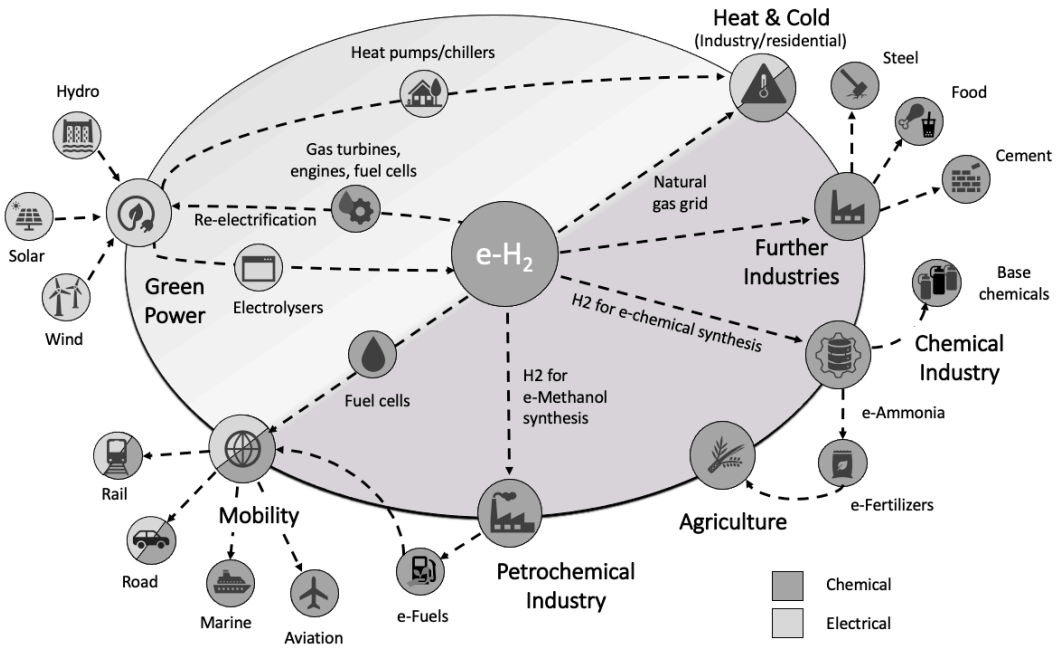

Figure 6. Sector Coupling under Power-to-X methods, adapted from [11]. e-H_2 means "green Hydrogen".

Hence, power-to-X is emerging as an interesting method for storing renewable energy excess as well as providing a low capital decarbonization pathway to produce green fuels and common chemical products [29].

To properly understand the benefits of Power-to-X (PtX) it is necessary to also introduce the term sector coupling. There are several definitions used in Germany, such as that of the German Federal Ministry for Economic Affairs [30], the German Technical and Scientific Association for Gas and Water [31], or the German Association of Energy and Water Industries (BDEW) [32], among others.

In this thesis, it has been decided to present the definition stated by the BDEW, which describes the concept of sector coupling as follows: "*the energy engineering and energy economy of the connection of electricity, heat, mobility and industrial processes, as well as their infrastructures, with the aim of decarbonization, while simultaneously increasing the flexibility of energy use in the sectors of industry and commercial/trade, households, and transport under the premises of profitability, sustainability and security of supply*" [32]. This concept in illustrated in Figure 7.

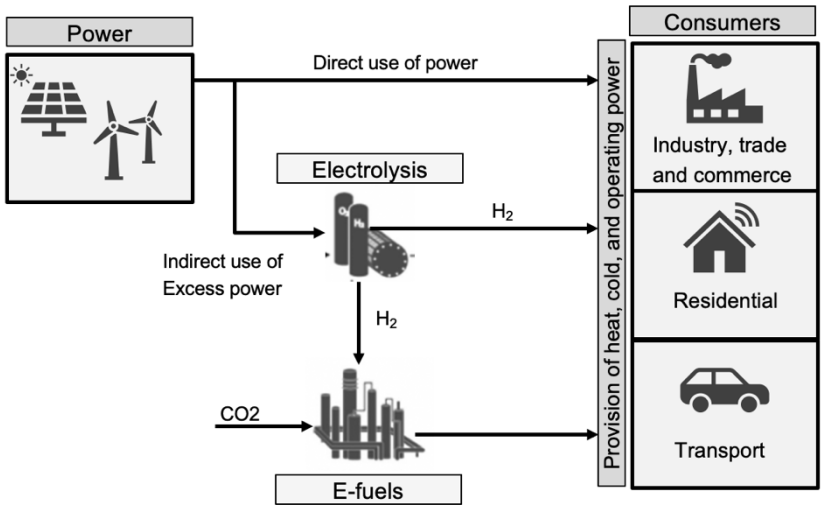

Figure 7. Principle of Sector Coupling, adapted from "Linking the power and transport sectors - Part 1: The principle of sector coupling" [34].

Furthermore, sector coupling via Power-to-X has the potential to reduce primary fossil fuels energy consumption by 50% even while global power demand grows by 25% [33]. Similarly, some authors have investigated the synergies of a coupled model that connects the power and transport sectors in Germany and Europe [34,35].

As it has it can be seen in Figure 6, e-Methanol synthesis is one of the most important Power-to-X routes and seem specially promising for the petrochemical industry and mobility sector. This together with the possible applications in energy storage and global methanol demand make e-Methanol one of the most important chemical products to substitute the petroleum. Thus, some authors have discussed the idea of a hypothetical future energy economy based on methanol. This is what is called "Methanol Economy" and it will be presented in the next section.

2.2 METHANOL ECONOMY

In the 1990s George A. Olah, awarded with the Nobel Prize in Chemistry in 1994, first discussed the idea of a hypothetical future energy economy based on methanol, which he personally named "Methanol Economy" [36,37].

Renewable energy systems pose challenges that should be addressed soon. These challenges are especially problematic for the two most promising and scalable renewable sources, solar and wind, which by nature are intermittent and highly fluctuating. Solar energy is not constant within the days neither within the seasons and is none at night. Similarly, wind is also variable during the seasons and the day [38].

This challenge implies the necessity to store electrical energy, which could be done in form of chemical energy (bonds) in compounds such as hydrogen, methanol, methane and higher hydrocarbons. Thereafter, these chemicals can also be used at later time to generate electricity or in other applications such as transport and heating [38,39,40].

The simplest and today´s most common compound that can be produced from renewable electrical energy excess is hydrogen, by the splitting of water through electrolysis. Hydrogen

has also been proposed as promising energy storage medium [41]. This process is really efficient and well researched and can achieve today overall system conversions higher than 75-85% [42,43].

However, other authors highlight that hydrogen, due to its physical and chemical properties, present several drawbacks. Since hydrogen has a low volumetric density, it requires either compression to high pressures (350-700 bar) or liquefaction at very low temperatures (-253ºC), which makes its storage difficult and energy intensive [38,44].

A liquid chemical storage medium would be preferable to a gaseous one because it would be easier to transport and store. Moreover, a renewable liquid fuel would be highly desirable to avoid the construction of an entirely new transportation/storage/distribution network [38].

A possible candidate fulfilling these requirements is methanol, which is liquid at ambient temperature [45]. Methanol could be an excellent substitute or additive for gasoline in internal combustion engines, since it can be efficiently used in modified diesel engines [46,47]. Moreover, it presents a very high octane rating and its emissions are clean in NO_x and SO_x [48].

Dimethyl ether (DME) can also be produced from methanol by dehydration. DME could also be good diesel fuel substitute [49,50]. Furthermore, methanol can also replace liquefied petroleum gas (LPG) in heating and they also are also superior fuels for electrical power generation in gas turbines [51].

Additionally, methanol could be also be transformed into gasoline through the methanol-to-gasoline process developed by Mobil in the 1980s [52]. Moreover, methanol is one of the most important products in the chemical industry with an estimated worldwide current annual production of over 110 million metric tons. The methanol production is still mostly based on fossil fuels (natural gas and coal) for economic reasons [53]. Thus, it seems crucial to explore the route of e-methanol and analyse how to improve the process conversion and profitability.

An interested reader is invited to read more information about the "Methanol Economy" concept in the following research works [25,36,37,38].

2.3 WORLDWIDE RENEWABLE METHANOL PLANTS

According to the Methanol Institute industry-estimations, renewable methanol could cut CO_2 by up to 95%, nitrogen oxide emissions by up to 80%, and completely eliminate the sulfur oxide emissions, compared to conventional fuels [54].

There are currently only a few projects for renewable methanol production (see Figure 8). In the context of the BMWi funded E2Fuels project, Siemens Energy, Stadtwerke Hassfurt, Man Energy Solutions and Academia are working together to develop the novel PtMethanol concept, which should be more efficient and operationally flexible, balancing the volatile RES production. Lab-scale tests of the synthesis concept and a pilot project were both planned for 2021 but unfortunately have been postponed [2].

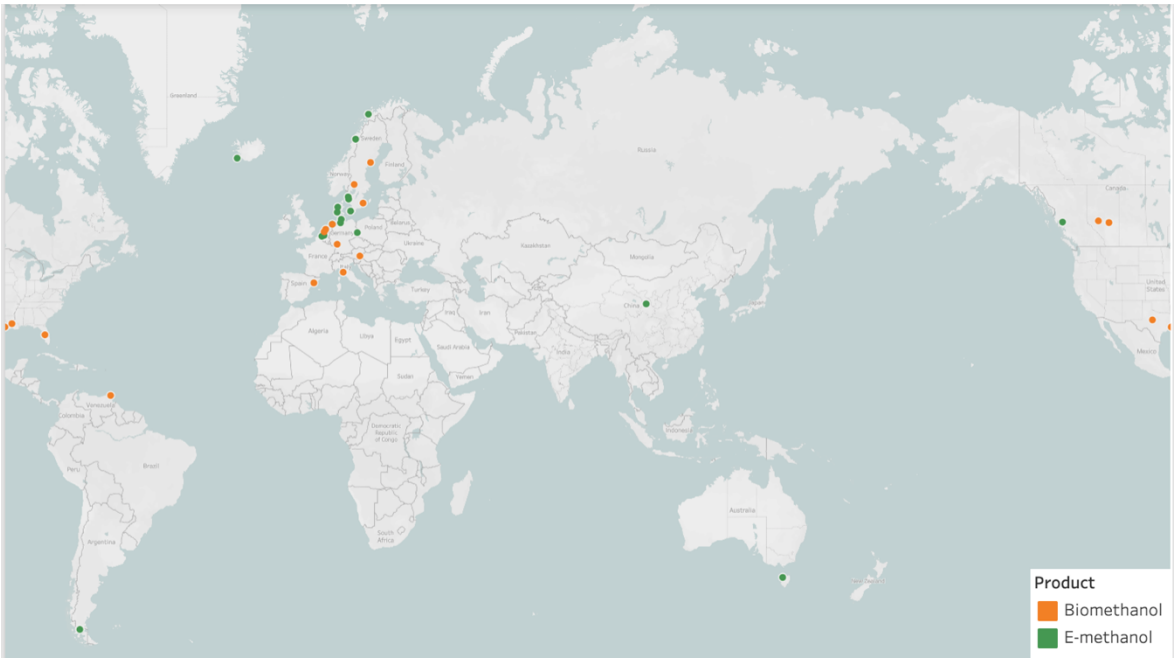

Figure 8. Renewable and Bio-methanol Projects 2021, taken from [54].

Moreover, parallel to small-scale pilot projects, scalability and maturity in large-scale plant operation should be confirmed and achieved quickly. These projects need to be located in regions with high renewable potential and low cost electricity production. Siemens Energy launched in December 2020 a PtMethanol plant (Haru Oni Project) to be constructed in Patagonia, Chile [55].

The PtMethanol plant will have a production capacity of 130,000 litres in 2022 during the pilot phase, 55 million during the first phase until 2024 and finally 550 million litres e-fuel per year during the second phase until 2026. The final products will be e-methanol and e-gasoline, which will be produced via methanol-to-gasoline process [2].

The Haru Oni Project will be the first commercial industrial-scale plant for climate-neutral e-fuels production and will be supported also by the German Federal Ministerium for Economic Affairs and Energy by funding under the National hydrogen Strategy program [56]. The project phases can be seen in Figure 9.

Figure 9. Haru Oni pilot plant, Patagonia (Chile), taken from [2].

Such Power-to-Liquid (PtL) plants can be designed using modular concepts with single train electrolysis of up to 200 MWel. This standardization together with economies-of-scale for both chemical synthesis and pre-manufactured components are essential to reduce investment costs and construction time. A simplified process flow diagram for a Power-to-Methanol plant is presented hereunder (see Figure 10) [2].

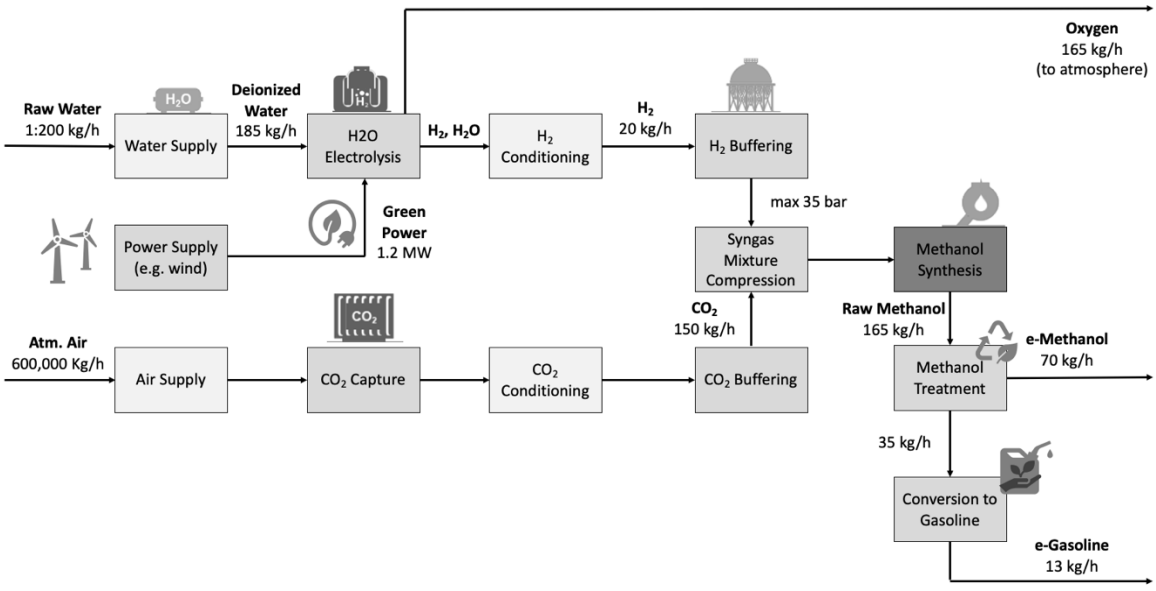

Figure 10. Simplified process flow diagram for a Power-to-Methanol plant, adapted from [2].

2.4 KINETIC MODELS FOR METHANOL SYNTHESIS

Up to date several kinetic models for methanol synthesis have been presented. The most used kinetic models are the ones from Graaf et al. [57], Vanden Bussche and Froment et al. [58] and Villa et al. [59]. Other authors have investigated other specific kinetic models for the methanol synthesis from renewable sources (H_2, CO_2 and/or CO) using a $Cu/ZnO/Al_2O_3$ catalyst [60].

Meyer et al. [61] compared the kinetic models of Graaf et al. [57] and Vanden Bussche and Froment et al. [58] for a methanol synthesis process by CO_2 hydrogenation. The authors conclude that results can be significantly different outside the equilibrium.

In the first kinetic models CO was considered to be the active component, CO_2 a stable component, and methanol was mainly produced from syngas. Later other research works proposed that CO_2 could be also a reactant as well and CO_2 hydrogenation terms were incorporated in kinetic models [57,62]. According to the PhD thesis of Tobias A.Henkel [63] the methanol synthesis kinetic models can be grouped in four categories.

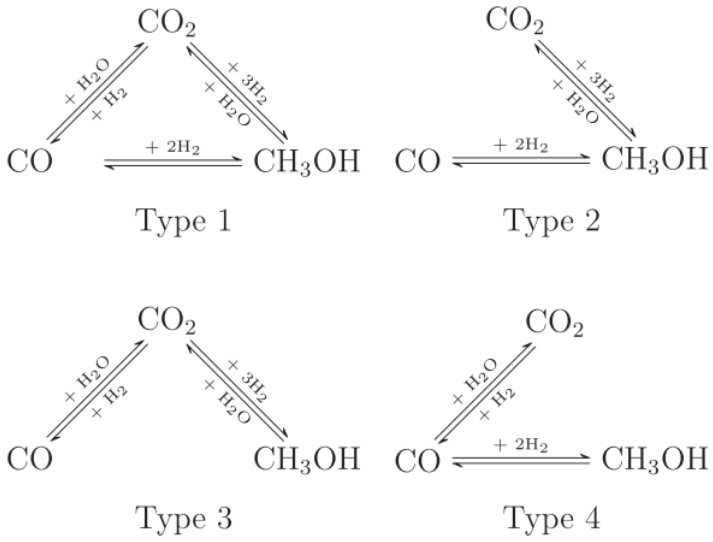

Figure 11. Classification of methanol synthesis in four types of kinetic models according to Slotboom et al. [65] and Henkel [63]. Type 1: all pathways can be taken [57,60,64]. Type 2: methanol is produced from both CO and CO_2, while the RWGS reaction rate is not considered [62,66]. Type 3: methanol is only produced from CO_2 [58,67,68,69] and Type 4: CO considered the main carbon source for methanol [59]. Taken from [65].

The first category (Figure 11, Type 1) is considered in the models of Takagawa et al. [64], Graaf et al. [57] and Seidel et al. [60]. In these models, methanol is assumed to be formed from both CO and CO_2 as carbon sources and the reverse water gas shift (RWGS) reaction rate needs to be included [65].

The second group (Figure 11, Type 2) assumes the methanol formation from CO_2 and CO. McNeil et al. [62] and Klier et al. [66] are typical examples of this approach. Here the two hydrogenation reactions are considered as the key reactions of synthesis. Thus, a reaction rate for the RWGS reaction is not taken into account and CO_2 cannot be directly converted to CO [65].

The third group (Figure 11, Type 3) considers the CO_2 hydrogenation reaction as the main reaction towards methanol. This approach is used by Skrzypek et al. [67], Askgaard et al. [68], Kubota et al. [69] and Vanden Bussche and Froment [58]. CO can be produced by the RWGS reaction, but this approach assumes methanol not to be converted directly from the RWGS reaction.

The fourth and last group assumes CO as the main carbon source for methanol (Figure 11, Type 4). This approach is assumed by Villa et al. [59].

Clearly, there is no consensus in what kinetic model represent best the reality. An interested reader in kinetic models and comparisons between them is referred to read the work of Slootboom et al. [65] and Meyer et al. [61] for more detail.

2.5 THERMODYNAMIC EQUILIBRIUM IN METHANOL SYNTHESIS

The reduction of CO_2 to methanol is usually performed over a copper-zinc oxide catalyst at 200-300ºC and a pressure of several tens of bar [57,70,71]. The chemical reactions involved in CO_2 hydrogenation to methanol according to Graaf kinetic model are shown in Figure 12.

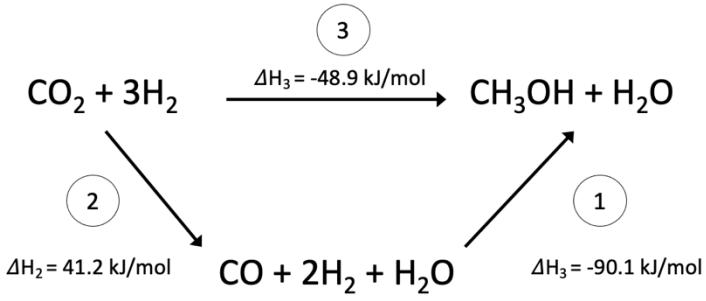

Figure 12. CO_2 hydrogenation to methanol involved reactions according to Graat et al. [57,70]. Reaction (3) is the direct hydrogenation of CO_2, Reaction (2) is the reverse water shift reaction (RWGS) and Reaction (1) is the hydrogenation of carbon monoxide. Adapted from "A simplified simulation of catalytic reactors for CO_2 reduction" [75].

Therefore, methanol production can be direct (reaction 3) or can produced via carbon monoxide as intermediate product (reactions 2 and 1). Note that the water shift reaction (RWGS) 2 competes for CO_2 with direct hydrogenation and it is the only endothermic reaction. Thus, increasing the reaction temperature will lead to an increase formation of CO and will consequently reduce the direct hydrogenation of CO_2 to methanol. Moreover, an increase in pressure will enhance the direct hydrogenation of CO_2 to methanol, since reaction 3 involves a reduction in the number of moles. These predictions agree and can be derived from le Chaterlier´s principle [72].

The equilibrium state in the conversion of CO_2 to CH_3OH is defined by thermodynamics and can be then determined using the temperature-dependent constants K^{eq}, which are derived from the change in Gibbs free energy at a given temperature.

$$K_3^{eq}(T) = \exp\left(\frac{-\Delta G_3^0}{RT}\right) = \exp\left(\frac{-\Delta H_3^0 + T\Delta S_3^0}{RT}\right)$$
$$= \exp\left(\frac{-\Delta H_{CH3OH}^0 - \Delta H_{H2O}^0 + -3\Delta H_{H2}^0 + \Delta H_{CO2}^0}{RT}\right) x \exp\left(\frac{S_{CH3OH}^0 + S_{H2O}^0 - 3S_{H2}^0 - S_{CO2}^0}{RT}\right)$$

where T is the absolute temperature, R is the gas constant, and ΔH^0 and S^0 are the standard enthalpy and entropy of formation of the corresponding reactant and product species (see Table 1, values obtained from Swaddle et al. [73]). The temperature-equilibrium constant $K_3^{eq}(T)$ refer to the direct conversion of CO2 to methanol (reaction 3), $K_2^{eq}(T)$ to the reverse water gas shift (RWGS) reaction (reaction 2) and $K_1^{eq}(T)$ to the CO hydrogenation to methanol (reaction 1).

Table 1. Standard enthalpy of formation and entropy involved species for CO_2 reduction to methanol. Values obtained from [73].

Components	$\Delta H^0[kJ/mol]$	$S^0[kJ/mol]$
CO	-110.52	197.67
CO_2	-393.51	213.74
H_2	0	130.68
H_2O	-241.82	188.82
CH_3OH	-200.66	239.81
CH_4	-74.81	186.26

In this way, one can estimate the equilibrium constants for the reactions involved in the methanol synthesis, as plotted as a function of inverse temperature in Figure 13 (reaction 1 and 3, depicted in red) and for the reverse water gas shift reaction (reaction 3, depicted in green).

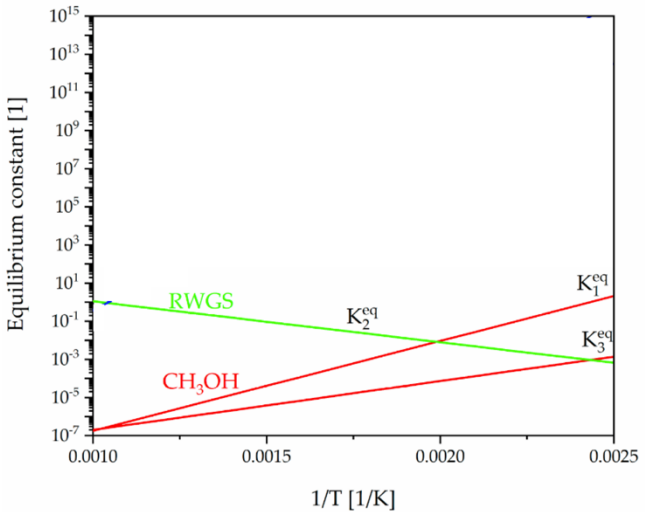

Figure 13. Equilibrium constants for methanol production reactions as a function of the inverse temperature. The green line shows the equilibrium constant of the reverse water gas shift reaction. Adapted from "Understanding catalysis-a simplified simulation of catalytic reactors for CO_2 reduction" [75].

Note that since the three reactions presented in Figure 12 are coupled, only two of the three equilibrium constants are independent, and the equilibrium constants can be presented as follows:

$$K_1^{eq}(T) \cdot K_2^{eq}(T) = K_3^{eq}(T) \quad (1)$$

At given temperatures and pressures, one can consider that the thermodynamic yield of a reaction is the equilibrium result that is approached after an infinite elapsed time. Because of their coupling (see equation 1), only two of the three equations need to be considered. The thermodynamic yield is then determined by equating the equilibrium constant with the corresponding reaction quotient [72]. By doing so and considering the reactions 2 and 3 of Figure 12, the following expressions can be derived (see below equations 2,3).

The reaction quotient measures the relative amounts of products and reactants present during a reaction at a particular point in time. Similarly, the reaction quotient can aid in figuring out

which direction a reaction is likely to proceed, given either the pressures or the concentrations of the reactants and products [74].

$$K_2^{eq}(T) = \frac{N_{CO} \cdot N_{H2O}}{N_{H2} \cdot N_{CO2}} \quad (2)$$

$$K_3^{eq}(T) = \frac{N_{CH3OH} \cdot N_{H2O} \cdot N_{tot}^2 \cdot P_0^2}{N_{H2}^3 \cdot N_{CO2} \cdot P^2} \quad (3)$$

The reaction quotients are determined by the reduced partial pressures p_j or molar concentrations N_j of the reactants and products species j, the reaction pressure P (assumed to be constant), and the atmospheric pressure P_0 [75].

On the other hand, the molar concentrations are related to the degrees of completion ξ_i of the individual reactions i. In this sense, the relationships between the equilibrium molar concentrations N_j and the degrees of completion ξ_i for the methanol synthesis are given by [75]:

$$N_{CO} = \xi_2 \cdot N_{CO2}^0$$
$$N_{CO2} = (1 - \xi_2 - \xi_3) \cdot N_{CO2}^0$$
$$N_{H2} = (SN + 1 - \xi_2 - 3\xi_3) \cdot N_{CO2}^0$$
$$N_{H2O} = (\xi_2 + \xi_3) \cdot N_{CO2}^0$$
$$N_{CH3OH} = \xi_3 \cdot N_{CO2}^0$$
$$N_{total} = N_{CO} + N_{CO2} + N_{H2} + N_{H2O} + N_{CH3OH} = (SN + 2 - 2\xi_3) \cdot N_{CO2}^0$$

where N_{total} is the total number of moles and SN is the "Stoichiometric number", defined as the ration the ratio between the difference of initial hydrogen and carbon dioxide concentrations and the sum of initial carbon monoxide and carbon dioxide [76].

$$SN = \frac{N_{H2}^0 - N_{CO2}^0}{N_{CO}^0 + N_{CO2}^0}$$

Note that in this thesis, we assume no initial CO concentration (i.e. $N_{CO}^{0} = 0$). The specification of SN, T and P allow one to numerically solve equations mentioned above and obtain the ξ_2 and ξ_3 variables. Note that ξ_3 represents the degree of conversion of CO_2 to methanol (i.e. methanol yield).

By solving these equations systems, one can obtain the following equilibrium conversions for the CO_2 reduction to methanol as function of T and P (see Figure 14)

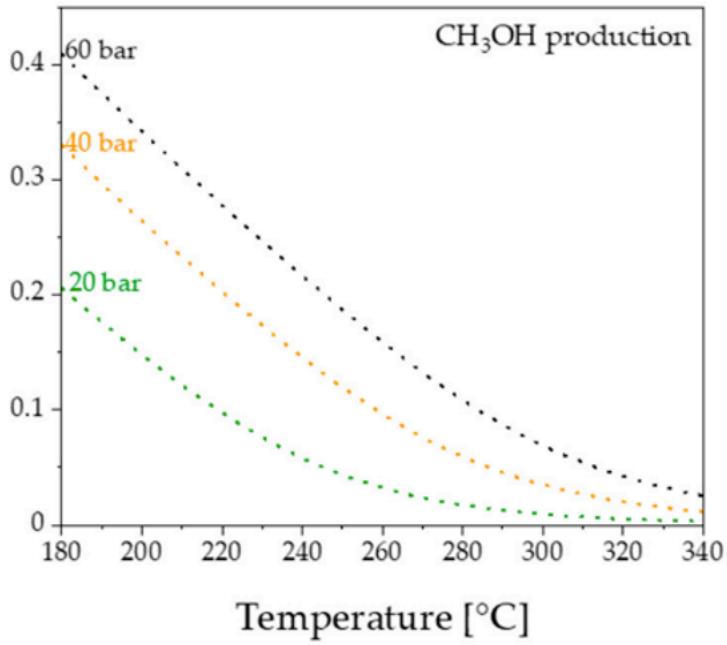

Figure 14. Equilibrium molar conversion for CO_2 to methanol hydrogenation as a function of temperature (180-340ºC) and pressure (20,40,60 bar). Adapted from [75].

Note that as predicted by Le Chaterlier´s principle, the equilibrium conversion of CO2 to methanol is enhanced with increasing pressure and decreases with increasing temperature. These results are also in good agreement with other previous published research works [77].

The steps for calculating the thermodynamic equilibrium have been taken from the work of Terreni et al. [75].

2.6 METHANOL PRODUCTION

Methanol has been used for millennia since the ancient Egyptians used it for embalming processes. However, it was not until 1661 when Robert Boyle produced pure methanol through further wood distillation. In 1834 the elemental composition of methanol was determined by Jean-Baptiste Dumas and Eugene Peligot [78].

To this date several techniques have been developed to produce methanol. The distillation of vinegar on wood and then dry wood distillation techniques were used until the first catalytic processes were discovered in the second decade of the XX century by the German chemical company BASF [79].

In the 1920s BASF designed a selective Zn/Cr catalyst and patented the high-pressure methanol synthesis process from synthesis gas (syngas) operated at up to 350 bar and 400ºC [80].

Later in the 1960s, the ICI Katalko company replaced previous Cr-based catalyst with a Cu-based catalyst and developed a low-pressure methanol process that could operate at 35-55 bar and 200-300ºC. This process is the most used today for large-scale methanol production [81].

Nowadays, methanol synthesis catalysts are a well-established design. Today the highest active and selective catalysts for methanol production are $Cu/ZnO/Al_2O_3$ catalysts and they have already been intensively studied. These catalysts have a good activity starting from 200°C and are selective toward the formation of methanol from H_2 and CO_2. Table 2 presents a typical composition of the catalysts used for the synthesis with respect to the producers [79].

Table 2. Typical composition for methanol synthesis catalysts, taken from Gallucci et al. [79]

Manufacturer	Cu (%)	Zn (%)	Al (%)
BASF	65-75	20-30	5-10
Süd Chemie	65-75	18-23	5-10
ICI	61	30	9
DuPont	50	19	31
Haldor Topsøe	50-60	21-25	15-28

Thus, today there is more research focus on reaction engineering and process design with the aim to increase the yield per pass and therefore, to reduce the recycle of unconverted reactants and increase the process efficiency [79].

According to the kinetic model proposed by Graaf et al [57], one of the most important kinetic models up to date, the methanol synthesis is indeed an equilibrium system represented by the following reactions:

$$CO + 2H_2 \Leftrightarrow CH_3OH \qquad \Delta H_{298K} = -90.7 \frac{kJ}{mol} \qquad (4)$$

$$CO_2 + H_2 \Leftrightarrow CO + H_2O \qquad \Delta H_{298K} = -41.19 \frac{kJ}{mol} \qquad (5)$$

$$CO_2 + 3H_2 \Leftrightarrow CH_3OH + H_2O \qquad \Delta H_{298K} = -49.51 \frac{kJ}{mol} \qquad (6)$$

The carbon sources needed for the methanol formation can either be CO_2 or CO as shown in Eqs (4) and (6). First the carbon source was considered to be CO [59], later CO_2 [58,67,69] and eventually both [57,60,82].

As stated before, one of the biggest challenges in methanol synthesis is the limitation of the methanol yield due to the chemical equilibrium. In most cases, only less than 30% methanol

yield can be achieved in one reactor run. According to Gallucci et al. [79], to circumvent the thermodynamic limitation that reduces the yield of conventional systems, two possible routes can be explored: (i) smart recycling of unconverted synthesis and (ii) in situ removal of the products of the reaction.

Option (i) is already well known but lead to high energy and plant costs due to the condensation and recycling process of the unreacted gases. Moreover, this option makes the process more complex and increase the associated capital and operating costs of the process. Because of this, research seems to be more interesting for option (ii).

In situ product removal can be achieved by selective adsorption of one or both liquid products. In this sense, while removing the methanol would only simplify the final product purification, the removal of water is also very important. By removing water, one can indeed achieve higher methanol production (because the Le Chatelier's effect on the equilibrium reactions is higher), and simultaneously can prevent unwanted methanol reforming reactions and deactivation of the catalyst (since water accelerates the crystallization of Cu and ZnO contained in a Cu/ZnO-based catalyst) [79].

The idea is not something new. In 1996 Struis et al. [83] analyzed the use of a Li-Nafion membrane reactor for the production of methanol. The conclusions show the capability of a Li-Nafion membrane to separate products from a commercially available catalyst bed operating on CO and H_2. However, the temperature limit around 200ºC limited the potential of the technology.

Since then, other authors have proposed different membranes that could be more suitable to produce methanol. These membranes and research works are detailed in the following sections.

2.7 MEMBRANES FOR METHANOL PRODUCTION

Membrane reactors can theoretically be used to increase conversion and selectivity (see Figure 15). Membrane reactors have a superior performance with respect conventional systems due to the combination of reaction and in-situ removal of products in a single system [79].

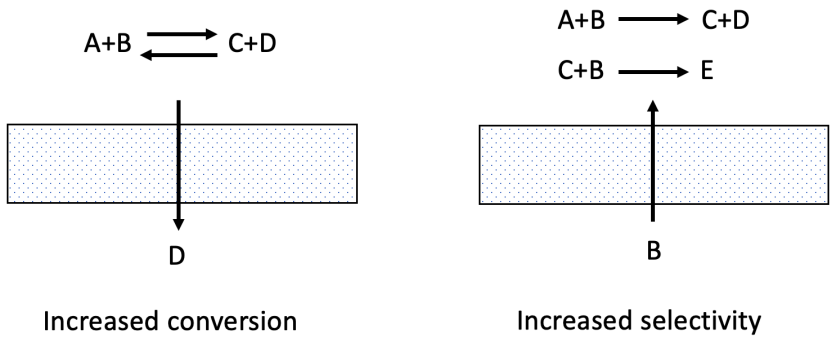

Figure 15. Process type of membrane reactors, adapted from "Increased product yield through the use of membrane reactors" [89]. A,B are the reactants and C,D the products for increased conversion case (left). A,B,C are the reactants and C,D,E the products for the increased selectivity case (right). The focus of this thesis is increased conversion (left).

As first demonstrated by Struis et al. [83], membrane reactors can improve both reactant´s conversion and methanol yield. In this research work the authors performed an experiment with a polymeric Nafion membrane. The authors conclude that a reactor equipped with this type of membrane can achieve higher methanol yields than conventional reactors without membranes.

However, as stated in section 2.6 Methanol Production, the improvements of this membrane type were limited by temperature. Nafion membranes were stable at around 150-200 ºC, which is too low for optimal methanol catalysts to be active. Typical operation conditions for methanol synthesis are around 250ºC (200-320ºC). Thus, there is a need to investigate other membranes that can separate water/methanol at temperatures interesting for methanol synthesis. In this range there are several inorganic membranes under investigation.

Today the most interesting seem to be carbon membranes and inorganic zeolite membranes. A brief introduction to these membranes is presented below. An interested reader is referred to read the literature review about inorganic membrane reactors presented by Gallucci et al. [79].

2.7.1 CARBON MEMBRANES

Microporous carbon membranes seem to be good candidates for methanol synthesis, because they have excellent permeation selectivity, high hydrothermal stability and high corrosion resistance [79].

Moreover, the porous structure and hydrophobicity/hydrophilicity of these membranes can be modified by working at the appropriate temperature and selecting the right polymer precursors [84]. The shape of these membranes is illustrated in Figure 16.

Up to date most research on this kind of membrane is focused on recovery of hydrogen from the methanol reforming reaction [85]. However, other authors suggest that carbon membranes can also be applied for methanol and water removal, if modifications in the membrane structure are conducted [86].

Similarly, according to the Zeolite-and Carbon Membranes Group from the Fraunhofer Institute for Ceramic Technologies and Systems (IKTS), carbon membranes are interesting materials for tasks in gas separation, pervaporation, vapor permeation and liquid filtration.

The gas transport through the membranes is strongly dependent on material structure, pore size and thickness of the membrane layer. According to Fraunhofer IKTS [87], carbon membranes are divided into two types: the molecular sieving carbon membrane (MSCM) and the adsorption-selective carbon membrane (ASCM).

The Fraunhofer IKTS is also investigating the increased product yield through the use of membrane reactors through the use of both zeolite and carbon membranes [88].

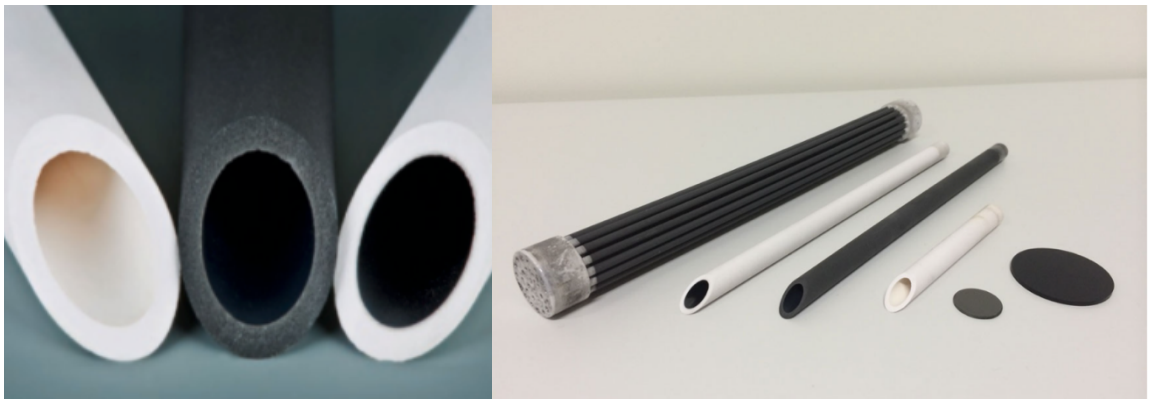

Figure 16. Carbon-based membranes for membrane reactors (left) and Carbon membranes on different ceramic substrates (right), taken from [88].

The Fraunhofer IKTS is working together with MUW Screetec GmbH on a membrane reactor for methanol synthesis from hydrogen and carbon dioxide. The simulation results prove a significant increase in methanol yield [89] (see Figure 17).

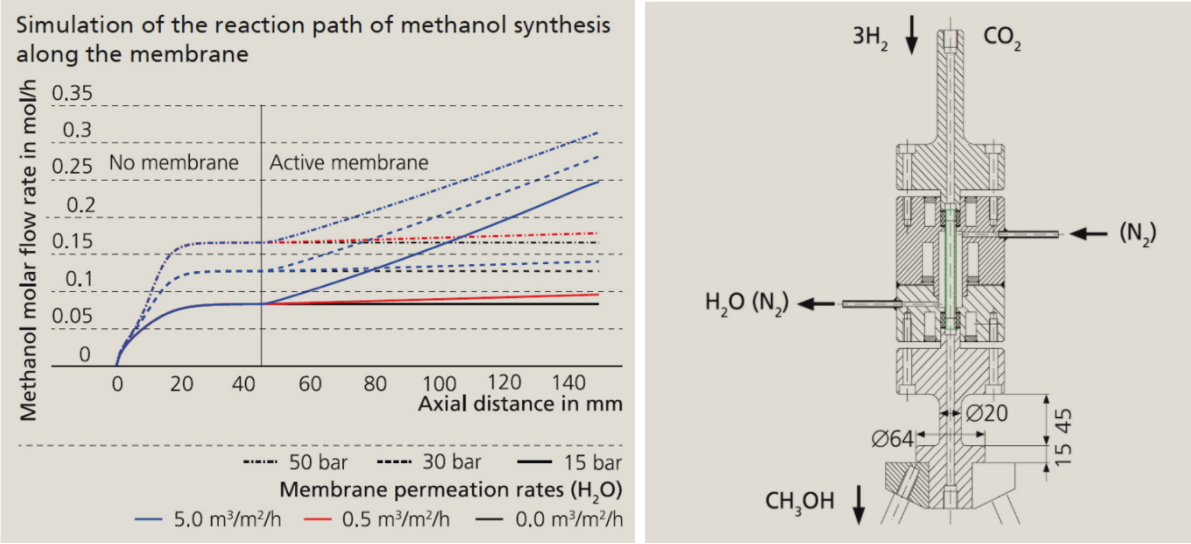

Figure 17. Simulation of the reaction path of methanol synthesis along the membrane reactor length (left) and membrane reactor schema (right), taken from "Increased product yield through the use of membrane reactors" [89].

2.7.2 INORGANIC ZEOLITE MEMBRANES

Zeolite membranes can selectively separate molecules based on their size. These membranes are very interesting due to their well-defined and narrow pore size distribution of the zeolites. Because of this, they can be used as a molecular sieve. These membranes are characterized by their regular pore structure of molecular dimensions. More than 1500 types of zeolite membranes have been synthesised and around 50 can be found in nature [79].

In general, two types of zeolite membranes can be considered: Polymeric zeolite filled membranes and Inorganic zeolite membranes. As discussed before, polymeric membranes are today generally discarded due to their temperature limitation (as Struis et al. [83] observed in their experiment).

Therefore, only inorganic zeolite membranes seem to be interesting for methanol synthesis, since they can stand typical operation conditions. The quality and the mass transport characteristics of the zeolite membranes mainly depend on the zeolite type, synthesis operation conditions and presence of a support [79].

Samawura et al. [90] evaluated the water-methanol-hydrogen separation properties of modernite membrane (a well-known type of zeolite membrane) at temperatures as high as 523K under pressurized conditions. This study showed that a mordenite membrane prepared on the outer surface of porous α-alumina tube supports by the secondary-growth method allowed selective permeation of water at high temperatures as high as 250ºC. On the other hand, methanol removal seems also important for membrane reactor applications, though this modernite membrane allowed water separation only.

Chen et al. [91] explore the use of a silicone rubber/ceramic membrane reactor for the methanol synthesis. First, this reactor was analysed theoretically and in a next step some results were tested and verified with experimental data. This study shows that the conversion of the main reaction with the membrane increased by 22% with respect to traditional fixed bed reactor.

Gorbe et al. [92] investigate the feasibility of using zeolite membrane reactors for CO_2 hydrogeneration to methanol. Promising water-permanent gas separation factors were obtained up to 240ºC suggesting that the use the use of zeolite membrane reactors is a promising technology.

Gallucci et al. [93] propose a zeolite membrane reactor (MR) to investigate the possibility to increase CO_2 conversion into methanol with respect to a traditional catalytic system. The experimental results of this work show that the zeolite membrane reactor gives the highest experimental value: 8.7%, compared to the corresponding value of 2.4% for traditional reactor (TR), and 2.5% of the lithiated Nafion membrane reactor studied by Struis et al. [83].

Van der Ham et al. [94] investigate the hydrogenation of CO_2 for methanol production through zeolite membranes. The result of this study confirm that zeolite membranes can remove the methanol and shift the equilibrium towards methanol. However, they conclude that the process is technically but not yet economically feasible.

In 2019 Leonzio et al. [95] analysed the use of a zeolite membrane reactor permeable to water. The simulation results suggest that at the same operating conditions, 55 bar and 493 K, the equilibrium CO_2 conversion to methanol is equal to 58%. When compared to results obtained with once-through reactor (TR), the higher conversion is due to the removal of water that shifts the reactions towards the products.

Likewise, today the Fraunhofer Institute or ceramic Technologies and Systems IKTS is also studying the increased product yield through the use of zeolite membrane reactors. Process simulations have proved a significant increase in the methanol yield [89]. Unfortunately, the total results and final findings are not public since it is a collaborative project between Fraunhofer Institute and industrial partners.

In this sense, the goal of this thesis is to investigate and evaluate the effects that membrane reactors have on the methanol synthesis. First, an overview on membrane reactors for the production of renewable methanol has been presented.

To the best of our knowledge, there is a lack of research comparing the effects of removing the different products formed in the methanol synthesis (water and methanol). Therefore, this thesis aims to cover this research gap investigating the effects of in-situ water and/or methanol removal via model steady-state simulations. Finally, the performance of membrane reactors with in-situ product removal will be compared to the conventional methanol synthesis based on methanol yield and methanol production rates.

2.7.3 ZEOLITE MEMBRANE PREPARATION

Although the Zeolite Membrane preparation is out of the scope of this thesis, it has been decided to include a brief introduction to offer the reader a basic overview. Without entering this topic in detail, it is worth to mention the following research works.

Zeolite membranes are usually mounted on ceramic porous supports, which mechanically sustain the thin zeolite layer (see Figure 18). Some authors have recently reported zeolite membrane formation on hollow fibers [96] and on PVC supports [97]. An interested reader is invited to read the recent the reviews of Pagis et al. [98], Dragomirova and Wohlrab et al. [99], Daer et al. [100] and Caro et al. [101].

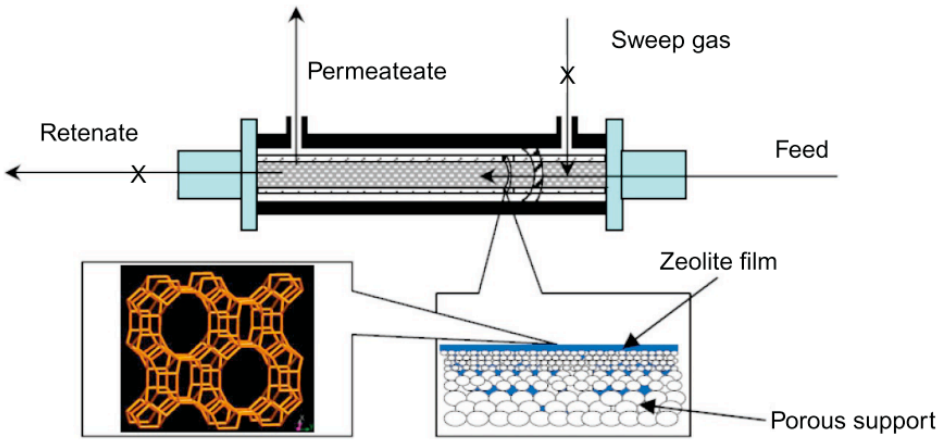

Figure 18. Schematic of a membrane reactor with thin film supported zeolite membrane. Reproduced from Tavolaro, A., Tavolaro, P., 2009.The preparation oftransition metal-containing mordenite catalytic tubular composite membranes. Catal. Commun., 10. https://doi.org/10.1016/j.catcom.2008.10.041 with permission of Elsevier. Taken from [79].

Zeolite membranes can be produced via three different approached [79]:

a) Deposition or embedding of preformed crystals on a substrate.
b) Hydrothermal synthesis (in situ synthesis).
c) Deposition of seeds and hydrothermal synthesis (secondary growth).

For membranes to be used in membrane reactors, the methods (b) and (c) are generally used for preparing the membrane. The hydrothermal synthesis is mainly used for the preparation of zeolite MFI, ferrite, and zeolite A composite membranes on porous supports [102].

To improve the performance of the membrane, the membrane layer can be produced via the so called multi in situ crystallization (MISDC) method. This method is based on forming films growing in subsequent hydrothermal steps. The membranes that are produced by this methodology are usually top performance defect-free membranes [103].

During the last decades other methods used for zeolite membrane preparation have been developed as for example vapor deposition and microwave-assisted deposition. The method reported by Kim et al. [104] based on a one step production process for zeolite membranes containing metal nanoparticles seems particularly interesting. This methodology allows the production of membranes, where both separation and high surface area are used for enhancing the conversion of chemicals.

An interested reader is referred to read the review on this topic presented by Gallucci et al. [79].

Chapter 3. METHODOLOGY

This chapter discusses the methodology used to evaluate and simulate the performance and potential of membrane reactors for renewable methanol production. First, the simulation methodology and the most important key performance indicators (KPIs) are presented. Thereafter, both conventional and membrane models are explained in detail. Finally, the model implementation and the validation process are clarified.

A representation of the methodology process followed to answer the research questions of the thesis is presented bellow (see Figure 19).

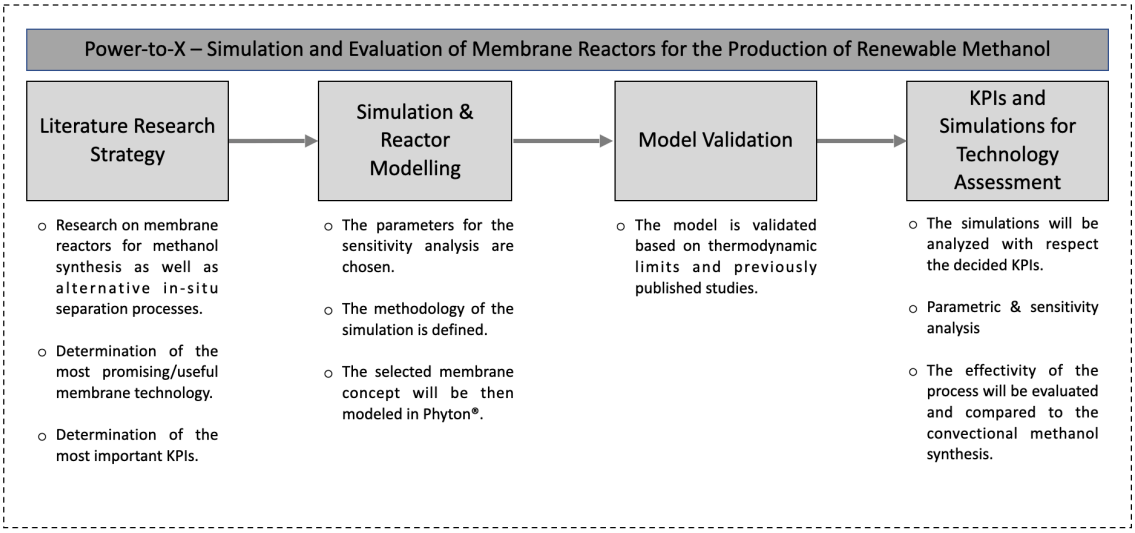

Figure 19. Representation of the methodology process for this thesis (own creation).

3.1 RESEARCH STRATEGY

During the first phase of the project a good body of literature was analyzed. One of the research objectives of this thesis is to identify the most important membrane types for renewable methanol production.

This information is presented in the State of the Art. To do this literature research, the following research strategy was implemented (see Figure 20).

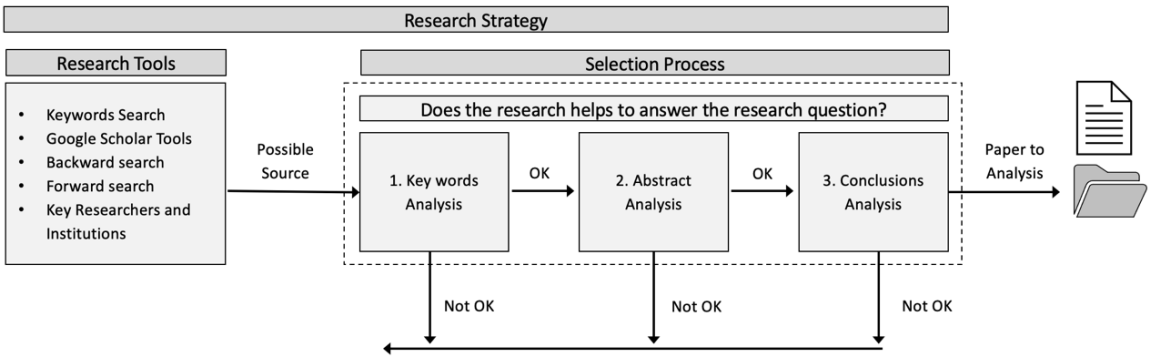

Figure 20. Research strategy and literature gathering method (own creation).

3.1.1 RESEARCH TOOLS

3.1.1.1 Iterative Search Using Key Words

The first step to start literature research is to define a list of key words. To do this, the topic was first broken into chanks and subtopics. The initial list of key words is provided in Table 3.

Table 3. Key words used in the research strategy

Key words
Methanol synthesis, membrane reactors, yield improvement, renewable methanol, Power-to-X

With these key words, the first research works appeared. In particular, the research work of Galluci et al. [79] provided a really good first overview of the topic and information about the two most promising membrane types for methanol production, carbon and zeolite membranes.

The papers given by Technical University of Munich were also analyzed. Once the most promising membrane types were known, a specific search for research works in zeolite and carbon membranes for renewable methanol production was started. For this search a second key words list was defined (see Table 4).

Table 4. Keywords list used in the research strategy

Key words
Methanol synthesis, zeolite membranes, carbon membranes, process improvements, circumvent of thermodynamic limit, in-situ product removal

This second list started to give insights on carbon and zeolite membrane reactors. The most relevant research works are presented in the State of the Art.

3.1.1.2 Utilization of Google Scholar Tools

Google Scholar offer users good tools to find literature. For example, Google scholar pulls up additional scholarly resources related to the search results that you selected before. This tool was also used to explore new related literature.

Moreover, Research Gate, Scopus, and Elsevier offer the users the possibility to set up alarms to stay up to date in the areas of interest.

3.1.1.3 Backwards Search

The citations of the articles yielded from the key words search were further examined. This method is also commonly known as “chain searching”. The goal of this tool is dual: (1) to

learn about the development of knowledge on the topic and (2) understand how the authors approached their research questions and the considered assumptions.

A second-level or second-generation backward reference search was also implemented. This is when a researcher examines the sources cited by the references used in an initial article.

The Backwards Search provides a good body of papers for the selection step.

3.1.1.4 Forward Search

Additional articles that have cited the reviewed literature were also selected as possible sources. Google Scholar shows papers that are related to the article you just read. This tool was also used to try to come up with other papers with focus on membrane reactors.

3.1.1.5 Key Researchers and Institutions

During the literature gathering process, key researchers, and institutions with publications in membrane reactors for methanol production were identified. This information was used to do specific research on these authors and institutions to come up with valuable literature.

The research of Prof. Fausto Gallucci from Eindohven University of Technology seems particularly interesting. Prof. Galluci investigates the development of membranes and novel multiphase reactors, in particular membrane reactors and dynamically operated reactors at the Inorganic Membranes and Membrane Reactors (SIR) research group. Particularly interesting application areas are methanol production in zeolite and carbon membranes, methane activation with oxygen selective membranes, the Fischer-Tropsch reaction in carbon based membrane reactors, and hydrogen production by reforming/dehydrogenation reactions with hydrogen selective membranes [105].

The Fraunhofer Institute is also investigating the increased product yield using membrane reactors. Dr.rer.nat. Adrian Simon is in charge of the Zeolite-and Carbon Membranes research Group within the Fraunhofer Institute for Ceramic technologies and Systems (IKTS). In their research, they develop membranes with properties for different kinds of membrane reactors. Moreover, together with MUW Screentec GmbH they are working on a

membrane reactor for methanol synthesis from hydrogen and carbon dioxide. Process simulations have already proved a significant increase in methanol yield (See Figure 17) [89]

Dr.rer.nat. Adrian Simon was contacted for further information about their project. However, this project is still confidential, and he could not provide more information about it. Nevertheless, he put us in contact with Dr.-Ing. Jörg Richter and Dr.rer.nat. Benjamin Jäger. Since that moment, both Dr.-Ing. Jörg Richter and Dr.rer.nat. Benjamin Jäger has supported this research project by answering technical questions, giving advice, and providing non-confidential information about membranes and membrane reactors.

The Laboratory for Advance Analytical Technologies, the Department of Chemistry from University of Zurich and the department of Chemical Engineering from Norwegian University of Science and Technology (NTNU) have recently demonstrated how one may simulate the simplified operation of a catalytic reactor using basic thermodynamic data, a kinetic model for the multi-steps reactions, and numerical solutions of reactor-specific differential equations describing the evolution from reactant to product chemical species [75].

The authors were also contacted to resolve questions about the modelling process.

3.1.2 SELECTION PROCESS

The second step for the research strategy is to select valuable information. For a research work is always crucial to come up with a good number of papers that shed light on the research questions. Therefore, it is important to be effective in the source evaluation.

This section briefly explains the decision-making process developed to evaluate if a source was valuable or not for this research. First, the key words and title were compared to the lists presented in Table 3 and Table 4. Then, the abstract was read and analyzed to identify the research questions, methodology and conclusions. Finally, the conclusions were analyzed to verify if their results could be useful for this work.

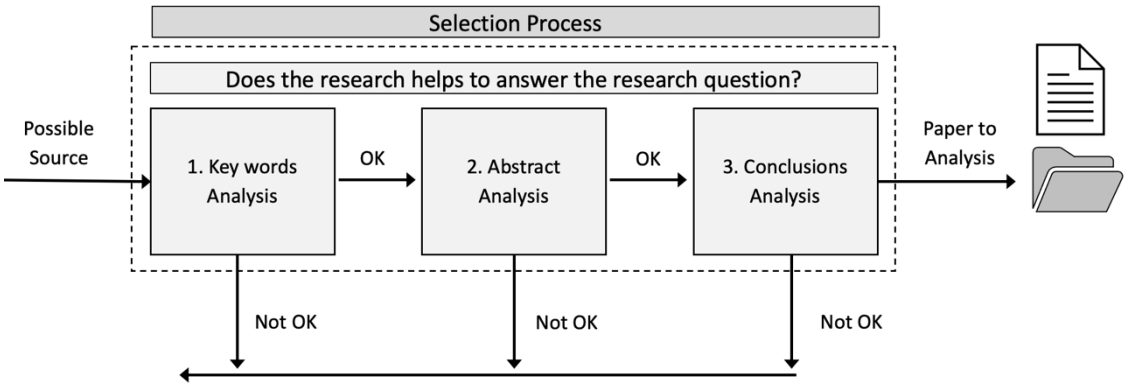

Figure 21. Selection process framework (own creation).

3.1.2.1 Key Words Analysis

The first step to assess the relevance of a research work is to analyze the key words and the title. The key words of the articles were compared to the lists presented in Table 3 and Table 4 to perform a quick first evaluation.

If two or more keywords matched the presented lists, the article was selected for the next step. Note that this first filter is especially useful for the literature that come from backward and forward search, since the literature yielded from keywords research was obviously matching some of the words. Moreover, it should be noted that synonyms of these words

were also considered (e.g. methanol production instead of methanol synthesis, among others).

3.1.2.2 Abstract Analysis

The next step to continue with the value assessment of literature is to conduct a critical analysis of the abstract. This can be seen as a second filter of the decision-making process. To evaluate if a research article is interesting for the research, the abstract need to be analyzed based on the research objectives and results. If the authors aimed to evaluate or investigate membrane reactors for methanol production, the article was sent to the next step.

3.1.2.3 Conclusions and Results Analysis

If the Abstract seems to be aligned with the research objectives of the thesis, the conclusions and results were further examined. The goal of this step is to evaluate if the conclusions of the papers give valuable information to answer the research questions of this thesis. In this sense, finally the papers offering information about membrane types and the effects of membrane reactors for methanol production were analyzed more in detail.

The output of this part of the thesis is presented in the State of the Art.

3.2 SIMULATION METHODOLOGY

The kinetic analysis was performed based on a plug flow reactor (PFR) developed in Python®. Equilibrium compositions for the outlet streams were calculated by numerically solving the PFR differential equations using the Graaf kinetic model [57,70]. The model was then modified to simulate the effects of in-situ water and/or methanol removal. Both membrane and conventional reactor model are explained more in detail in the following section.

For this thesis, the following two scenarios were considered: (1) conventional CO2 hydrogenation to methanol process and (2) CO2 hydrogenation to methanol with in-situ water and/or methanol removal. The effects of the following methanol synthesis reactor operation conditions were analyzed for both investigated scenarios: temperature ($180-340ºC$), pressure ($20, 40, 60\ bar$), H_2/CO_2 molar ratio (1,2,3,4) and permeation parameters λ_k $(0, 0.4, 0.8, 1.2, 1.6, 2)$. The examined operation conditions used for the parameter study are given in Table 5.

The parametric analysis examined the influence of the above parameters on methanol yield and methanol production. Methanol yield can be defined as the number of CH_3OH moles produced (N_{CH3OH}^{out}) divided by the number of moles of CO_2 in the feed stream of the reactor (N_{CO2}^{in}).

$$MeOH\ yield = \frac{N_{CH3OH}^{out}}{N_{CO2}^{in}} \cdot 100\ [\%]$$

Similarly, methanol production is defined as the number of moles of CH_3OH produced at the reactor outlet for a given temperature, pressure, and H_2/CO_2 molar ratio.

Table 5. Reactor operation conditions to be examined in the simulation sensitivity analysis.

Reactor Operation Conditions	Values
Temperature	180-340 ºC
Pressure	20,40,60 bar
H2/CO2 molar ratio	1,2,3,4
$\boldsymbol{\lambda_k}$	0, 0.4, 0.8, 1.2, 1.6, 2 m^{-1}

3.3 REACTOR MODELLING

Catalytic reactor design is a complex task involving the coupled phenomena of chemical thermodynamics, multi-step chemical reactions, hydrodynamic flow and generation, as well as conduction and dissipation of heat. Normally, software packages like Aspen Plus® and Aspen Hysys® are used to aid the reactor designer. However, to our knowledge none of this software packages have an integrated operational reactor with membrane technology.

Because of this, in this work a simplified model of a catalytic reactor needs to be developed. This has been done using a kinetic model for the multi-step reactions and numerical solutions of reactor-specific differential equations that describe the evolution of the product chemical species trough the reactor length. To do this, it was decided to follow the approach suggested by Patterson et al. [75] and to develop the reactor model in Pyhton®.

To simplify the model and the discussion, constant and uniform reaction temperature and pressure are assumed, and issues of heat flow are neglected. Furthermore, it is assumed that all reactant and products behave as ideal gases. These assumptions are in line with the model proposed by Prof. Hillestad and Prof. Patterson in their research work "A Simplified Simulation of Catalytic Reactors for CO2 Reduction" [75]. All assumptions are detailed in the next section. The simulation procedure is shown in Figure 22.

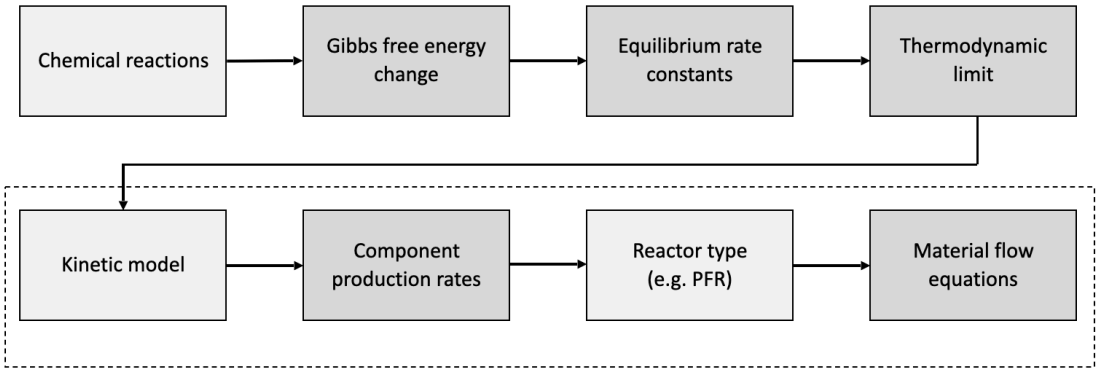

Figure 22. Schematic diagram illustrating the catalytic reactor simulation procedure. Light grey boxes indicate the external input of information. Dotted box represents the focus of the model, since the boxes above are given by the chosen kinetic model. Adapted from "A simplified simulation of catalytic reactors for CO_2 reduction" [75].

Dynamic reactor simulation requires knowledge of the concentration-, T-, and P-dependent production rates for every chemical component involved. This information is usually found in published kinetic models, which depends on the catalyst used. Then, the reactor designer should choose the type of reactor to be implemented. For this thesis, it has been decided to define a Plug Flow Reactor based on the Graaf kinetic model, because of simplicity. Moreover, this type of reactor (PFR) captures the fixed bed reactors that are typically applied in industry. Thereafter, once the reactor type has been defined, the corresponding differential equations describing the chemical component flows were set up in the model.

These equations need to be numerically solved to yield the position-dependent concentration of each chemical component afterwards. These steps are explained more in detail in section 3.3.5. Model Implementation.

3.3.1 KINETIC MODEL

In real chemical reactors, a catalyst is commonly used to selectively accelerate the desired reaction. However, it should be noted that the presence of a catalyst cannot by it itself increase the reaction yield beyond the thermodynamic limit but only increase the rate at which the reaction takes place [106].

As explained before in the State of the Art, the kinetics of methanol have been studied by several authors. In this work, it has been decided to use the model of Graaf et al. [57,70] who modeled the reduction of CO_2 to methanol over a $Cu/ZnO/Al_2O_3$ catalyst.

According to the Graaf Model, the following rate expressions should be considered for the methanol synthesis [57].

$$r_1 = k_1 \cdot K_{CO} \cdot \left(p_{CO} \cdot p_{H2}^{\frac{3}{2}} - \frac{p_{CH3OH}}{P_{H2}^{\frac{1}{2}} \cdot K_1^{eq}} \right) / denom$$

$$r_2 = k_2 \cdot K_{CO2} \cdot \left(p_{CO2} \cdot p_{H2} - \frac{p_{H2O} \cdot p_{CO}}{K_2^{eq}} \right) / denom$$

$$r_3 = k_3 \cdot K_{CO2} \cdot \left(p_{CO2} \cdot p_{H2}^{\frac{3}{2}} - \frac{p_{CH3OH} \cdot p_{H2O}}{P_{H2}^{\frac{3}{2}} \cdot K_3^{eq}} \right) / denom$$

$$denom = (1 + K_{CO} \cdot p_{CO} + K_{CO2} \cdot p_{CO2}) * \left[p_{H2}^{\frac{1}{2}} + \left(\frac{K_{H2O}}{K_{H2}^{\frac{1}{2}}} \right) \cdot P_{H2O} \right]$$

In these equations the production rate for every chemical species can be seen as a 5-component vector.

$$R = \left(R_{CO}, R_{CO2}, R_{H2}, R_{H2O}, R_{CH3OH}\right) = (-r_1 + r_2, -r_2 - r_3, -2r_1 - r_2 - 3r_3, r_2 + r_3, r_1 + r_3)$$

It should be noted that in the Graaf model, component fugacities are used instead of the partial pressures. However, as for this work it is assumed ideal gas behavior for all the species, fugacities can be substituted by partial pressures. This assumption is explained more in detail in the section 3.3.2 Assumptions and Methods.

The kinetic factors in the equations presented above can also be written in Arrhenius form (see Table 6). The Arrhenius formula was first proposed by Svante Arrhenius in 1889 and relate the reaction rates with the temperature [107].

$$K_n(T) = a_n \cdot e^{\left(\frac{b_n}{R \cdot T}\right)}$$

The values proposed by Graaf et al. for the Arrhenius parameters are presented in Table 6.

Table 6. Arrhenius parameters for the Graaf kinetic model [57,70] temperature-dependent factors. Taken from "A simplified simulation of catalytic reactors for CO2 reduction" [75].

Variable	a	b $[\frac{J}{mol}]$
K_1^{eq}	2.39×10^{-13}	9.84×10^{4}
K_2^{eq}	1.07×10^{2}	-3.91×10^{4}
K_3^{eq}	2.56×10^{-11}	5.87×10^{4}
K_1	$4.89 \times 10^{7} [\frac{mol}{kg*s}]$	-1.13×10^{5}
K_2	$9.64 \times 10^{11} [\frac{mol}{kg*s}]$	-1.53×10^{5}
K_3	$1.09 \times 10^{5} [\frac{mol}{kg*s}]$	-0.875×10^{5}
K_{Co}	2.16×10^{-5}	0.468×10^{5}
K_{CO2}	7.05×10^{-7}	0.617×10^{5}
$K_{H2O}/K_{H2}^{1/2}$	6.37×10^{-9}	0.840×10^{5}

3.3.2 ASSUMPTIONS AND METHODS

As stated before, some assumptions have been considered to simplify the discussion and the model. All these assumptions are in line with previous research works and the model approach proposed by Terrani et al [75].

It is assumed that all the reactant and product species behave as ideal gases. According to the Gibbs-Dalton law, which states that as the pressure of a real gas approaches zero (meaning that the real gas becomes "perfect" or "ideal"), the fugacity of each component in the mixture approaches its partial pressures [108,109]. The gas at the typical temperature for methanol synthesis is not far from being ideal. Because of this, fugacities and partial pressures are not very different and can be substituted in the kinetic model to simplify the calculations.

The Graaf kinetic model was chosen since it is one of the most used in academia and industry. Temperature and pressure are assumed to be constant and uniform along the reactor tubes as it assumed in their model by Terrani et al. [75]. This assumption is discussed more in detail in Chapter 5.

The kinetic rate factors were obtained from published models based on experimental data [57,70]. The numerical computations for solving the differential equations describing the position-dependent component flows were performed using Phyton® and function package Odeint. A detailed explanation of the code and function is presented in section 3.3.5 Model Implementation.

3.3.3 PLUG FLOW REACTOR

The plug flow reactor model (PFR, also known sometimes as continuous tubular reactor, CTR) is normally the name given to a model used in chemical engineering to describe chemical reactions in continuous, flowing systems of cylindrical geometry [110].

In a one-dimensional Plug Flow Reactor model, axial diffusion effects are neglected. Moreover, this type of reactor assumes that reactants and products flow with a constant mass flow through one or more parallel tubes filled with loosely packed catalyst [75,111].

Therefore, the fluid going through a plug flow reactor is modelled as it flows as a series of infinitely thin coherent "plugs", each of them having a uniform composition. These plugs travel through the axial direction of the reactor and change its composition at every longitude differential. The key assumption here is that the fluid is considered to be perfectly mixed in the radial direction but not mixed in the axial direction, meaning that every plug can be considered as a separate entity [110].

A stationary steady state flow is assumed for the simulations. The stationary PFR is governed by the ordinary equations presented in Figure 23. Then, the solutions of these equations can then be calculated providing appropriate boundary conditions. The material balance of every species along the reactor axial length is given by:

$$[Accumulation] = [in] - [out] + [generation] - [consumption]$$

It should be noted that accumulation is 0 under steady state. Hence, the mass balance can be re-written as follows:

$$F_i(x) - F_i(x + dx) + A_t dx \alpha_i r_i = 0$$

where,

- x is the reactor tube axial position $[m]$
- dx is the differential thickness of the plug/section
- the index "i" refers to the species "i"
- $F_i(x)$ is the molar flow rate of species "i" at the position x $[mol/s]$
- A_t is the tube transverse cross sectional area $[m^2]$
- α_i is the stoichiometric coefficient
- r_i is the reaction rate for the specie "i" $[{}^{mol}/_{m^3 s}]$

Graaf et al. also assumed that the fixed bed reactor behaves as a plug flow reactor in his research [70]. The working principle is detailed in Figure 23.

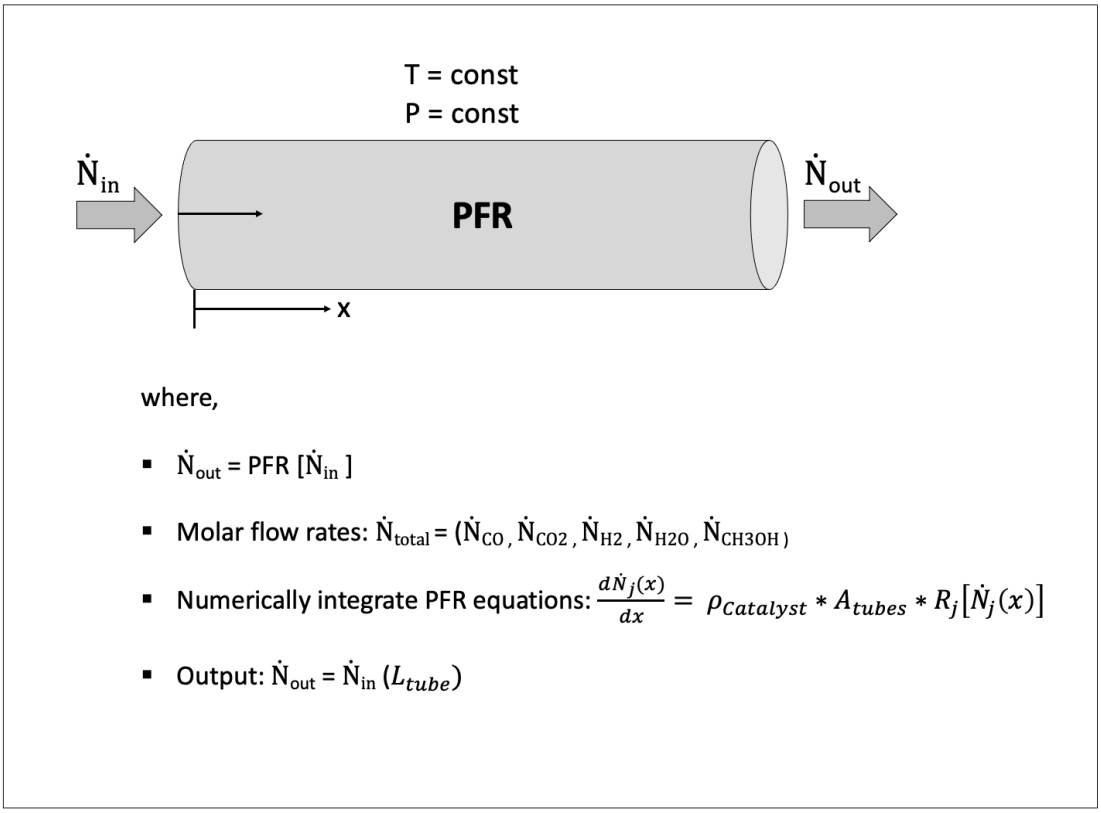

Figure 23. Computational scheme for a plug flow reactor (PFR). Definition of the PFR function and differential equations, which relates the input and output component molar flow rates. Adapted from "A simplified simulation of catalytic reactors for CO_2 reduction" [75].

The vector Ṅ refers to the x position-dependent molar flow rates (mol/s) of the components carbon monoxide (CO), carbon dioxide (CO_2), hydrogen (H_2), water (H_2O) and methanol (CH_3OH). The kinetic ratio constants are derived from the Graaf model $R_j[\dot{N}_j(x)]$, which are also x position-dependent, since they depend on the partial pressure and thus, on the number of moles of each component. As the gases proceed along the reactor tubes, the initial reactants CO_2 and H_2 are converted to the product species CO, H_2O and CH_3OH.

3.3.4 MEMBRANE MODELLING

As stated before, to circumvent the thermodynamic limitation that reduces the yield of conventional systems, two possible routes can be used: (i) smart recycling of the unconverted gases and (ii) in situ product removal of the products of the reaction [79].

In this thesis, the second route is explored via membrane reactors. In-situ product removal can be achieved by separation of both methanol and water or by separation of only one of the components (i.e. either water or methanol). By removing only water, it is possible to achieve higher methanol production (as the Le Chaterlier´s effect on equilibrium reactions is higher). Furthermore, by doing this, the deactivation of the catalyst and unwanted methanol reforming reactions can simultaneously be prevented simultaneously (since water accelerates the crystallization of Cu and ZnO contained in a Cu/ZnO-based catalyst) [112].

To simulate this behavior, one can include a permeation/separation factor to the model presented in Figure 24. The idea of this design is that the product (both water and methanol, or either water or methanol independently) is constantly removed from the gas stream by a suitable membrane (in reality it could be a zeolite or carbon membrane) and consequently, shift the equilibrium towards the product side [113].

It is possible to model such a reactor simply by introducing a second parallel channel ("Membrane channel") and a permeation/separation parameter in the PFR equations (λ_k). This term simply gives a weight to the permeation/removal capacity, meaning that a higher value of λ_k implies a greater product removal trough the membrane. The units of the term

λ_k should be given in m^{-1}, so the new modification has also units as the reactor model without the membrane (i.e. $\frac{mol}{m \cdot s}$).

The symbol $\delta_{j,k}$ ist the "Kronecker delta". This term is one for methanol and water and zero for the rest of the components. In other words, it is simply used to express the modified PFR equations in a matrix form.

The kinetic model and methodology are the same as for the reactor model without membrane. The implementation of both models is explained in detail in Model Implementation. The model scripts can also be founded in Appendix A and Appendix B.

The vector $\dot{N}^1$ refers to the x position-dependent molar flow rates (mol/s) of the components carbon monoxide (CO), carbon dioxide (CO_2), hydrogen (H_2), water (H_2O) and methanol (CH_3OH) through the PFR. Similarly, the vector $\dot{N}^2$ refers to the x position-dependent molar flow rates (mol/s) of the components water (H_2O) and methanol (CH_3OH) through the membrane channel, in other words, the amount of water and/or methanol that is removed by the membrane.

The initial conditions in the membrane channel imply zero molar flow in the beginning of the channel. As the gases proceed along the reactor tubes, the initial reactants CO_2 and H_2 are converted to the product species CO, H_2O and CH_3OH within the PFR. Then part of the water and/or methanol is in-situ removed by the membrane, achieving higher methanol yield and production rates. The working principle of such a reactor is detailed in Figure 24.

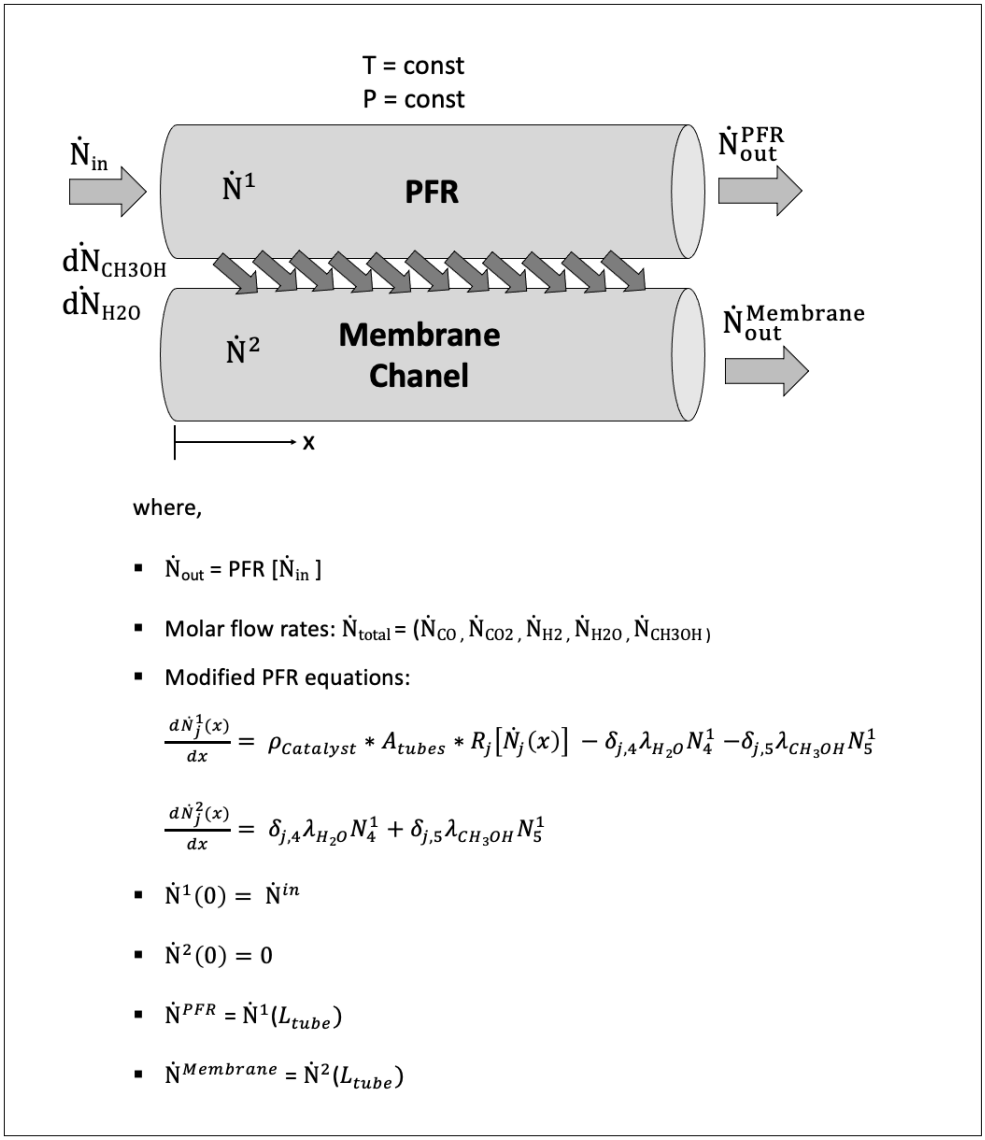

where,

- $\dot{N}_{out}$ = PFR [$\dot{N}_{in}$]
- Molar flow rates: $\dot{N}_{total}$ = ($\dot{N}_{CO}$, $\dot{N}_{CO2}$, $\dot{N}_{H2}$, $\dot{N}_{H2O}$, $\dot{N}_{CH3OH}$)
- Modified PFR equations:

$$\frac{d\dot{N}_j^1(x)}{dx} = \rho_{Catalyst} * A_{tubes} * R_j\left[\dot{N}_j(x)\right] - \delta_{j,4}\lambda_{H_2O}N_4^1 - \delta_{j,5}\lambda_{CH_3OH}N_5^1$$

$$\frac{d\dot{N}_j^2(x)}{dx} = \delta_{j,4}\lambda_{H_2O}N_4^1 + \delta_{j,5}\lambda_{CH_3OH}N_5^1$$

- $\dot{N}^1(0) = \dot{N}^{in}$
- $\dot{N}^2(0) = 0$
- $\dot{N}^{PFR} = \dot{N}^1(L_{tube})$
- $\dot{N}^{Membrane} = \dot{N}^2(L_{tube})$

Figure 24. Computational scheme of the membrane plug flow reactor. Note the presence of a parallel channel representing the "membrane". Through this channel only methanol and water can selectively flow. The symbol $\delta_{j,k}$ is the "Kronecker delta". Definition of the PFR function and differential equations, which relates the input and output component molar flow rates. Adapted from "A simplified simulation of catalytic reactors for CO_2 reduction" [75].

3.3.5 MODEL IMPLEMENTATION

The reactor has been modelled in Python® [114]. The function odeint from the Scipy.integrate package has been used to integrate and solve the PFR differential equations. This function requires three inputs [115]:

$$y = odeint(model, y0, x)$$

1. **Model:** Function name that returns derivative values at requested y and t values as $dydt = model(y, t)$. For this case, the model contains the kinetic rate calculations and PFR differential equations.
2. **y0** = initial conditions of the differential states. For this model the initial conditions are the number of moles of each component in the beginning of the reactor. In other words, the molar flow input.
3. **x**: length points at which the solution should be reported. The x value should be a linspace vector. Additional internal points are often calculated to maintain accuracy of the solution but are not reported.

Odeint numerically solves the differential equations at each given x-position point. More information about the method and function can be read in the scipy.integrate.odeint manual [116].

First, the needed packages are imported. Some important packages for this model are numpy, matplotlib, scipy.integrate, pandas, and seaborn (this last one for the results visualization). Then, the reactor specification parameter values used in the simulation of methanol synthesis are introduced. These values are presented in Table 7.

Thereafter, the model dy is defined. Here the kinetic rates are estimated based on partial pressures for every x-position iterative solution. Furthermore, this model also contains the differential equations to be solved. Once the kinetic ratios are calculated, odeint numerically solves the PFR differential equations and returns the solutions for the next dx.

These solutions are sent to the model, so the solver can use these values to numerically solve the differential equations for the next dx. In other words, the function odeint interactively calls the model and returns the solution for every given dx.

This process is calculated for different temperatures and pressure ranges, so the effect of these two parameters can also be analyzed. The solution is saved in a pandas data frame. Finally, all these solutions are visualized in different manners so better conclusions can be extracted from the model.

Table 7. Plug flow reactor parameter values used in the present simulation of methanol synthesis. Note that the values λk are only used in the membrane reactor simulation and not for the conventional methanol synthesis.

Parameter	Value
Catalyst	$Cu/ZnO/Al_2O_3$
Catalyst density $\rho_{catalyst}$	$1000\ kg/m^3$
Number of parallel tubes $\boldsymbol{n_{tubes}}$	10,000
Tube diameter $\boldsymbol{d}$	$2\ cm$
Tube area $\boldsymbol{A_{tube} = n_{tube}\pi(d^2/4)}$	$3.14\ m^2$
Tube length $\boldsymbol{L_{tube}}$	$3\ m$
H_2/CO_2 molar ratio	1,2,3,4
Temperature range $\boldsymbol{T}$	$180 - 340\ ºC$
Pressures $\boldsymbol{P}$	$20, 40, 60\ bar$
$\boldsymbol{\lambda_k}$	0, 0.4, 0.8, 1.2, 1.6, 2

For the membrane model, one need to include in the model an extra parameter in the model, the so-called permeation/removal parameter (λ_k). In this thesis, the effects of the removal of water and/or methanol are explored.

As stated before, this term simply gives a weight to the separation capacity, meaning that a higher value of λ_k implies a greater removal trough the membrane. The units of the term λ_k should be given in m^{-1}, so the new equation has also units as the reactor model without the membrane (i.e. $\frac{mol}{m \cdot s}$).

Simulations for different λ_k values are conducted in this thesis. In this sense, it has been decided to try the following values ($\lambda_k = [0, 0.4, 0.8, 1.2, 1.6, 2]$). This range was chosen based on previous try and error simulations to confirm the percentage of product removal for different λ_k values. In this model, a λ_k value of 2 m^{-1} represent around 80-90% of product removal and λ_k value of 0.4 m^{-1} a 50% of product removal. Similarly, a λ_k value of 0 m^{-1} refers to the conventional reactor (i.e. no in-situ product removal through the membrane). These parameters should be included in the differential equations as explained in Figure 24 and in section 3.3.4 Membrane Modelling.

The PFR model script is reported in Appendix A and the membrane reactor in Appendix B. The code itself and its explanatory notes explain the rest of the implementation. The visualization possibilities based on simulation data are presented in Appendix C.

3.4 MODEL VALIDATION

In this section, the validation methodology for the model is presented. First, the reactor model is compared to equilibrium curves to assure its validity. To do this, the error is checked with respect the thermodynamic limit and equilibrium values.

The membrane model cannot be compared to the equilibrium curves, since the goal of the membrane is to circumvent the thermodynamic limitation, and thus, the results will be higher and not comparable. To validate the membrane model, the results are compared to Prof. Patterson and Prof. Hillestad's published results [75].

In the end, the results of both membrane and convectional plug flow reactor were compared to previously published studies to confirm their validity.

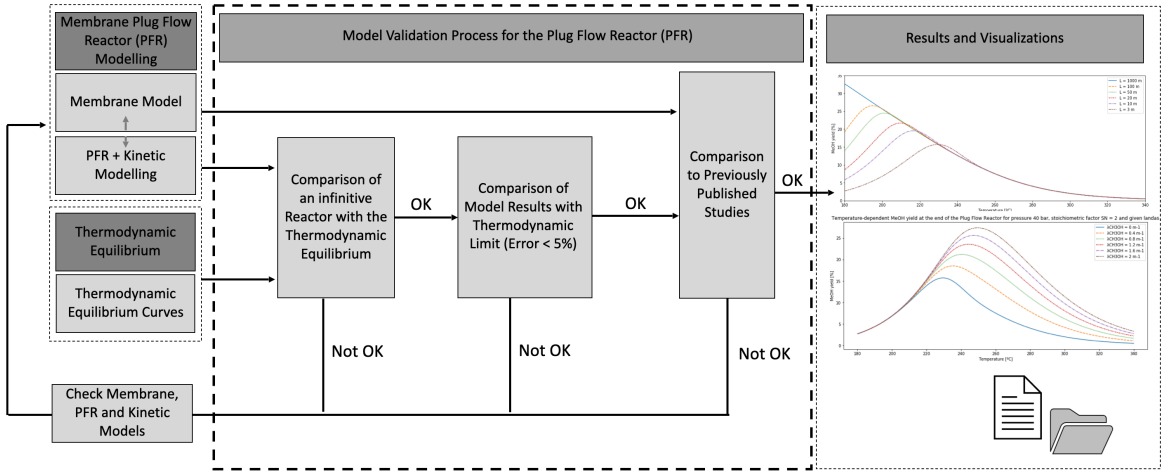

Figure 25. Model validation process (own creation).

3.4.1 COMPARISON OF THE THERMODYNAMIC EQUILIBRIUM WITH THE REACTOR RESULTS ASSUMING INFINITIVE TUBES LENGTH

A simple way to validate the kinetic model implementation is to extend the length (to impractical sizes) of the reactor tubes and estimate the methanol yield of such a reactor. By doing this, one should approach the thermodynamic limit if the kinetic model is well implemented [75]. This principle is shown in Figure 26, where the length of the reactor is assumed to increase from 3 m to 100 m.

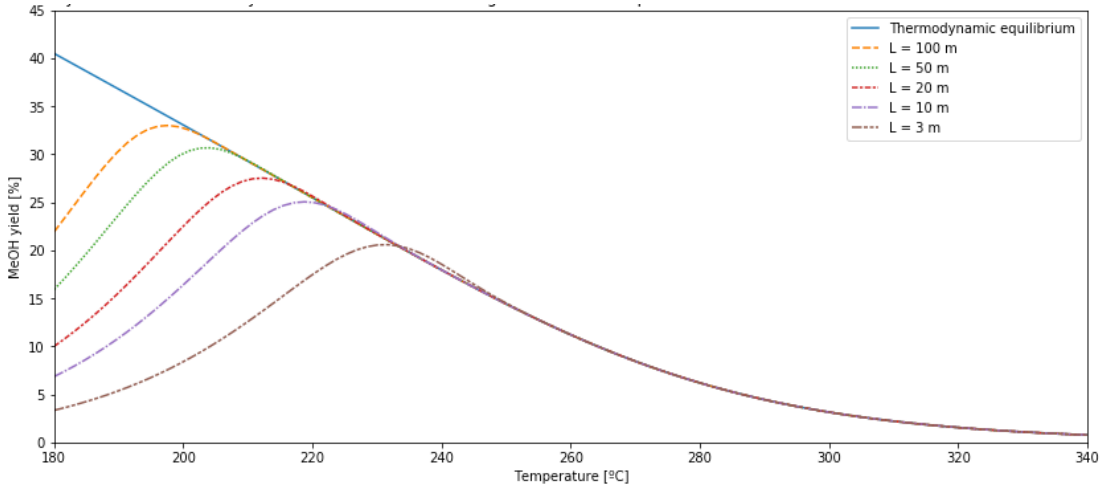

Figure 26. Demonstration that extending the tube length of a plug flow reactor leads the molar conversion of CO_2 to methanol to approach the limit given by equilibrium thermodynamics. Simulation done for 60 bar and SN = 2.

Similarly, one should compare the thermodynamic limit with the temperature-dependent molar conversion of CO_2 to methanol in a reactor with "infinitive" tubes (e.g. $L = 1000\ m$) for the given pressures $20, 40\ and\ 60\ bar$.

As it can be seen in Figure 26, the results obtained from this simulation are in good agreement with the thermodynamic equilibrium, meaning that the kinetic model is well implemented.

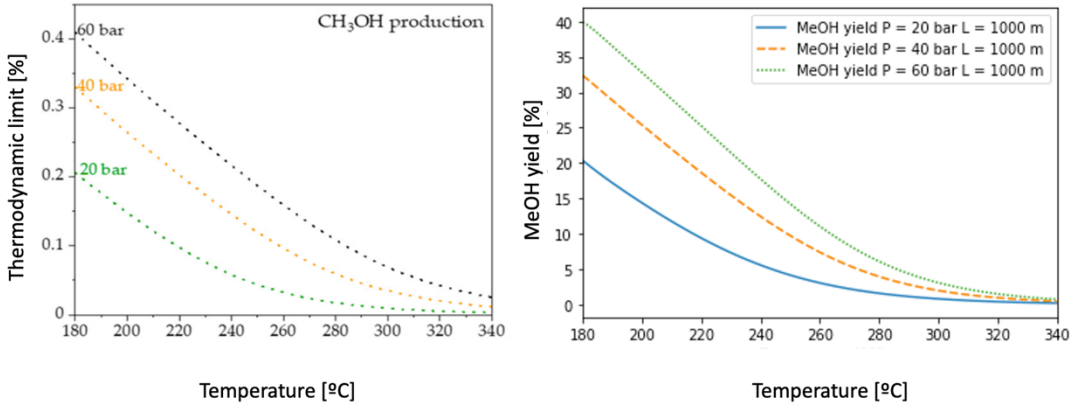

Figure 27. Comparison between the equilibrium molar conversion for the reduction of CO_2 to methanol with the molar conversion obtained with the PFR assuming "infinitive" length tubes. Thermodynamic limit taken from Patterson et al. [75] calculations (left), own simulation of the PFR assuming "infinitive" length tubes (right).

However, the predicted behavior of the conversion rate should not exceed the equilibrium value (blue line in Figure 26). A slight overshoot of the kinetic data can be seen in Figure 26 for the reactor length $L = 3\ m$ (real length of the reactor).

This error is also presented in the work of Patterson et al. [75]. The authors attribute this slight overshoot of the kinetic data to slight inconsistencies in the parameter values of Graaf et al [57,70]. Despite this, it was decided to estimate the maximum absolute error before proceeding to the next step, and in this way assess the impact of this error (see Table 8).

The maximum difference can be estimated by subtracting the methanol yield obtained in the PFR from the estimated thermodynamic equilibrium. To do this, one can simply subtract both data frames and obtain the temperature point at which the difference is the highest.

To quantify and size this error, it was decided to apply the maximum absolute error. This error can be estimated as follows:

$$\max\left(e_{absolute}\right) = \left|MeOH_{yield}^{PFR\ (L=3m)} - Estimated\ Thermodynamic\ Equilibrium\right|$$

The results of this calculation are presented in Table 8. The error has been estimated for pressures $20,40,60\ bar$, H_2/CO_2 ratios of 1,2,3,4 and given reactor parameters (see Table 5). The error is demonstrated to be higher for low pressures (20 bar) and high H_2/CO_2 ratios. The maximum absolute error founded is 1.805%, so it was decided to disregard this effect and attribute this slight overshot to inconsistencies in the Arrhenius parameters for the temperature-dependent factors in the Graaf model. Thus, results for low pressures ($20\ bar$) may be less trustful than results for high pressures ($60\ bar$). One could have explored different kinetic models and use the one with lowest error. However, it was decided to assume this error due to time constraints and leave this aspect out of the scope of the thesis.

Table 8. Maximal absolute error between the obtained MeOH yield and the estimated thermodynamic equilibrium.

H_2/CO_2	P [bar]	T [ºC]	MeOH yield [%]	Limit [%]	Max error [%]
1	20	223.63	3.738	2.451	1.287
1	40	228.48	6.179	5.146	1.033
1	60	231.71	7.899	7.089	0.809
2	20	230.10	6.431	4.837	1.593
2	40	233.33	10.993	9.959	1.044
2	60	236.57	14.036	13.312	0.723
3	20	233.30	8.459	6.727	1.732
3	40	236.50	14.475	13.471	1.003
3	60	238.18	19.049	18.424	0.624
4	20	236.56	9.857	8.052	**1.805**
4	40	238.18	17.438	16.497	0.942
4	60	239.79	22.909	22.374	0.534

3.4.2 COMPARISON WITH OTHER RESEARCH WORKS

To finally assess the validity of the model, the results were compared to other published studies. Especially the research work of Patterson et al. [75] offers a good comparison, since the model developed in this thesis is inspired by their modelling suggestions. The authors analyzed both models, conventional and adsorption reactor, with product in-situ removal, involving repeated "pressure swings". From the mathematical perspective, this adsorption process is similar to a membrane reactor with permeation capability on a specialized catalyst.

In this sense, the input reactor parameter values used for their simulation are also introduced in our model to compare results and asses the validity of our calculations. A summary of the plug flow input values used for their simulation of methanol synthesis is presented in Table 9.

Note that the same catalyst density, number of parallel tubes, tube diameter and tube length are used as input parameter for our analysis (see Table 5), since the effects of reactor design are out of the scope of this thesis. However, it was decided to examine different H_2/CO_2 ratios and intermediate permeation parameters λ_k in our model.

The focus of Patterson et al. research work is to demonstrate how one can may simulate and model the simplified operation of catalytic reactor using basic thermodynamic data, a kinetic model for the multi-step reactions and numerical solutions methods. Therefore, they only offer a couple of figures that are of the interest for this thesis. However, these graphics can then be used to check the validity and accuracy of our model.

Table 9. Plug flow reactor parameter values used in the simulation of methanol synthesis performed by Patterson et al. that are important for the validation.

Parameter	Value
Catalyst	$Cu/ZnO/Al_2O_3$
Catalyst density $\rho_{catalyst}$	$1000\ kg/m^3$
Number of parallel tubes n_{tubes}	10,000
Tube diameter d	$2\ cm$
Tube area $A_{tube} = n_{tube}\pi(d^2/4)$	$3.14\ m^2$
Tube length L_{tube}	$3\ m$
SN	2
Temperature range T	$180 - 340\ ºC$
Pressures P	$20, 40, 60\ bar$
Adsorption factor λ_k	0, 2

3.4.2.1 Conventional Reactor Comparison

For the conventional reactor Patterson et al. show the position-dependent component molar flows through their plug flow reactor (40 bar, 230ºC and SN =2). By introducing the parameters presented in Table 7 and the given operation conditions in our model, one can explore to the same case study as the one presented in their research work.

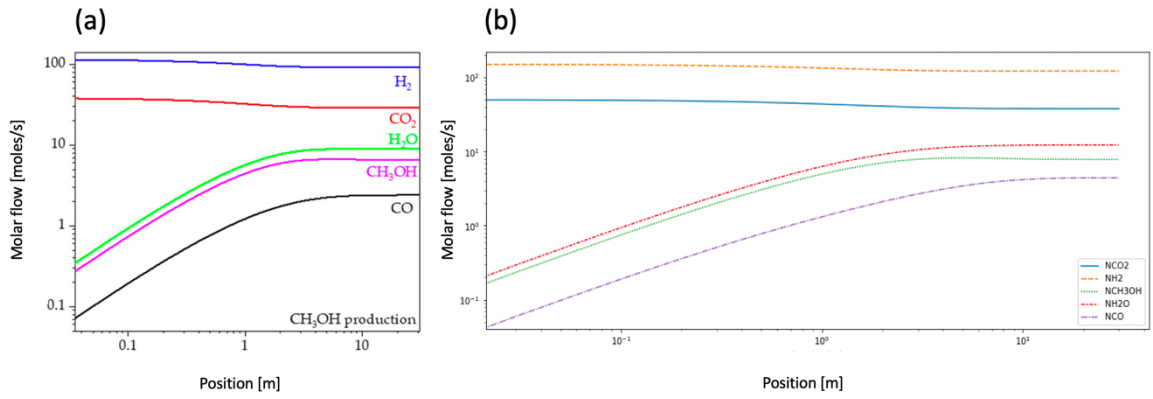

Figure 28. Comparison of the position-dependent component molar flow in a plug flow reactor. (a) Results taken from Patterson et al. (b) results obtained with our plug flow reactor model.

As it can be seen in Figure 28, the results of the developed plug flow reactor model are in qualitative good agreement with the results obtained by Patterson et al. in their research work. Moreover, these position dependencies are also comparable to those found previously by Van-Dal et al. [117], who use the software Aspen Plus® to simulate a methanol production plant.

3.4.2.2 Membrane Reactor Comparison

Patterson et al. also shows how to model a sorption-enhanced PFR, which from the mathematic perspective is the same as modeling a membrane reactor. The authors simulate the conversion of CO_2 to methanol in the sorption-enhanced PFR assuming (a) water adsorption and (b) simultaneously water and methanol adsorption. They show these simulations for a pressure of 40 bar and a stoichiometric factor $SN = 2$. In this sense, here we can also compare the same case study, by simply introducing the same input and operation conditions in our membrane plug flow reactor model.

As it can be inferred from Figure 29, the results of our model match the prediction of Patterson et al., meaning that both the kinetic and membrane model are well implemented.

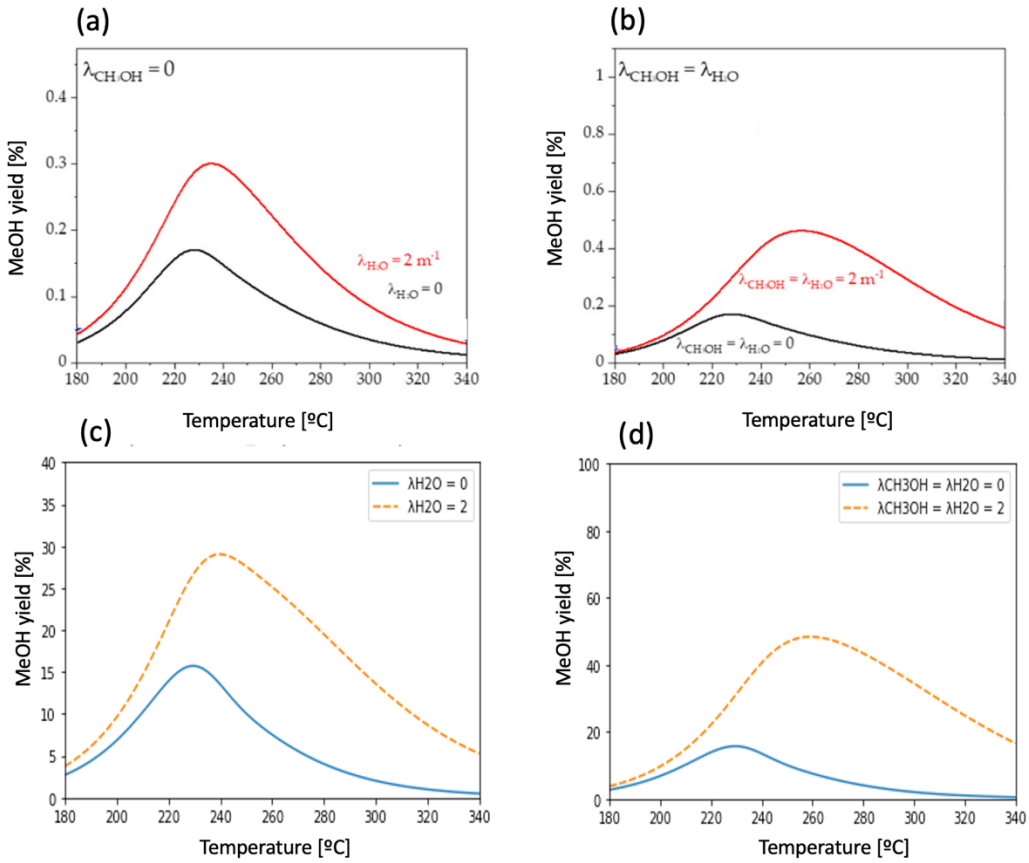

Figure 29. Simulated membrane PFR MeOH yield: (a) and (b) are taken from Patterson et al. [75] and (c) and (d) are obtained with the developed membrane plug flow reactor. (a,b) consider water in-situ removal, (b,c) consider simultaneous in-situ water and methanol removal.

Chapter 4. RESULTS

This chapter gives insight in the results of the thesis. First, the results of the conventional plug flow reactor are presented. These results confirm that at practical pressures, only a low degree of conversion to methanol can be obtained ($< 25\%$). The results are presented for different temperatures ($180ºC - 340ºC$), pressures ($20,40,60\ bar$) and H_2/CO_2 molar ratios ($1,2,3,4$). Moreover, they are also position-dependent depicted, so one can understand and visualize the component molar flow rates through the reactor.

Then, the results for the membrane reactor are also presented. Here the results are reported similarly for different temperatures ($180ºC - 340ºC$), pressures ($20,40,60\ bar$), stochiometric number values ($1,2,3,4$), and water and methanol permeation values [$\lambda_{H2O}, \lambda_{Ch3OH}$] ($0,0.4,0.8,1.2,1.6,2\ m^{-1}$). The results for the membrane reactor are also position-dependent depicted.

Finally, the results are compared with respect to methanol yield and methanol production and discussed in Chapter 5.

4.1 CONVENTIONAL PLUG FLOW REACTOR (PFR) SIMULATIONS

4.1.1 MEOH YIELD IN THE PLUG FLOW REACTOR

The resulting temperature and pressure-dependent MeOH yield is presented in Figure 30. These results agree with previously published studies [118,119] and confirm that at practical pressures, only a low degree of conversion to methanol per pass can be obtained (25%).

The simulations were performed for the operation conditions and reactor parameters presented in Table 7. In this sense, the model was run for different pressures $(20{,}40{,}60\ bar)$, a temperature range $(180 - 340ºC)$, and for different H_2/CO_2 molar ratios $(1{,}2{,}3{,}4)$. The results are shown in Figure 30 and Table 10.

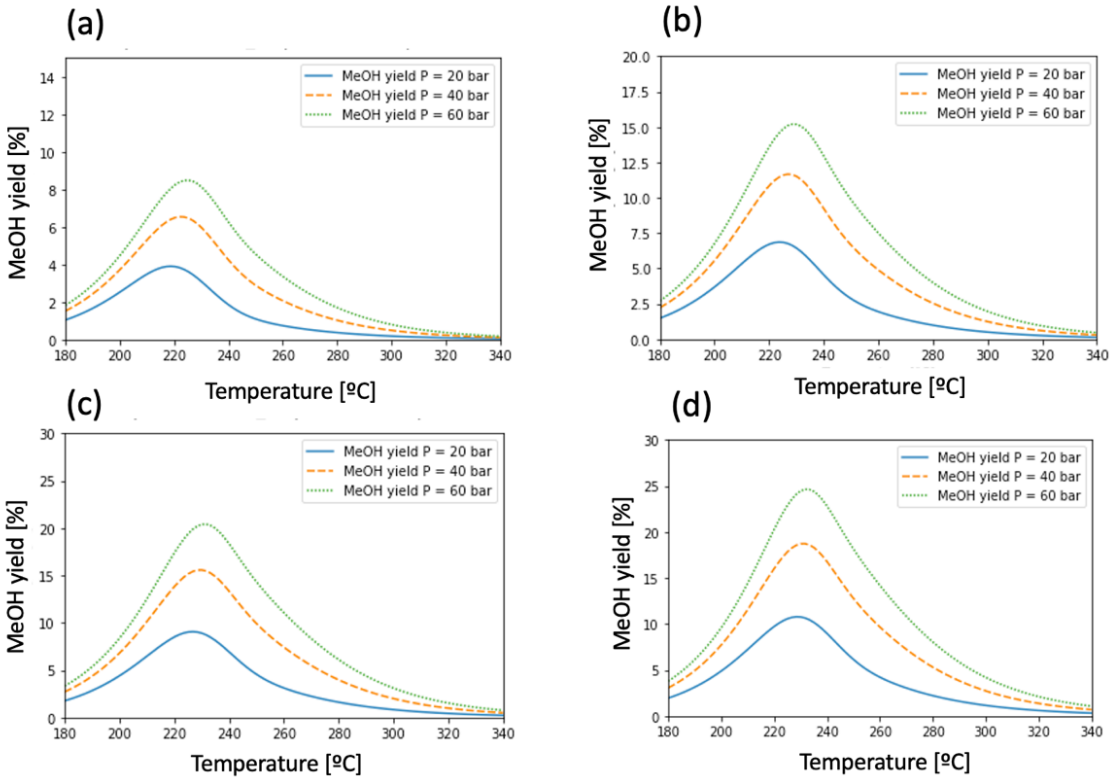

Figure 30. MeOH yield as a function of temperature (180-340ºC) and pressure (20,40,60 bar), (a) H_2/CO_2 = 1, (b) H_2/CO_2 = 2, (c) H_2/CO_2 = 3, (d) H_2/CO_2 = 4.

As it can be observed in Figure 30, methanol yield is favored for both higher pressures and higher H_2/CO_2 molar ratios. A maximum methanol yield of 24.63% is obtained for a H_2/CO_2 molar ratio equal to 4 (i.e. $N_{H2}^{in} = 200$, $N_{CO2}^{in} = 50$) at 60 bar and T = 231.71ºC (see Figure 31). The other maximum values are detailed in Table 10.

Table 10. Maximum MeOH yield [%] for the explored operation conditions in the Plug Flow Reactor (PFR).

Reactor Operation Conditions	Max MeOH value
H_2/CO_2 = 1, P = 20 bar, T = 218.79 ºC	3.90%
H_2/CO_2 = 1, P = 40 bar, T = 222.02 ºC	6.54%
H_2/CO_2 = 1, P = 60 bar, T = 225.25 ºC	**8.48%**
H_2/CO_2 = 2, P = 20 bar, T = 223.64 ºC	6.86%
H_2/CO_2 = 2, P = 40 bar, T = 226.87 ºC	11.66%
H_2/CO_2 = 2, P = 60 bar, T = 228.48 ºC	**15.20%**
H_2/CO_2 = 3, P = 20 bar, T = 226.87 ºC	9.05%
H_2/CO_2 = 3, P = 40 bar, T = 230.10 ºC	15.58%
H_2/CO_2 = 3, P = 60 bar, T = 231.71 ºC	**20.41%**
H_2/CO_2 = 4, P = 20 bar, T = 228.48 ºC	10.77%
H_2/CO_2 = 4, P = 40 bar, T = 231.71 ºC	18.73%
H_2/CO_2 = 4, P = 60 bar, T = 231.71 ºC	**24.63%**

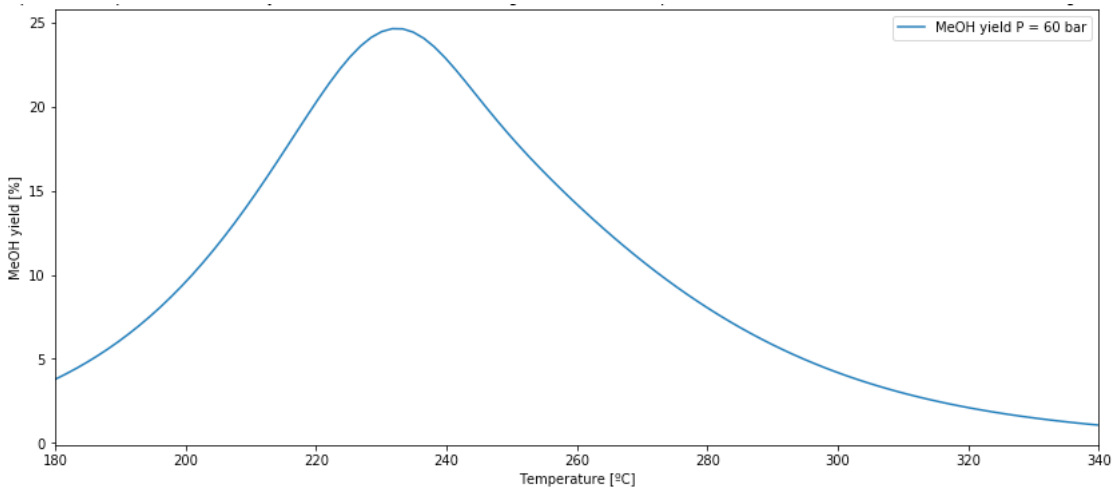

Figure 31. Temperature-dependent MeOH yield [%]. Operation conditions: pressure = 60 bar, H_2/CO_2 molar ratio = 4. Max MeOH yield value of 24.64 % at T = 231.71 ºC.

4.1.2 METHANOL PRODUCTION IN THE PLUG FLOW REACTOR

Moreover, the plug flow reactor allows to explore the position-dependent molar flow through the reactor length. To assess the maximum methanol production through the reactor, the position-dependent molar flows are plotted for the pressures and temperature points at which the MeOH yield is highest. These results are shown in Figure 32.

In this sense, the maximum methanol production of 12.42 mol is obtained for a pressure of 60 bar and a temperature of 231.71 ºC. Note that the figures are in logarithmic scale, since this scale allows a better visualization for each component. The molar position-dependent molar flow rates for each scenario are presented in Appendix D (see Table 36-Table 39).

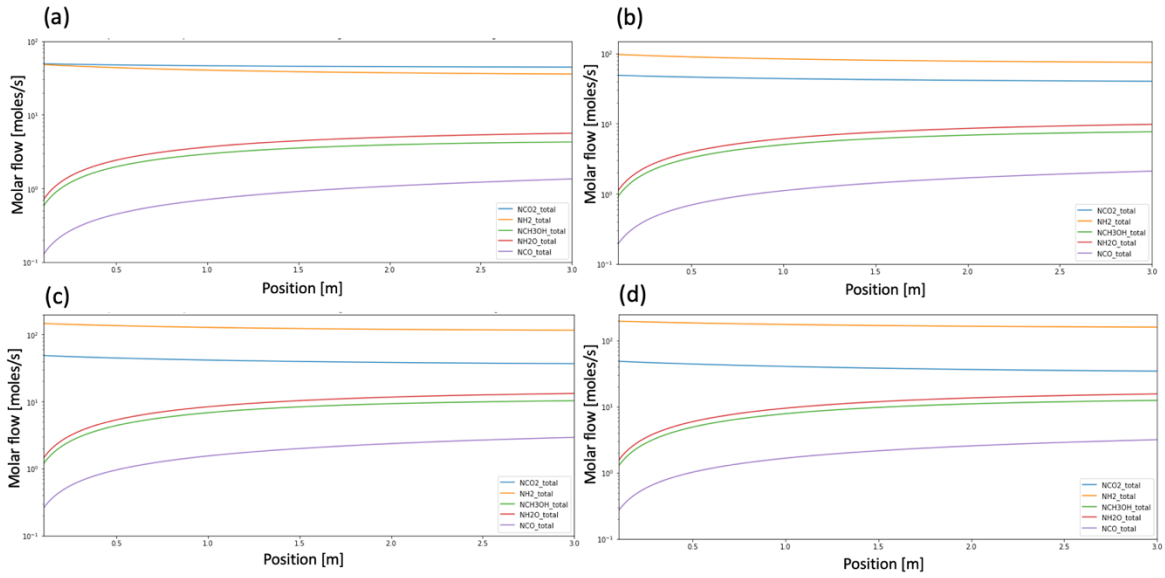

Figure 32. Position-dependent component molar flow rates through the plug flow reactor (PFR). (a) H_2/CO_2 = 1 ($N_{H2}^{in} = 50\ mol, N_{CO2}^{in} = 50\ mol$), P = 60 bar, T = 225.25ºC, (b) H_2/CO_2 = 2 ($N_{H2}^{in} = 100\ mol, N_{CO2}^{in} = 50\ mol$), P = 60 bar, T = 228.48ºC, (c) H_2/CO_2 = 3 ($N_{H2}^{in} = 150\ mol, N_{CO2}^{in} = 50\ mol$), P = 60 bar, T = 231.71ºC, (d) H_2/CO_2 = 4 ($N_{H2}^{in} = 200\ mol, N_{CO2}^{in} = 50\ mol$), P = 60 bar, T = 231.71ºC.

4.2 MEMBRANE PLUG FLOW REACTOR SIMULATIONS

This section shows the main results obtained from the membrane plug flow reactor model. The simulations confirm that in-situ product removal can increase both methanol yield and methanol production.

4.2.1 EFFECT OF MEMBRANE REACTORS ON MEOH YIELD AND METHANOL PRODUCTION

As mentioned in the State of the Art, membrane reactors can circumvent the thermodynamic equilibrium and increase the MeOH yield per pass by in situ product removal. In this thesis, the effects of water, methanol, and simultaneous water and methanol in-situ removal are explored via model simulation.

4.2.1.1 Membrane Reactor with simultaneous in-situ Methanol and Water Removal

The simulations are performed for different pressures $(20,40,60\ bar)$, temperature ranges $(180-340ºC)$, permeation factors λ_k $(0,0.4,0.8,1.2,1.6,2)$ and different H_2/CO_2 ratios $(1,2,3,4)$. According to the simulations, the MeOH yield is especially improved when both methanol and water are removed (see Figure 33).

Note that although the reactor performance with water removal is similar to the performance with methanol removal, this is not exactly the same. Removing the water seems to be more interesting than methanol, since it can increase more the methanol yield. For example, at 60 bar and a H_2/CO_2 ratio of 3 the methanol yield can increase up to 37.92% with respect to 35.36% with methanol removal. This is further discussed in Chapter 5.

Moreover, as in the conventional plug flow reactor, the MeOH increases for higher pressures and H_2/CO_2 molar ratios (see Figure 34).

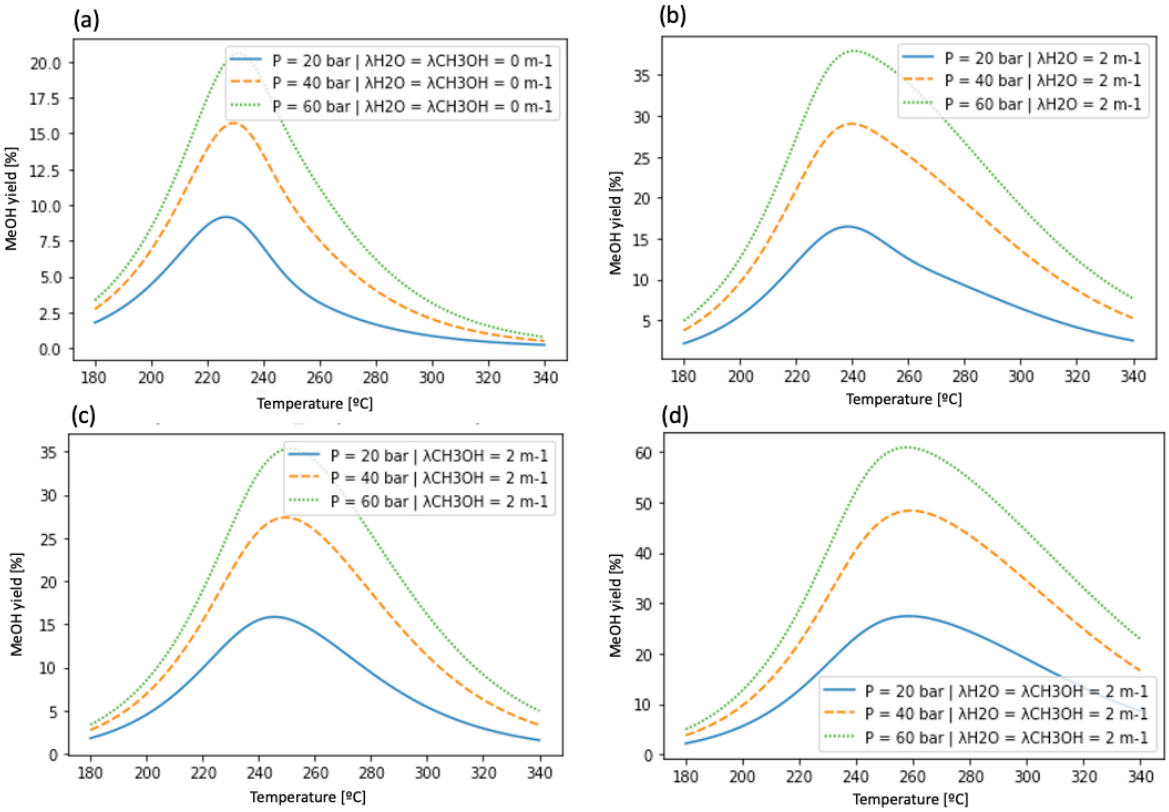

Figure 33. Comparison between removing water, methanol or simultaneous water and methanol removal. Operation conditions for all cases: P = 20,40,60 bar, H_2/CO_2 = 3 (i.e. $N_{H2}^{in} = 150, N_{H2}^{in} = 50$) and given landas. (a) no in-situ product removal – conventional reactor, (b) in-situ water removal, (c) in-situ methanol removal and (d) simultaneous in-situ water and methanol removal.

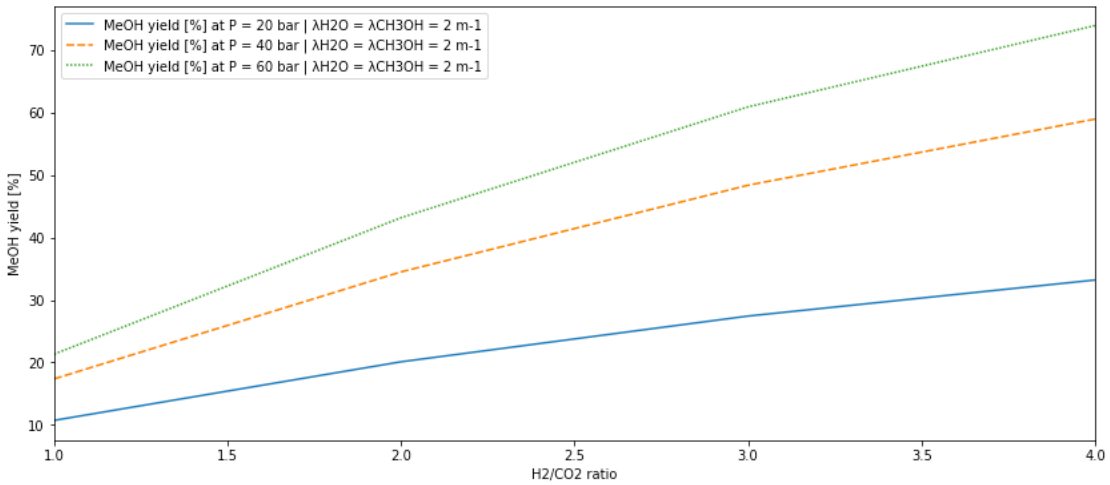

Figure 34. MeOH yield as function of H_2/CO_2 ratio at 20,40 and 60 bar. All cases for $\lambda_{H2O} = \lambda_{CH3OH} = 2$.

The MeOH yield simulation results for 20,40,60 bar and a H_2/CO_2 ratio of 4 are presented in Figure 35 and more in detail in Table 11. This figure illustrates that the enhancement of the MeOH yield for higher pressures and higher permeation factors ($\lambda_{H2O}, \lambda_{CH3OH}$).

According to the simulations, a 50% of water and methanol removal can increase the MeOH yield with respect conventional reactors by 42% on average. In other words, the methanol yield could rise to 35.57%. Similarly, the simulations suggest that a membrane reactor with the capability of removing 90% of the produced water and methanol could achieve a methanol yield of 73.91%. This confirms that simultaneous methanol and water in-situ removal can circumvent the thermodynamic equilibrium and achieve higher methanol production.

Comparably to the conventional reactor, the membrane model allows to plot the position-dependent molar flow rates through the reactor too (see Figure 36). Membrane reactors also allow a higher CO_2 consumption, since they can be used to circumvent the thermodynamic equilibrium and push the reaction to the product side.

A maximum methanol production of 36.96 mol/s can be obtained for 60 bar, a H_2/CO_2 molar ratio of 4 and a permeation factor $[\lambda_{CH3OH}, \lambda_{H2O}]$ of 2 m^{-1} (see Appendix D, Table 23). Similarly, by removing only 50% of both water and methanol and assuming same operation conditions (60 bar, H_2/CO_2 molar ratio of 4) one could obtain a methanol production ratio of 17.78 mol/s (see Appendix D, Table 20).

A conventional reactor would in contrast produce 12.41 mol/s for the same operation conditions (see Appendix D, Table 17). These values show the effectiveness of water and methanol in-situ removal to increase methanol production rates and methanol yield.

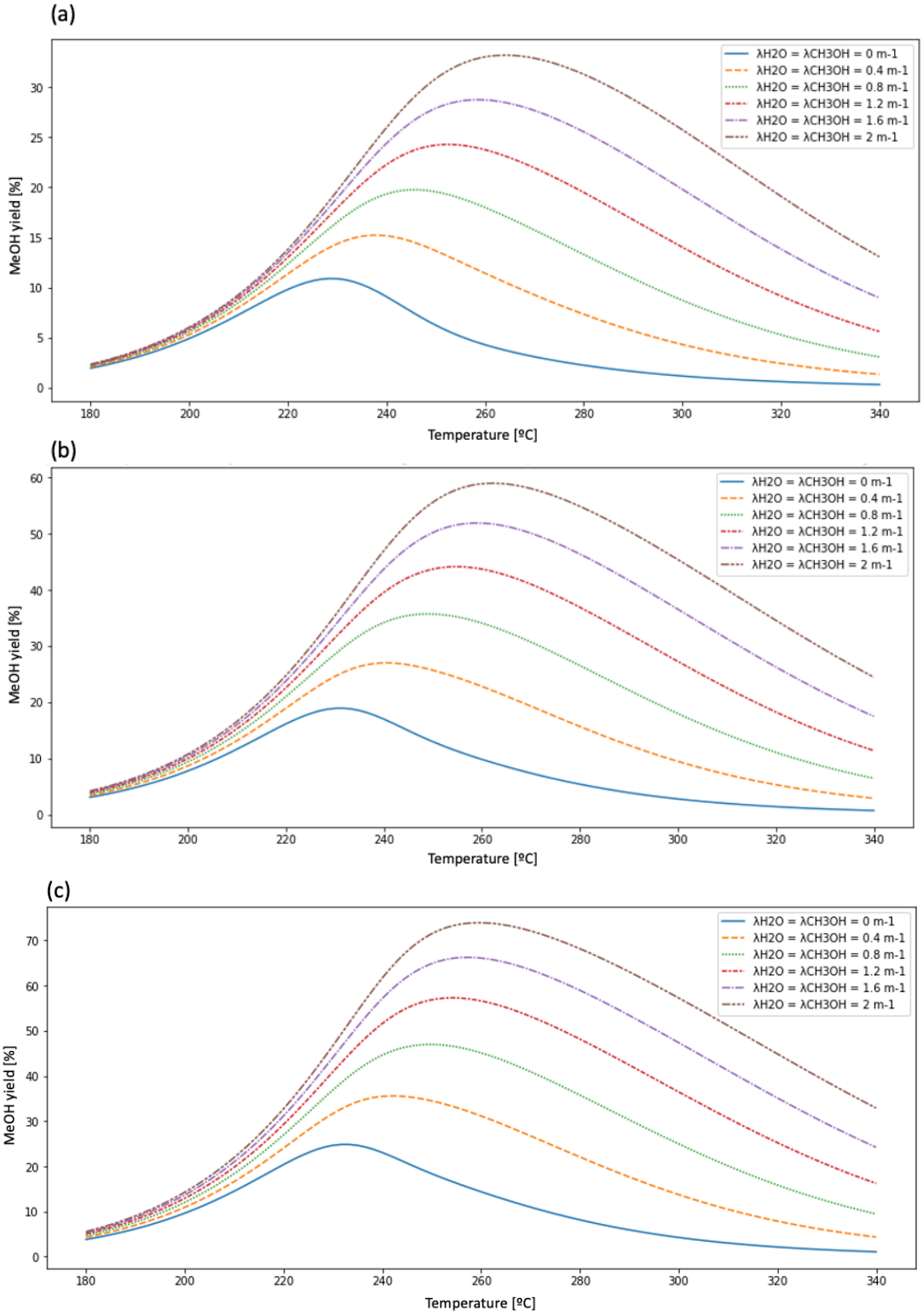

Figure 35. MeOH yield [%] in the membrane plug flow reactor (MPFR). Operation conditions: (a) P = 20 bar, (b) P = 40 bar and (c) P = 60 bar. For all cases given $\lambda_{H2O}, \lambda_{CH3OH}$ and $H_2/CO_2 = 4$.

Table 11. MeOH yield and H_2O/CO_2 percentage of absorption in the membrane plug flow reactor. Operation conditions P = 20,40,60 bar, T = 180-340ºC, H_2/CO_2 ratio = 4 (i.e. $N_{H2}^{in} = 200, N_{H2}^{in} = 50$) and given $\lambda_{H2O} = \lambda_{CH3OH}$.

Pressure [bar]	$\lambda_{H2O} = \lambda_{CH3OH}$ [m^{-1}]	T [ºC]	max MeOH [%]	%H_2O / %CH_3OH absorbed
20	0	228.48	10.77	0/0
20	0.4	238.12	15.24	48.60/49.47
20	0.8	246.26	19.77	68.32/68.32
20	1.2	252.72	24.74	79.69/76.52
20	1.6	259.19	28.75	85.78/81.00
20	**2**	**264.04**	**33.19**	**89.36/83.97**
40	0	231.71	18.73	0/0
40	0.4	239.79	26.97	50.98/50.70
40	0.8	249.49	35.69	69.7/69.11
40	1.2	254.34	44.10	82.00/77.42
40	1.6	259.19	51.87	87.35/82.49
40	**2**	**262.42**	**58.95**	**90.50/86.00**
60	0	231.71	24.63	0/0
60	0.4	241.41	35.57	52.52/51.60
60	0.8	249.49	46.96	73.57/70.14
60	1.2	254.34	57.28	83.01/78.74
60	1.6	257.57	66.24	88.1/84.11
60	**2**	**259.19**	**73.91**	**91.11/87.74**

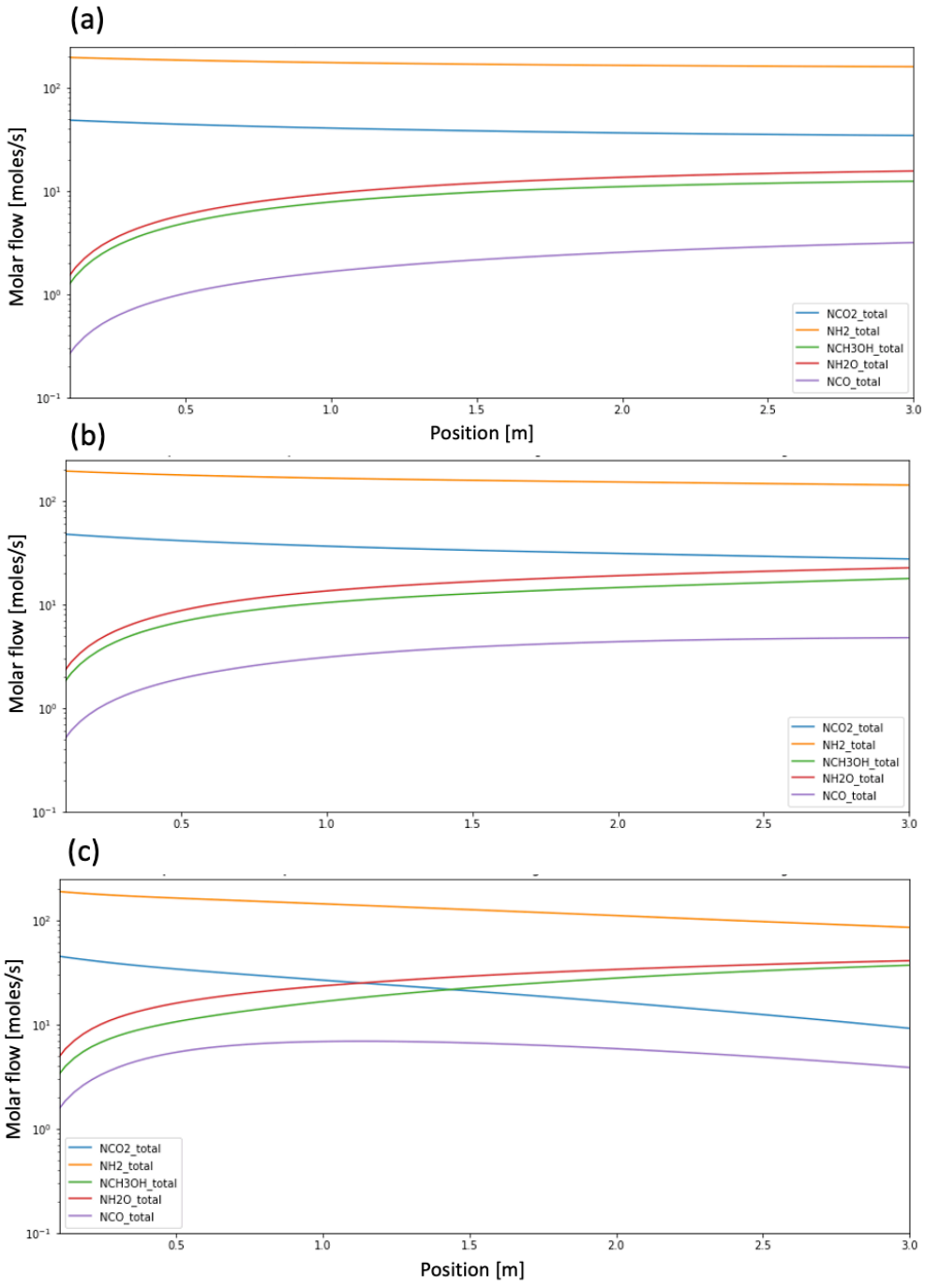

Figure 36. Position-dependent molar flow rates. Operation conditions at which MeOH is maximum for all cases. (a) $\lambda_{H2O} = \lambda_{CH3OH} = 0\ m^{-1}$, *T= 231.71 ºC, (b)* $\lambda_{H2O} = \lambda_{CH3OH} = 0.4\ m^{-1}$, *T = 241.41 ºC, (c)* $\lambda_{H2O} = \lambda_{CH3OH} = 2\ m^{-1}$, *T = 259.19ºC. For all cases P = 60 bar.*

4.2.1.2 Membrane Reactor with Water in-situ Removal

The simulations are performed for different pressures (20,40,60 bar), temperature ranges ($180-340ºC$), permeation factors λ_{H2O} (0,0.4,0.8,1.2,1.6,2) and different H_2/CO_2 ratios (1,2,3,4). According to the simulations, the MeOH yield is especially improved for high pressures and H_2/CO_2 molar ratios (see Figure 37 and Figure 38).

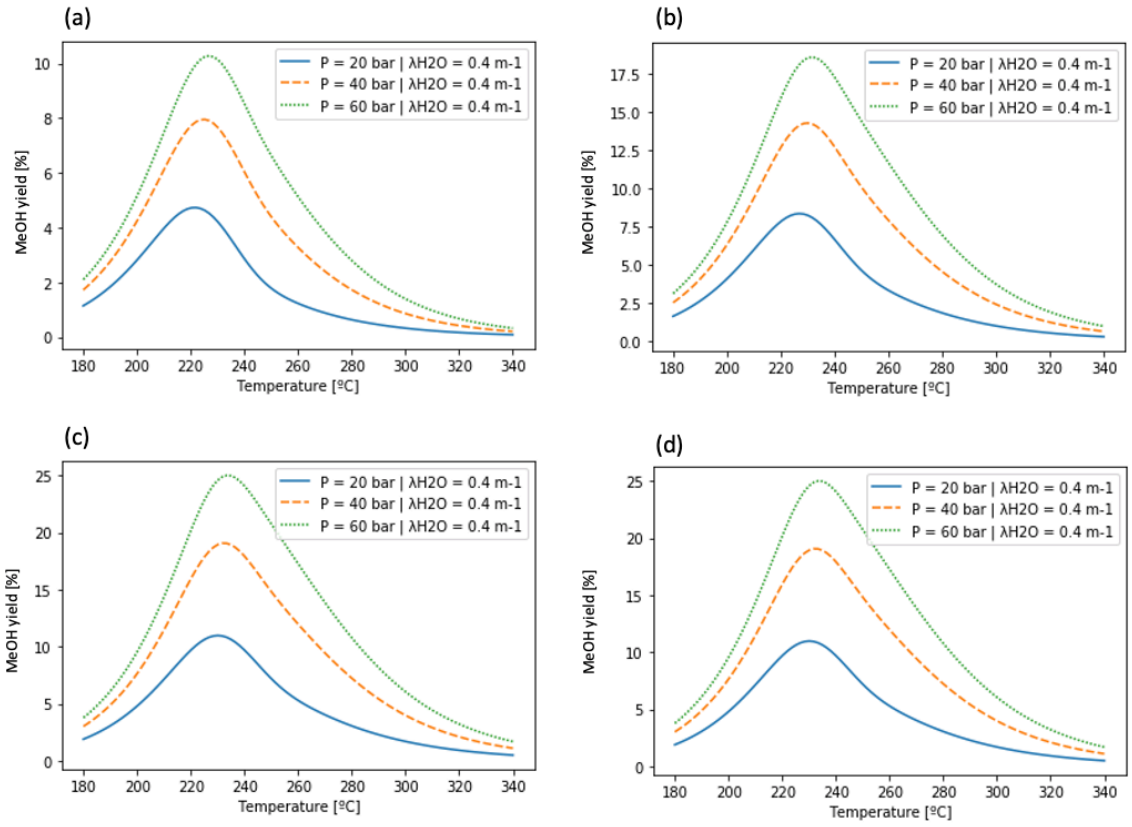

Figure 37. Effects of pressure and H_2/CO_2 molar ratio on MeOH yield. (a) H_2/CO_2 = 1 (i.e. $N_{H2}^{in} = 50, N_{CO2}^{in} = 50$, (b) H_2/CO_2 = 2 (i.e. $N_{H2}^{in} = 100, N_{CO2}^{in} = 50$, (c) H_2/CO_2 = 3 (i.e. $N_{H2}^{in} = 150, N_{CO2}^{in} = 50$, (d) H_2/CO_2 = 4 (i.e. $N_{H2}^{in} = 200, N_{CO2}^{in} = 50$. All cases for P = 20,40,60 bar, T=180-340ºC and $\lambda_{H2O} = 0.4$.

The effects of in-situ water removal on the methanol yield are shown in Figure 39 for a H_2/CO_2 molar ratio of 4 (i.e. $N_{H2}^{in} = 200, N_{H2}^{in} = 50$). A more detailed table with the operation conditions at which the methanol yield is maximum is presented in Table 12.

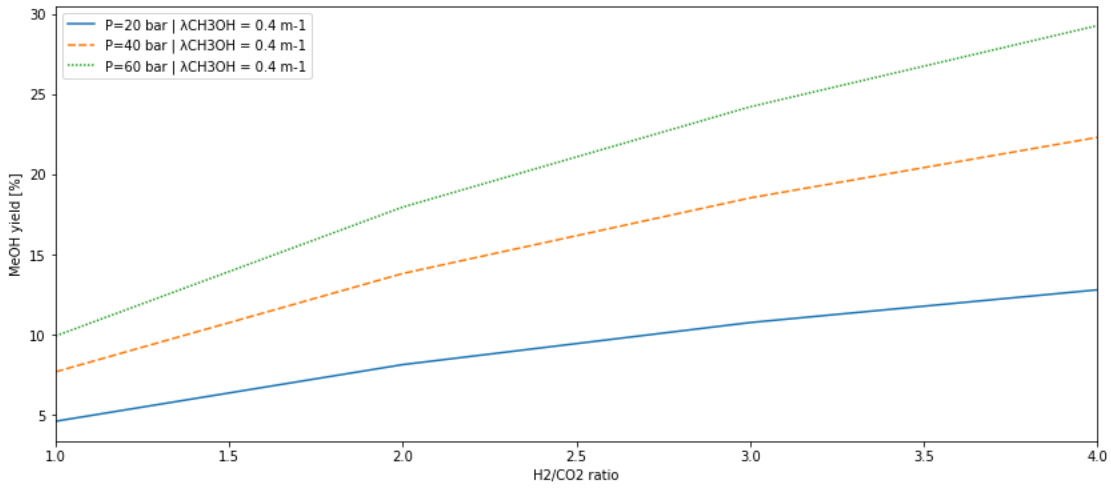

Figure 38. Effects of pressure and H_2/CO_2 molar ratio on Methanol yield. All cases for $\lambda_{H2O} = 0.4$.

Figure 39 visualizes the enhancement of the MeOH yield for higher pressures and higher permeation factors λ_{H2O}. According to the simulations, a 60% of water removal can increase around 22% the MeOH yield with respect conventional reactors. This confirms that in-situ water removal can also circumvent the thermodynamic equilibrium and achieve higher methanol production than a conventional reactor.

Like the previous case, the position-dependent molar flow rates through the reactor are shown in Figure 40. In situ-water removal also allows a higher CO_2 consumption, since they can be used to circumvent the thermodynamic equilibrium and push the reaction to the product side.

A maximum methanol production of 23.14 mol/s can be obtained for 60 bar, H_2/CO_2 molar ratio of 4, permeation factor λ_{H2O} of 2 m^{-1} and pressure of 60 bar (see Appendix D, Table 29). A conventional reactor would in contrast produce 12.41 mol/s for the same operation conditions (see Appendix D, Table 17). These values show the effectiveness of water in-situ removal to increase methanol production rates and methanol yield.

These results are further discussed in Chapter 5.

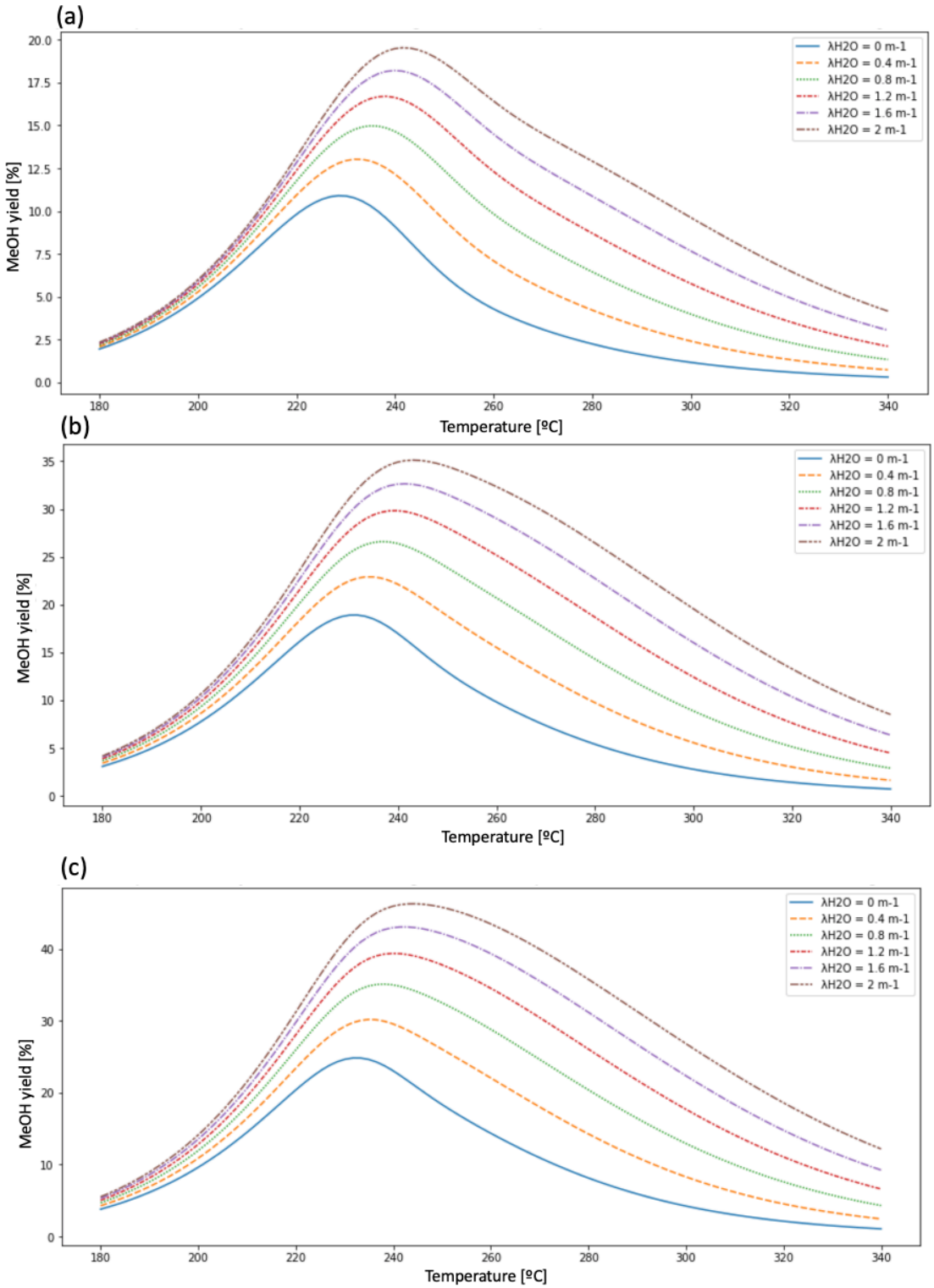

Figure 39. MeOH yield [%] in the membrane plug flow reactor (MPFR). Operation conditions: (a) P = 20 bar, (b) P = 40 bar and (c) P = 60 bar. For all cases given λ_{H2O} and $H_2/CO_2 = 4$.

Table 12. MeOH yield and H_2O/CO_2 percentage of absorption in the membrane plug flow reactor. Operation conditions P = 20,40,60 bar, T = 180-340ºC, H_2/CO_2 ratio = 4 (i.e. $N_{H2}^{in} = 200, N_{H2}^{in} = 50$) and given λ_{H2O}.

Pressure [bar]	**λ_{H2O} [m^{-1}]**	**T [ºC]**	**max MeOH [%]**	**%H_2O absorbed**
20	0	228.48	10.90	0
20	0.4	231.72	13.03	62.17
20	0.8	234.95	14.97	80.85
20	1.2	238.18	16.69	88.61
20	1.6	239.80	18.20	92.54
20	**2**	**241.41**	**19.53**	**94.80**
40	0	231.71	18.90	0
40	0.4	234.95	22.90	62.35
40	0.8	236.56	26.59	80.95
40	1.2	239.80	29.82	88.71
40	1.6	241.41	32.64	92.63
40	**2**	**243.03**	**35.11**	**94.85**
60	0	231.71	24.83	0
60	0.4	234.90	30.18	62.41
60	0.8	238.18	35.10	81.03
60	1.2	239.80	39.38	88.72
60	1.6	241.41	43.06	92.69
60	**2**	**244.65**	**46.28**	**94.88**

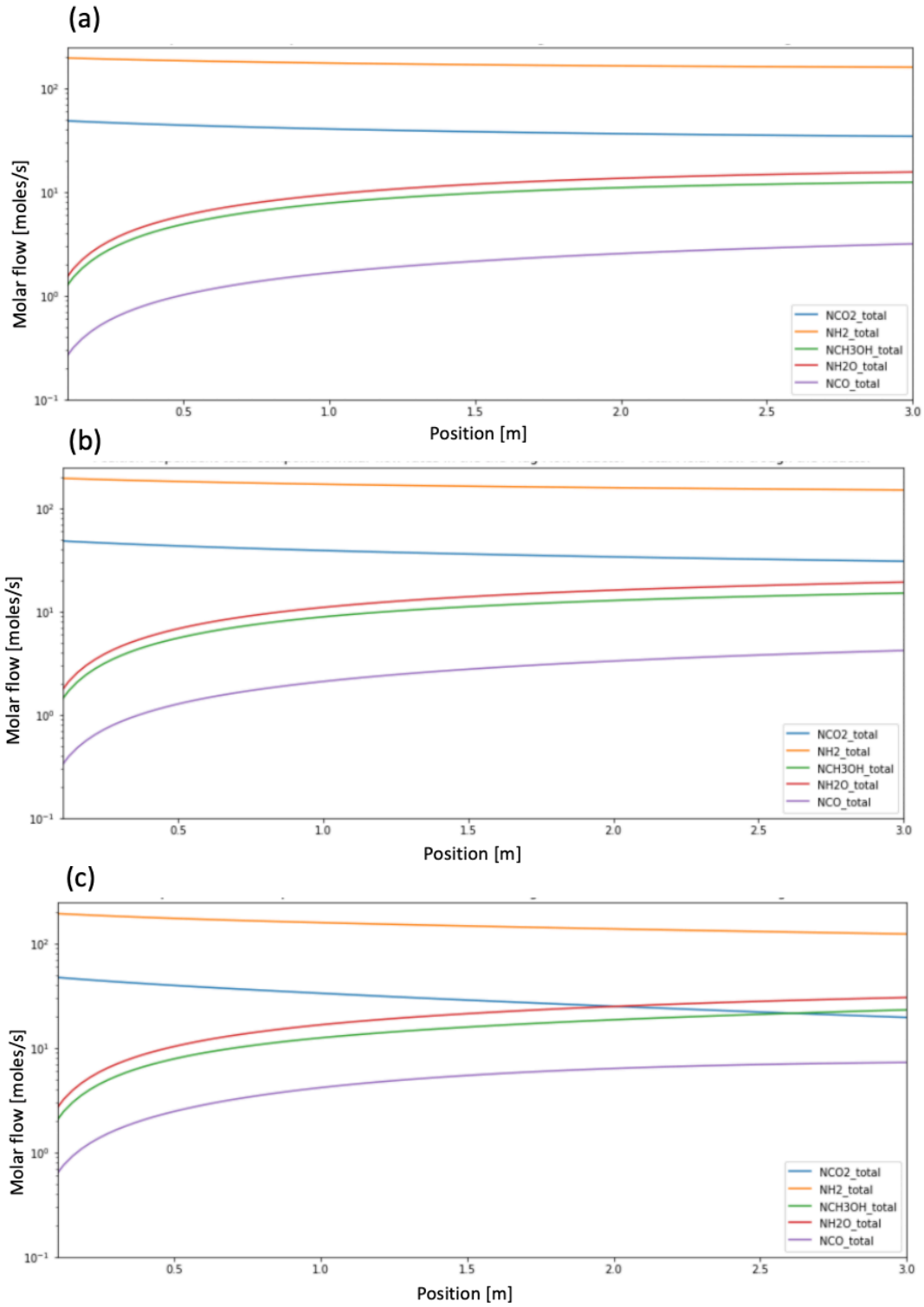

Figure 40. Position-dependent molar flow rates. Operation Conditions at which MeOH is maximum: (a) $\lambda_{H2O} = 0\ m^{-1}$, *T= 231.71 ºC, (b)* $\lambda_{H2O} = 0.4\ m^{-1}$, *T = 241.41 ºC, (c)* $\lambda_{H2O} = 2\ m^{-1}$, *T = 259.19ºC. For all cases P = 60 bar.*

4.2.1.3 Membrane Reactor with Methanol in-situ Removal

The simulations are performed for different pressures (20,40,60 bar), temperature ranges ($180-340ºC$), permeation factors λ_{CH3OH} (0,0.4,0.8,1.2,1.6,2) and different H_2/CO_2 ratios (1,2,3,4). Here, the MeOH yield is also improved for high pressures and H_2/CO_2 molar ratios (see Figure 41 and Figure 42). The effects of in-situ methanol removal on the methanol yield are shown in Figure 43 for a H_2/CO_2 molar ratio of 4 (i.e. $N_{H2}^{in} = 200, N_{H2}^{in} = 50$). A more detailed table with the operation conditions at which the methanol yield is maximum is presented in Table 13.

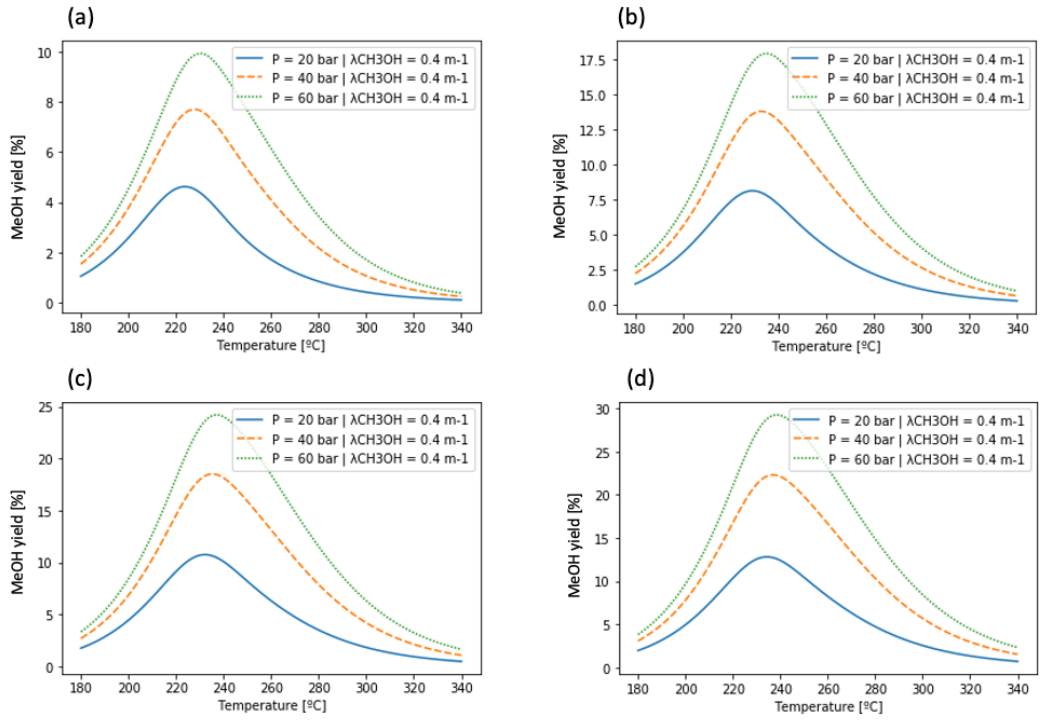

Figure 41. Effects of pressure and H_2/CO_2 molar ratio on MeOH yield. (a) H_2/CO_2 = 1 (i.e. $N_{H2}^{in} = 50, N_{CO2}^{in} = 50$, (b) H_2/CO_2 = 2 (i.e. $N_{H2}^{in} = 100, N_{CO2}^{in} = 50$, (a) H_2/CO_2 = 3 (i.e. $N_{H2}^{in} = 150, N_{CO2}^{in} = 50$, (d) H_2/CO_2 = 4 (i.e. $N_{H2}^{in} = 200, N_{CO2}^{in} = 50$. All cases for P = 20,40,60 bar, T=180-340ºC and $\lambda_{CH3OH} = 0.4$.

Figure 43 confirms that the enhancement of the MeOH yield for higher pressures and higher permeation factors λ_{CH3OH}. According to the simulations, a 55% of water removal can increase around 17.84% the MeOH yield with respect to conventional reactors.

This confirm that in-situ methanol removal can also circumvent the thermodynamic equilibrium and achieve higher methanol production than a conventional reactor.

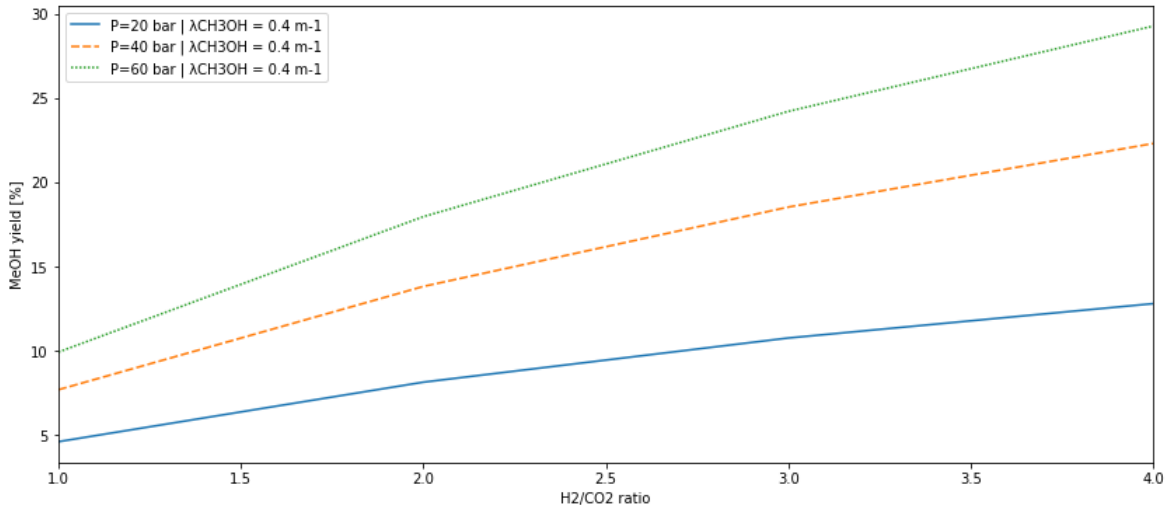

Figure 42. Effects of pressure and H_2/CO_2 molar ratio on Methanol yield. All cases for $\lambda_{CH3OH} = 0.4$.

In situ-methanol removal also allow a higher CO_2 consumption, since they can be used to circumvent the thermodynamic equilibrium and push the reaction to the product side. The position-dependent molar flow rates through the reactor are presented in Figure 44.

A maximum methanol production of 21.42 mol can be obtained for 60 bar, a H_2/CO_2 molar ratio of 4, a permeation factor λ_{CH3OH} of 2 m^{-1} and a pressure of 60 bar (see Appendix D, Table 35). As stated before, a conventional reactor would in contrast produce 12.41 mol/s for the same operation conditions (see Appendix D, Table 17). These values show the effectiveness of in-situ methanol removal to increase both methanol production rates and methanol yield. However, in-situ methanol removal was demonstrated to be the less effective strategy to increase both methanol yield and production rates. This is further discussed in Chapter 5.

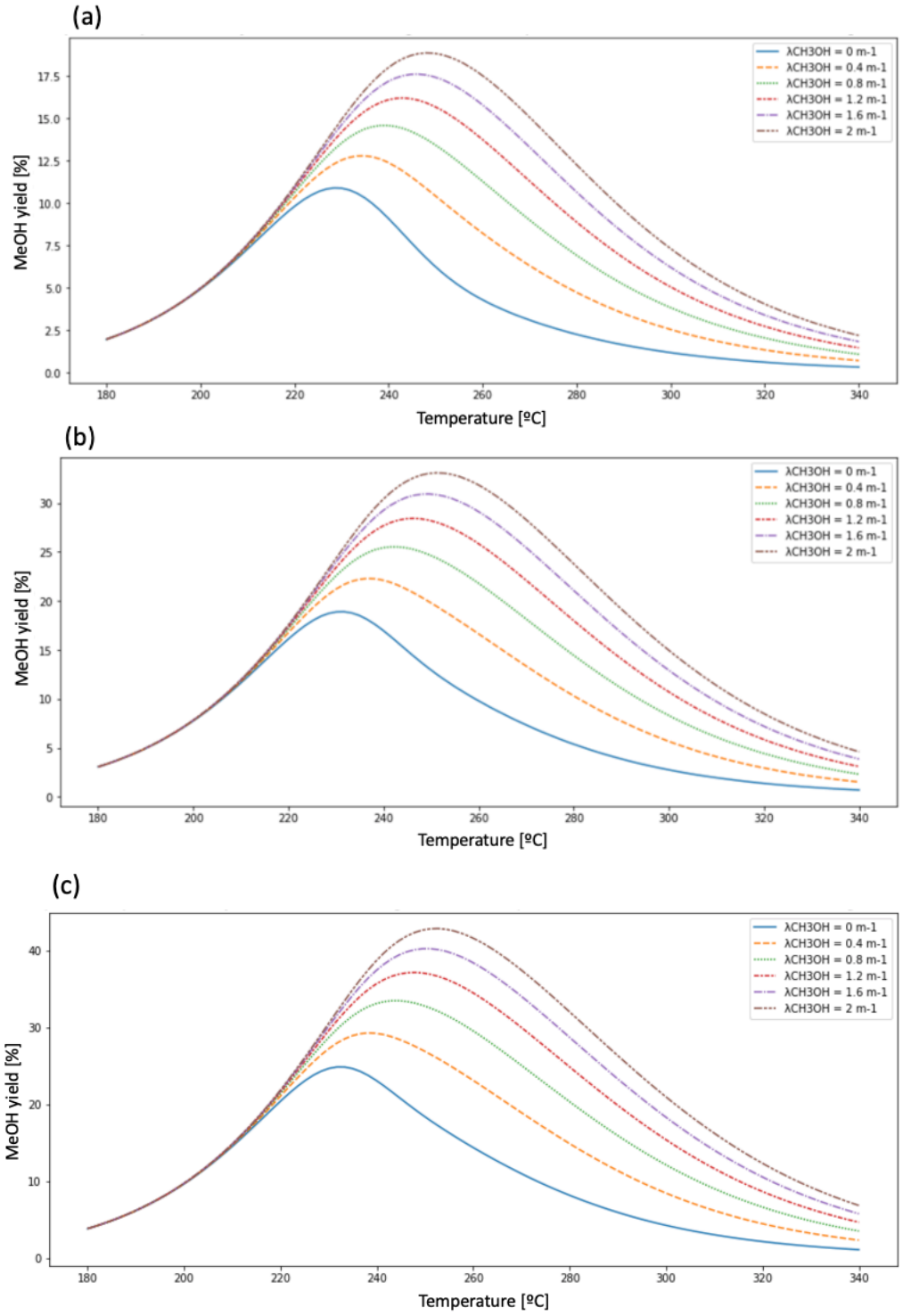

Figure 43. MeOH yield [%] in the membrane plug flow reactor (MPFR). Operation conditions: (a) P = 20 bar, (b) P = 40 bar and (c) P = 60 bar. For all cases given λ_{CH3OH} and $H_2/CO_2 = 4$.

Table 13. MeOH yield and CH_3OH percentage of absorption in the membrane plug flow reactor. Operation conditions P = 20,40,60 bar, T = 180-340ºC, H_2/CO_2 ratio = 4 (i.e. $N_{H2}^{in} = 200, N_{H2}^{in} = 50$) and given λ_{CH3OH}.

Pressure [bar]	λ_{CH3OH} [m^{-1}]	T [ºC]	max MeOH [%]	%CH_3OH absorbed
20	0	228.48	10.90	0
20	0.4	234.95	12.80	55
20	0.8	239.80	14.59	71.09
20	1.2	243.03	16.21	78.78
20	1.6	246.26	17.63	83.27
20	**2**	**247.88**	**18.88**	**86.27**
40	0	231.71	18.91	0
40	0.4	236.57	22.30	54.97
40	0.8	243.03	25.52	71.21
40	1.2	246.26	28.42	78.97
40	1.6	249.49	30.91	83.52
40	**2**	**251.11**	**33.07**	**86.50**
60	0	231.71	24.83	0
60	0.4	238.18	29.26	55.08
60	0.8	244.64	33.45	71.41
60	1.2	247.88	37.14	79.23
60	1.6	251.11	40.41	83.81
60	**2**	**252.73**	**42.84**	**86.81**

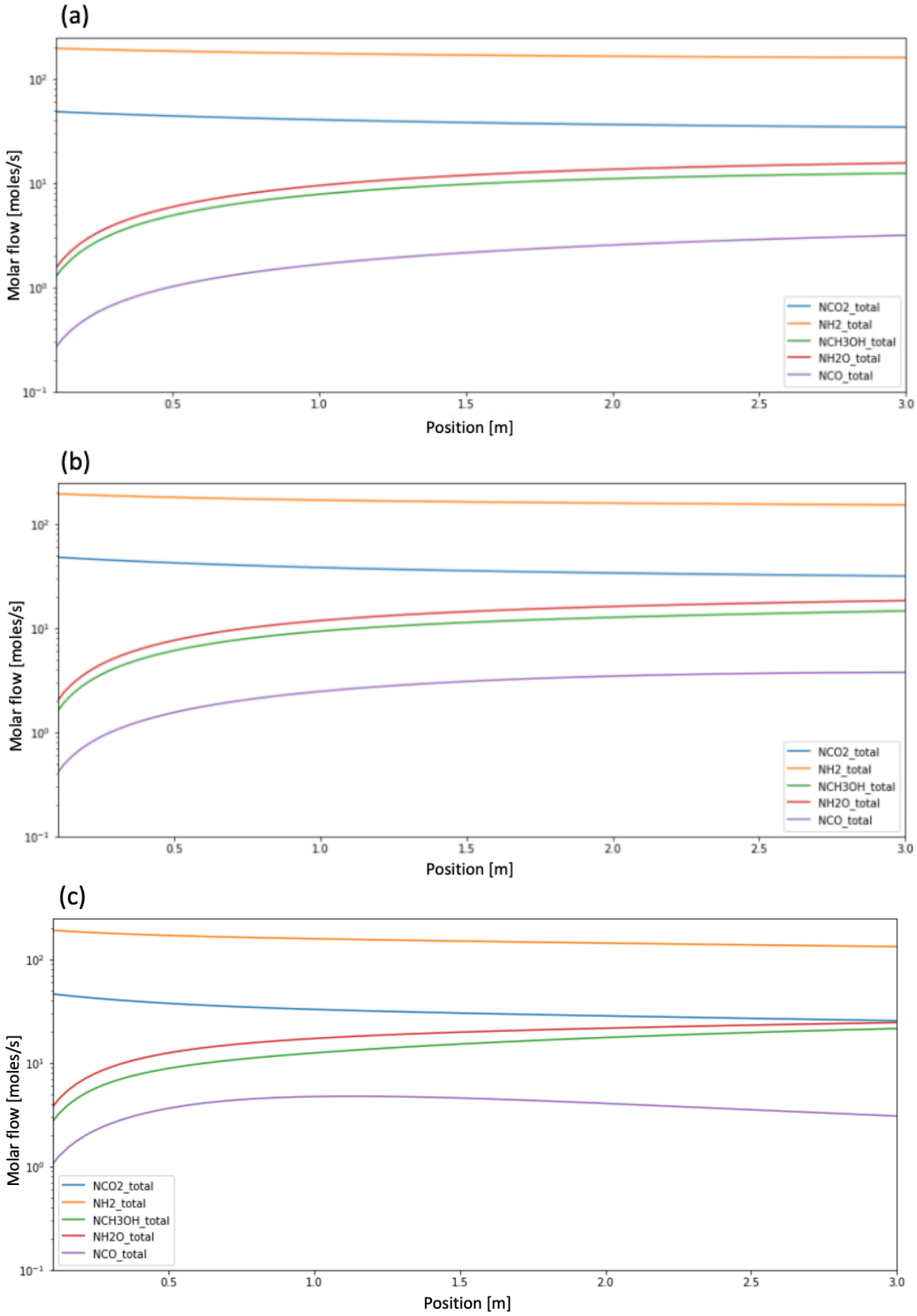

Figure 44. Position-dependent molar flow rates. Operation Conditions at which MeOH is maximum: (a) $\lambda_{CH3OH} = 0\ m^{-1}$, *T= 231.71 ºC, (b)* $\lambda_{CH3OH} = 0.4\ m^{-1}$, *T = 241.41 ºC, (c)* $\lambda_{CH3OH} = 2\ m^{-1}$, *T = 259.19ºC. For all cases P = 60 bar.*

Chapter 5. DISCUSSION

In this chapter, the impacts of different operating parameters on the performance of both conventional and membrane PFR are analyzed. In this sense, the effects of the temperature, pressure, H_2/CO_2 molar ratio, in-situ water removal, in-situ methanol removal, and simultaneous in-situ water and methanol removal on methanol yield and methanol production are explained in detail.

Thereafter, the simulation results for both conventional and membrane plug flow membrane reactor with in-situ water and/or methanol are analyzed and compared. Finally, the limitations of the model used to evaluate the performance of membrane reactors are highlighted and explained.

A summary of the thesis and an outlook on research gaps that can be tackled to further investigate the effects of membrane reactors on methanol synthesis are provided in Chapter 6 Summary and Outlook.

5.1 EFFECTS OF TEMPERATURE ON MEOH YIELD AND METHANOL PRODUCTION

The temperature effect was investigated in the range of 180-340 ºC. The conventional PFR simulations confirm that the methanol yield is reduced for high temperatures. CO_2 hydrogenation to methanol is favored at low temperatures, since it is a strongly exothermic reaction. This leads the methanol yield to decrease fast for high temperatures (> 260 ºC). At this temperature range, the RWGS reaction starts to be favored, leading to a higher CO production, and reducing the methanol generation.

In Figure 31, one can see that the MeOH yield is nearly zero at 340ºC in the conventional plug flow reactor. At this temperature, a pressure of 60 bar and a H_2/CO_2 molar ratio of 4, only 0.54 mol/s of methanol can be obtained compared to 18 mol/s of CO, meaning that at this temperature range almost only the reduction of CO_2 to CO takes place (see Appendix D, Table 17).

On the other hand, the kinetics of methanol are very low for low temperatures (e.g. 100 ºC). This requires that methanol synthesis processes must be performed at higher temperature ranges (220-270ºC), leading the CO_2 to methanol reduction to be thermodynamically limited. Moreover, it can be seen from Figure 30 and Table 10 that the optimal temperature for methanol production is within the range of 218.79-231.71 ºC for all investigated operation conditions in the conventional reactor.

As stated in the State of the Art, this thermodynamical limitation can be circumvent using membrane reactors to in-situ remove the products. The continuous product removal shifts the thermodynamic equilibrium and drives the reaction of CO_2 to a higher conversion, meaning higher methanol yield and methanol production.

Removing the water helps to minimize the effects of the RWGS reaction at high temperatures, leading the maximum methanol yield to be obtained at higher temperatures

(around 250ºC). Moreover, the decrease of the methanol yield is lower than for conventional reactors at high temperatures. This trend can be seen in Figure 39.

5.2 EFFECTS OF PRESSURE ON MEOH YIELD AND METHANOL PRODUCTION

In the absence of in-situ product removal (i.e. conventional reactor case), pressure elevation positively affects both methanol yield and methanol production rates. This can be seen in Figure 30, where the rest of operation conditions are fixed (T=180-340 ºC and H_2/CO_2 molar ratios of 1,2,3,4).

Assuming 230ºC and a H_2/CO_2 molar ratio of 4, the methanol yield can increase from 10.8% to 24.60% (127% increase) by elevating the pressure from 20 bar to 60 bar. Similar to methanol yield, the methanol production is maximized for higher pressures. For a molar ratio of 4 (i.e. $N_{H2}^{in} = 200\ mol$, $N_{CO2}^{in} = 50\ mol$), the methanol production is increased from 5.45 mol/s (see Appendix D, Table 15) to 12.41 mol/s (see Appendix D, Table 17) simply by elevating the pressure from 20 bar to 60 bar.

These results (see Appendix D, Table 15-Table 17) are in good agreement with Le Chaterlier´s principle, since CO_2 hydrogenation to methanol is a strongly volume decreasing reaction and is favored at high pressures. Note that CO production is less affected, since there is no volume increase in the RWGS reaction. Same conclusions are drawn by Zachopoulos et al. [120] in their research.

According to the simulations, it is evident that CO_2 hydrogenation to methanol requires high pressures to achieve a high methanol yield and production rates. However, even at high pressures the maximum methanol yield that can be obtained in the conventional reactor is 24.63% due to the thermodynamic limit of the reaction. Additionally, high reaction pressures imply high operation costs and energy needs. Thus, it is believed that these two factors should also be considered to estimate the optimal operation conditions needed to minimize

methanol production costs. Despite this analysis being out of the scope of this thesis, it is believed that this should be mentioned.

The membrane PFR simulations also shows the positive effects of increasing the pressure in the reaction with in-situ product removal. Considering simultaneous in-situ water and methanol removal (see Table 11), the methanol yield could increase up to 73.91% at 60 bar compared to 32.94 at 20 bar (H_2/CO_2 molar ratio = 4, $\boldsymbol{\lambda_{H2O} = \lambda_{CH3OH}} = 2$).

These positive effects of elevating the pressure can also be seen for concurrent in-situ water removal and in-situ methanol removal. These results can be seen in Figure 39 and Figure 43.

The methanol production is also positively influenced by high pressures in membrane reactors. Assuming a temperature of 230ºC, a H_2/CO_2 molar ratio of 4 and a permeation factor of 2, the methanol production can increase 137% by elevating the operation pressure from 20 to 60 bar (from 9.82 to 23.36 CH_3OH mol/s). Similar improvements can also be founded for other temperatures and H_2/CO_2 molar ratios.

Note that in-situ product removal via membrane reactors can achieve similar methanol yields and production rates as the ones obtained by conventional reactors at less drastic conditions (e.g. lower pressures). For example, only by removing water (permeation factor of 2), the methanol yield could be increased up to 35.12% at 40 bar, whereas the conventional reactor obtains a maximum methanol yield of 24.61% at 60 bar (see Table 12).

This could be translated into potential high operation costs savings and a reduced methanol production cost. To verify this potential, future research works should analyze the investment and construction costs of membrane reactors for renewable methanol production.

5.3 EFFECTS OF H_2/CO_2 MOLAR RATIO ON MEOH YIELD AND METHANOL PRODUCTION

The H_2/CO_2 molar ratio in the feed stream can significantly affect the equilibrium of the reactions. The conventional PFR simulation shows that the methanol yield is positively influenced by high H_2/CO_2 molar ratios. The improvements are especially bigger if H_2/CO_2 molar ratios increase from 1 to 3. Increasing more the H_2/CO_2 molar ratio brings minor improvements. This can be seen in Figure 30, where the slope of the curve reduces as the H_2/CO_2 molar ratio increases.

Assuming a temperature of 230ºC and 60 bar, the methanol yield can increase from 8.22% to 24.63% if the H_2/CO_2 molar ratio is increased from 1 (i.e. $N_{H2}^{in} = 50$, $N_{CO2}^{in} = 50$) to 4 (i.e. $N_{H2}^{in} = 200$, $N_{CO2}^{in} = 50$). Assuming same operation conditions, the methanol production can reach 12.32 mol/s compared to 4.11 mol/s for a molar ratio of 4 and 1, respectively.

This shows that the production of methanol is favored when more H_2 is added to the feed stream. As stated before, the improvements are especially visible up to a H_2/CO_2 ratio of 3 and then levels off, which makes sense considering that the stoichiometric ratio of H_2/ CO_2 is 3 for the methanol synthesis reaction and 1 for RWGS.

The effects of H_2/CO_2 ratio are even greater in case of membrane reactors with in-situ product removal. The increase of the hydrogen in the feed drives the equilibrium to the product side, meaning a higher methanol yield and methanol production rates. This trend can also be seen in Figure 34.

Considering however the high value of hydrogen, one should perform a techno-economical evaluation to estimate the exact optimum H_2/CO_2 ratio. This analysis should balance the additional benefits of excess hydrogen compared to the increased energetic consumption and elevated costs. This is also mentioned in the research work of Zachopoulos et al. [120] when analyzing the performance of a water-sorption reactor.

5.4 EFFECTS OF SIMULTANEOUS METHANOL AND WATER IN-SITU REMOVAL

The simulations are performed for different pressures (20,40,60 bar), temperature ranges ($180 - 340ºC$), water and methanol permeation factors [λ_{H2O}, λ_{CH3OH}] (0,0.4,0.8,1.2,1.6,2) and different H_2/CO_2 ratios (1,2,3,4).

According to the simulations, membrane reactors with in-situ water and methanol removal seem to be especially promising. Both methanol yield and methanol production are maximized when removing both products. This can be seen in Figure 33.

Assuming a pressure of 60 bar, a H_2/CO_2 molar ratio of 4 and a 90% of water and methanol removal, the maximum methanol yield can increase up to 73.91% compared to 24.63% in conventional reactors at same operation conditions (see Table 11).

These degrees of water and methanol removal may be too optimistic with today's membranes but theoretically possible in the future. However, the effects of more realistic degrees of in-situ methanol and water removal (50%) lead to 44% increase in the methanol yield with respect conventional reactors at same operation conditions (see Table 11).

In-situ water and methanol removal also allow higher methanol production rates. Assuming same operation conditions as the mentioned above and a temperature of 260 ºC, the methanol production rate can be increase up to 36.95 mol/s compared to 12.31mol/s (conventional production).

Note however that for the high permeation case (λ_k values of 2), the total number of moles of both methanol and water at the end of the reactor surpass the H_2 ones (see Figure 36 and Appendix D- Table 32). Although this is theoretically possible, it does not seem that could happen under non-ideal conditions. Therefore, it is believed that the methanol production rates may be somewhat overestimated for high λ_k permeation values.

The simulation results confirm the effectivity of in-situ simultaneous methanol and water removal via membrane reactors to circumvent the thermodynamic equilibrium and achieve higher methanol yield and production rates.

Nonetheless, the simultaneous removal of both products brings the need to subsequently separate the methanol from the water subsequently. Therefore, it would be needed to install a separation unit at the reactor outlet, which would lead to higher investment and operating costs. Thus, it is recommended for future research works to study the techno-economic viability of such a process and to evaluate if in reality it is more interesting to remove both products or only one of the two as explained in the following sections.

5.5 EFFECTS OF WATER IN-SITU REMOVAL

To analyze the effects of in-situ water removal on the methanol yield and methanol production rates, the simulations are performed for different pressures (20,40,60 bar), temperature ranges ($180 - 340ºC$), water permeation factors λ_{H2O} (0,0.4,0.8,1.2,1.6,2) and different H_2/CO_2 ratios (1,2,3,4).

The in-situ water removal trough the membrane has a positive impact on the methanol yield. This trend is shown in Figure 39 for a H_2/CO_2 molar ratio of 4 (i.e. $N_{H2}^{in} = 200, N_{H2}^{in} = 50$). Similar to conventional reactors, Figure 39 and Table 12 confirms that in-situ water removal process is enhanced for high pressures and high H_2/CO_2 molar ratios.

According to the simulations, a 60% of water removal can increase the MeOH yield about 22% compared to the respective conventional reactor at 60 bar. Similarly, if 92% of water removal is considered, the methanol yield could be increased up to 46.28% at same pressure conditions (see Table 12).

Removing water can be interesting because one can prevent unwanted methanol reforming reactions and deactivation of the catalyst (since water accelerates crystallization of Cu and ZnO contained in a Cu/ZnO-based catalyst). Although, this last advantage is not important for the presented model, it is interesting in real applications.

As it can be seen in Table 29, a maximum methanol production of 23.14 mol/s can be obtained for 60 bar, H_2/CO_2 molar ratio of 4 and a permeation factor λ_{H2O} of 2 m^{-1}. A conventional reactor would in contrast produce 12.41 mol/s for the same operation conditions and optimal temperature (see Appendix D, Table 17). These values show the effectiveness of in-situ water removal to increase both the methanol production rates and methanol yield.

In case of high λ_{H2O} values (2 m^{-1}), the simulations show that the moles of both water and methanol slightly exceed the H_2 ones at the end of the reactor tubes (see Figure 40 and Appendix D- Table 29). As in the in-situ methanol and water removal case, it is believed that this may not be totally realistic, meaning that the effects of in-situ water removal on methanol production rates may be a little overestimated for high λ_{H2O} values.

5.6 EFFECTS OF METHANOL IN-SITU REMOVAL

As in the previous cases, the simulations are performed for different pressures $(20{,}40{,}60\ bar)$, temperature ranges $(180-340ºC)$, water permeation factors λ_{H2O} $(0{,}0.4{,}0.8{,}1.2{,}1.6{,}2)$ and different H_2/CO_2 ratios $(1{,}2{,}3{,}4)$.

The in-situ water removal trough the membrane has a positive impact on the methanol yield. This trend is shown in Figure 43 for a H_2/CO_2 molar ratio of 4 (i.e. $N_{H2}^{in} = 200, N_{H2}^{in} = 50$). Similar to conventional reactors, Figure 42 and Table 13 confirm that the in-situ methanol removal process is enhanced for high pressures and high H_2/CO_2 molar ratios.

According to the simulations, a 55% of methanol removal can increase the MeOH yield about 17.85% compared to the conventional reactor at 60 bar. Similarly, if 92% of methanol removal is considered, the methanol yield could be increased up to 42.84% at same pressure conditions.

A maximum methanol production of 21.42 mol/s can be obtained for 60 bar, a H_2/CO_2 molar ratio of 4 and a permeation factor λ_{H2O} of 2 m^{-1} (see Appendix D, Table 35). A conventional reactor would in contrast produce 12.42 mol/s for the same operation conditions and optimal

temperature (see Table 17). These values show the effectiveness of water in-situ removal to increase methanol production rates and methanol yield. Furthermore, the removal of methanol would simplify the final product purification, which could be economically interesting and reduce the methanol production costs.

This effect could give this approach a competitive advantage against the in-situ water removal. Therefore, it is recommended for future research works to balance this potential advantage with the minor improvements that in-situ methanol removal brings on both methanol yield and production rates with respect in-situ water removal.

5.7 COMPARISON BETWEEN CONVENTIONAL PLUG FLOW REACTOR (PFR) AND MEMBRANE PLUG FLOW REACTOR FOR METHANOL PRODUCTION

The PFR simulations proved that at practical pressures (20,40,60 bar) and temperatures (180ºC-340ºC) only a low per-pass conversion to methanol can be obtained (<25%). This is demonstrated in Figure 30, where the reactor model was simulated for the operation conditions given in Table 7.

A maximum methanol yield of 24.63% is obtained in the conventional plug flow reactor for a H_2/CO_2 molar ratio equal to 4 (i.e. $N_{H2}^{in} = 200$, $N_{CO2}^{in} = 50$) at 60 bar and 231.71ºC. These results agree with previously published studies [118,119].

The PFR model also allows to visualize the position-dependent molar flow through the reactor and thus, it gives insight on the production of methanol and other subproducts such as water and carbon monoxide.

A maximum conventional methanol production of 12.42 mol/s is obtained at 60 bar, 231.71 ºC and a H_2/CO_2 molar ratio of 4 (i.e. $N_{H2}^{in} = 200\ mol$, $N_{CO2}^{in} = 50\ mol$). These results are depicted in Table 39 and can be visualized in Figure 32. Note that both methanol yield and methanol production are limited by thermodynamics.

Membrane reactors can however circumvent this thermodynamic limitation by removing in-situ the products of the reaction (as the Le Chatelier´s effect on the equilibrium reactions is higher). In this thesis, the in-situ removal of water and/or methanol was explored. Results seem specially promising when both methanol and water are removed, leading to a potential methanol yield of 73.91%, if approximately 90% of the products could be in-situ removed (operation conditions: 60 bar, 259.19 ºC and H_2/CO_2 molar ratio of 4).

At these same operation conditions, the maximum methanol production could reach 36.96 mol/s, leading to a 197% increase with respect the maximum production of the conventional plug flow reactor (12.41 mol/s).

Water seems to be the second most interesting product to be removed. According to the simulations, the methanol yield can increase up to 46.28% by in-situ removing 90% of the produced water (operation conditions: 60 bar, H_2/CO_2 molar ratio of 4). At the same operation conditions, in-situ water removal would lead the methanol yield to reach 30.18%, if only 60% of the water could be removed.

Assuming only in-situ water removal, the maximum methanol production rate can be 23.13 mol/s (see Appendix D, Table 29). This shows that removing both methanol and water could be more interesting to enhance the methanol production. However, one should consider that the methanol critical temperature is around 240 ºC and the membrane reactor achieves this maximum production at 259.19 ºC, meaning that the results of in-situ water and methanol removal case may be a little overestimated for high permeation values (2 m^{-1}). This is further discussed in the following section Model Limitations and Critical Analysis.

Finally, the in-situ methanol removal has also been investigated via model simulation. Results suggest that this approach may be less effective to enhance both methanol yield and production rates. The methanol yield could be increased up to 42.84 if 86% of the methanol could be removed through the membrane. Similarly, if 55% of the methanol is removed, the methanol yield would reach 29.26% (5% more than the conventional methanol yield).

For this approach, the maximum methanol production rate is 21.41 mol/s. As one can see both methanol yield and production rates values are smaller than for in-situ water and simultaneous water and methanol removal.

On the other hand, this process would allow to separate the methanol within the reactor and thus, to save a separation unit at the end of the process and simplify the final product purification. This advantage could be economically interesting from the process perspective. Therefore, it is recommended for future research works to investigate if this advantage can overcome the methanol yield disadvantage and obtain a better methanol production price.

Similarly, the performance of both conventional membrane reactors is enhanced for high pressures and H_2/CO_2 molar ratios. If the pressure is fixed for example to 60 bar in the conventional plug flow reactor, the methanol yield increases from 8.48% to 24.63% by increasing the H_2/CO_2 molar ratio from 1 to 4.

Likewise, if the H_2/CO_2 molar ratio is fixed to 4 and the pressure is elevated from 20 to 60 bar, the maximum methanol yield increased from 10.77% to 24.63%. The same applies to the membrane reactors, where the methanol yield is also increased for high pressures and H_2/CO_2 molar ratios. This correlation is illustrated in Figure 34 for in-situ methanol and water removal.

A comparative analysis of the three mentioned approaches with the conventional reactor is presented bellow in Table 14.

Table 14. Comparative analysis of conventional and membrane reactor, this last with simultaneous in-situ water and methanol removal, in-situ water removal and in-situ methanol removal.

	Pressure [bar]	$\lambda_{H2O}/\lambda_{CH3OH}$ [m^{-1}]	T [ºC]	max MeOH [%]	Max MeOH production [mol/s]
Conventional plug flow reactor	20	0/0	228.48	10.77	5.45
	40	0/0	231.71	18.73	9.45
	60	0/0	231.71	24.63	12.42
PFR with in-situ water removal	20	0.4/0	231.72	13.03	6.51
	40	0.4/0	234.95	22.90	11.45
	60	0.4/0	234.90	30.18	15.09
	20	2/0	241.41	19.53	9.76
	40	2/0	243.03	35.11	17.56
	60	2/0	244.65	46.28	23.14
PFR with in-situ methanol removal	20	0/0.4	234.95	12.80	6.40
	40	0/0.4	236.57	22.30	11.15
	60	0/0.4	238.18	29.26	14.63
	20	0/2	247.88	18.88	9.44
	40	0/2	251.11	33.07	16.54
	60	0/2	252.73	42.84	21.42
PFR with in-situ methanol and water removal	20	0.4/0.4	238.12	15.24	7.62
	40	0.4/0.4	239.79	26.97	13.49
	60	0.4/0.4	241.41	35.57	17.70
	20	2/2	264.04	33.19	16.60
	40	2/2	262.42	58.95	29.48
	60	2/2	259.19	73.91	36.96

5.8 MODEL LIMITATIONS AND CRITICAL ANALYSIS

Note that the model presented in this thesis is a one-dimensional model and therefore, it does not precisely represent the reality. This approach assumes that the temperature and pressure are constant and uniform through the reactor. This is not exactly what will happen in a real reactor, where the temperature and pressure would change along the reactor tubes.

Since the two reactions involved in the methanol synthesis are exothermic, it would be necessary to have a cooling agent to assure that the process is isothermal. This aspect has not been included in the model because it does not affect to the calculations. Other authors have also assumed isothermal behavior to model their processes and methanol reactors [91, 75]. However, in real applications one would not achieve a perfect isothermal process, meaning that our reactor is working in an ideal case and therefore, the results may be overestimated.

Moreover, the parameter λ_k used to model the membrane working principle has its limitations. One should note that this parameter is only a mathematical term to give weight to the in-situ product removal process. A few experimental data on permeability has been found apart from the research works of Gorbe et al. [92], Gallucci et al [93], and Sawamura et al. [90]. This data was unfortunately not implementable in our model. Therefore, it was decided to use this λ_k parameter to estimate how far in-situ product removal could improve the methanol yield and production rates.

This λ_k parameter has been assumed to be constant for both pressure and temperature variations, which is not exactly what would happen a real process with product permeation, since it is subject to little variations for both pressure and temperature changes. The percentage of removal strongly depends on the process parameters such as flow velocity, transmembrane pressure, temperature, and sweep gas (this last if applies). This has not been considered in the analysis, but it is important in real process applications. Therefore, it is recommended for future research works to do a Computational Fluid Dynamics (CFD) membrane reactor model to better simulate the permeability.

Furthermore, the simulations suggest that high degrees of in-situ product removal (around 90%) lead the methanol yield to be achieved at temperatures of 250ºC. Note that this temperature is higher than the methanol critical temperature. This effect may favor the H_2 diffusion in a real membrane, meaning that for high temperatures our results may be overestimated.

Finally, one should also note that the research in membranes suggest that to date less than 50% of the products could be removed. Therefore, although the results for high permeation values (2 m^{-1}) are theoretically possible, they do not seem possible with the current technology.

However, even low permeability values (0.4 m^{-1}) also bring improvements to the process that may reduce the methanol production costs. It is recommended for future research studies to perform a techno-economic analysis in membrane reactors with low permeability capacity.

Despite these limitations, it is believed that the model can predict quickly and effectively the effects of in-situ water and/or methanol removal. Therefore, the model may be used in the future to perform fast calculations and visualize both methanol yield and methanol production rates.

Chapter 6. SUMMARY AND OUTLOOK

In this thesis, the effects of in-situ water and/or methanol removal on both methanol yield and methanol production have been investigated via model simulation. The results confirm that at practical pressures, a low degree of per-pass conversion to methanol can be obtained in the conventional plug flow reactor (<25%). This is because the methanol synthesis is limited thermodynamically.

Membrane reactors could be used to circumvent this thermodynamic limit by in-situ removing the products from the reaction. This shifts the equilibrium towards the products and allows for higher methanol yield and production rates.

The simulations confirm this hypothesis and suggest that membrane reactors have a promising potential for methanol production. The most promising membrane types for methanol production are inorganic membranes and in particular carbon and inorganic zeolite membranes since they can stand the high temperatures and pressures needed for methanol synthesis.

According to the simulations, the methanol yield can be increased up to 73.91%, if both methanol and water are simultaneously in-situ removed from the reaction. This would mean a potential methanol yield improvement of almost 200% with respect conventional reactors.

The simulations also confirm that both methanol yield and methanol production rates are enhanced for high pressures and H_2/CO_2 molar ratios for both membrane and conventional plug flow reactors. The optimal point for both benchmarks is found for 60 bar and a H_2/CO_2 molar ratio of 4. Considering however the high prices of hydrogen, an excess of hydrogen could increase the energetic consumption and elevate the cost of the process. Thus, the optimal H_2/CO_2 molar ratio is a matter of a techno-economical evaluation. It is suggested for future studies to balance the additional benefits of excess hydrogen with its potential costs increase.

Membrane reactors with in-situ water and methanol removal can obtain a methanol production rate of 36.96 mol/s if operated at 60 bar and with a H_2/CO_2 molar ratio of 4. A conventional reactor would in contrast produce 12.41 mol/s for the same operation conditions.

The removing of only water or methanol brings smaller improvements with respect to methanol yield and methanol production rates. According to the simulations, by removing exclusively water from the reactor, membrane reactors could achieve a methanol yield of 46.28% and a methanol production rate of 23.14 mol/s. Similarly, if only methanol is in-situ removed from the reaction, the methanol yield could be increased up to 42.84% and a methanol production rate of 21.42 mol/s.

A reactor with simultaneous in-situ methanol and water removal would need however an extra separation unit with respect reactors with only in-situ water or in-situ methanol removal, which would lead to higher operation and investment costs.

Thus, a techno-economic analysis should be performed in future research works to evaluate if the removal of both products is the most interesting approach. Likewise, the investment costs of membrane reactors should be analyzed to explore if they can achieve competitive methanol prices.

BIBLIOGRAPHY

[1] "CO2 emissions – Global Energy Review 2021 – Analysis - IEA." https://www.iea.org/reports/global-energy-review-2021/co2-emissions (accessed Jun. 26, 2021).

[2] W. Paper, "A universal green fuel," pp. 1–22, 2020.

[3] F. Kublik, A. Stones, M. von Glischinski-Kurc, C. Khong, A. Borggreve, and J. Whysall, "Shell Energy Scenarios: Germany," p. 24, 2017.

[4] "E2Fuels - Lehrstuhl für Energiesysteme." https://www.mw.tum.de/es/forschung/projekte/e2fuels/ (accessed May 01, 2021).

[5] Stefan Siegemund *et al.*, "E-Fuels Study," pp. 1–175, 2017, [Online]. Available: https://www.vda.de/en/services/Publications/«e-fuels»-study---the-potential-of-electricity-based-fuels-for-low-emission-transport-in-the-eu.html.

[6] C. Hobson and C. Márquez, "Renewable Methanol Report," *Methanol Inst.*, vol. 103, no. September, pp. 1–26, 2018, [Online]. Available: http://dx.doi.org/10.1016/j.energy.2016.02.092%0Awww.methanol.orgwww.methanol.org.

[7] International Energy Agency, "Technology Roadmap, Delivering Sustainable Bioenergy", 2017.

[8] I. Ridjan, B. V. Mathiesen, D. Connolly, and N. Duić, "The feasibility of synthetic fuels in renewable energy systems," *Energy*, vol. 57, pp. 76–84, 2013, doi: 10.1016/j.energy.2013.01.046.

[9] P. Schmidt and W. Weindorf, "Power-to-Liquids: Potentials and Perspectives for the Future Supply of Renewable Aviation Fuel," *Ger. Environ. Agency*, no. september,

pp. 1–36, 2016, [Online]. Available: https://www.umweltbundesamt.de/en/publikationen/power-to-liquids-potential-perspectives-for-the.

[10] E. Union, "State of the Art on Alternative Fuels Transport Systems in the European Union," *Futur. Transp. Fuels*, p. 128, 2015, [Online]. Available: https://ec.europa.eu/transport/sites/transport/files/themes/urban/studies/doc/2015-07-alter-fuels-transport-syst-in-eu.pdf%250Ahttp://ec.europa.eu/transport/sites/transport/files/themes/urban/studies/doc/2015-07-alter-fuels-transport-syst-in-eu.pdf.

[11] "Hydrogen Solutions | Renewable Energy | Siemens Energy Global." https://www.siemens-energy.com/global/en/offerings/renewable-energy/hydrogen-solutions.html?gclid=EAIaIQobChMI5Z69uOaR8gIVFs93Ch2LzQr-EAAYASAAEgJZc_D_BwE (accessed Aug. 02, 2021).

[12] D. Chiaramonti, "Sustainable aviation fuels: The challenge of decarbonization," *Energy Procedia*, vol. 158, pp. 1202–1207, 2019, doi: 10.1016/j.egypro.2019.01.308.

[13] J. Scheelhaase, S. Maertens, and W. Grimme, "Synthetic fuels in aviation - Current barriers and potential political measures," *Transp. Res. Procedia*, vol. 43, pp. 21–30, 2019, doi: 10.1016/j.trpro.2019.12.015.

[14] "Initial IMO GHG Strategy." https://www.imo.org/en/MediaCentre/HotTopics/Pages/Reducing-greenhouse-gas-emissions-from-ships.aspx (accessed Aug. 01, 2021).

[15] C. J. McKinlay, S. R. Turnock, and D. A. Hudson, "Route to zero emission shipping: Hydrogen, ammonia or methanol?," *Int. J. Hydrogen Energy*, vol. 46, no. 55, pp. 28282–28297, Aug. 2021, doi: 10.1016/J.IJHYDENE.2021.06.066.

[16] H. Lund and E. Münster, "Integrated transportation and energy sector CO2 emission control strategies," *Transp. Policy*, vol. 13, no. 5, pp. 426–433, 2006, doi:

10.1016/j.tranpol.2006.03.003.

[17] E. Pursiheimo, H. Holttinen, and T. Koljonen, "Inter-sectoral effects of high renewable energy share in global energy system," *Renew. Energy*, pp. 1119–1129, 2019, doi: 10.1016/j.renene.2018.09.082.

[18] M. Moser *et al.*, "Synthetic Liquid Hydrocarbons from Renewable Energy – Results of the Helmholtz Energy Alliance," *Chemie-Ingenieur-Technik*, vol. 89, no. 3, pp. 274–288, 2017, doi: 10.1002/cite.201500154.

[19] C. Change and R. Communities, "Integration erneuerbarer Energien durch Sektorkopplung: Analyse zu technischen Sektorkopplungsoptionen," 2019.

[20] T. Pregger *et al.*, "Future Fuels—Analyses of the Future Prospects of Renewable Synthetic Fuels," *Energies*, vol. 13, no. 138, pp. 1–36, 2020.

[21] A. Santasalo-Aarnio *et al.*, "Application of Synthetic Renewable Methanol to Power the Future Propulsion," *SAE Tech. Pap. Ser.*, vol. 1, Sep. 2020, doi: 10.4271/2020-01-2151.

[22] K. Räuchle, L. Plass, H. J. Wernicke, and M. Bertau, "Methanol for Renewable Energy Storage and Utilization," *Energy Technol.*, vol. 4, no. 1, pp. 193–200, 2016, doi: 10.1002/ente.201500322.

[23] E. Moioli, R. Mutschler, and A. Züttel, "Renewable energy storage via CO2 and H2 conversion to methane and methanol: Assessment for small scale applications," *Renew. Sustain. Energy Rev.*, vol. 107, no. March, pp. 497–506, 2019, doi: 10.1016/j.rser.2019.03.022.

[24] S. S. Araya *et al.*, "A review of the methanol economy: The fuel cell route," *Energies*, vol. 13, no. 3, 2020, doi: 10.3390/en13030596.

[25] G. A. Olah, "Towards oil independence through renewable methanol chemistry," *Angew. Chemie - Int. Ed.*, vol. 52, no. 1, pp. 104–107, 2013, doi:

10.1002/anie.201204995.

[26] Q. I. Roode-Gutzmer, D. Kaiser, and M. Bertau, "Renewable Methanol Synthesis," *ChemBioEng Rev.*, vol. 6, no. 6, pp. 209–236, 2019, doi: 10.1002/cben.201900012.

[27] "Communications materials – United Nations Sustainable Development." https://www.un.org/sustainabledevelopment/news/communications-material/ (accessed May 01, 2021).

[28] G. Buffo, P. Marocco, D. Ferrero, A. Lanzini, and M. Santarelli, *Power-to-X and power-to-power routes*. Elsevier Inc., 2019.

[29] IRENA, *Innovation landscape for a renewable-powered future: Solutions to integrate variable renewables*. 2019.

[30] "BMWi Newsletter Energiewende - Was bedeutet 'Sektorkopplung'?" https://www.bmwi-energiewende.de/EWD/Redaktion/Newsletter/2016/14/Meldung/direkt-erklaert.html (accessed Sep. 28, 2020).

[31] "DVGW: Sektorenkopplung." https://www.dvgw.de/themen/energiewende/sektorenkopplung/ (accessed Sep. 28, 2020).

[32] "Positionspapier: 10 Thesen zur Sektorkopplung | BDEW." https://www.bdew.de/service/stellungnahmen/10-thesen-sektorkopplung/ (accessed Sep. 28, 2020).

[33] Siemens, "Power-to-X: The crucial business on the way to a carbon-free world," 2021, [Online]. Available: file:///C:/Users/Sony/Downloads/20211202_Power-to-X-white-paper.pdf.

[34] M. Robinius *et al.*, "Linking the power and transport sectors - Part 1: The principle of sector coupling," *Energies*, vol. 10, no. 7, 2017, doi: 10.3390/en10070956.

[35] M. Robinius *et al.*, "Linking the power and transport sectors - Part 2: Modelling a sector coupling scenario for Germany," *Energies*, vol. 10, no. 7, pp. 1–23, 2017, doi: 10.3390/en10070957.

[36] G. A. Olah, "Beyond oil and gas: The methanol economy," *Angew. Chemie - Int. Ed.*, vol. 44, no. 18, pp. 2636–2639, 2005, doi: 10.1002/anie.200462121.

[37] G. A. Olah, "After oil and gas: Methanol economy," *Catal. Letters*, vol. 93, no. 1–2, pp. 1–2, 2004, doi: 10.1023/b:catl.0000017043.93210.9c.

[38] A. Goeppert, G. A. Olah, and G. K. Surya Prakash, *Toward a Sustainable Carbon Cycle: The Methanol Economy*. Elsevier Inc., 2018.

[39] "Chemical Energy Storage - Google Libros." https://books.google.de/books?hl=es&lr=&id=Fm9PdzVCA34C&oi=fnd&pg=PR15&dq=Schlögl+R.+Chemical+energy+storage.+Berlin/Boston:+Walter+de+Gruyter%3B+2013&ots=yYyxjwXnR_&sig=5YWikQZm6TqXP3iXRGkBSpbAiX0&redir_esc=y#v=onepage&q&f=false (accessed Aug. 03, 2021).

[40] "Beyond Oil and Gas: The Methanol Economy - George A. Olah, Alain Goeppert, G. K. Surya Prakash - Google Libros." https://books.google.de/books?hl=es&lr=&id=T4VqDwAAQBAJ&oi=fnd&pg=PR13&dq=Olah+GA,+Goeppert+A,+Prakash+GKS.+Beyond+oil+and+gas:+the+methanol+economy.+2nd+ed.+Weinheim,+Germany:+Wiley-VCH%3B+2009&ots=A85M_kwpG2&sig=2-FbnYHUeGb8lo2fQ6GSR4RDpng&redir_esc=y#v=onepage&q&f=false (accessed Aug. 03, 2021).

[41] W. W. Clark and J. Rifkin, "A green hydrogen economy," *Energy Policy*, vol. 34, no. 17, pp. 2630–2639, 2006, doi: 10.1016/j.enpol.2005.06.024.

[42] A. Loh, "Development of Electrocatalysts for Oxygen Electrodes in Alkaline Electrochemical Systems," no. April, 2019.

[43] A. Ursúa, L. M. Gandía, and P. Sanchis, "Hydrogen production from water electrolysis: Current status and future trends," *Proc. IEEE*, vol. 100, no. 2, pp. 410–426, 2012, doi: 10.1109/JPROC.2011.2156750.

[44] U. Bossel, "Does a hydrogen economy make sense?," *Proc. IEEE*, vol. 94, no. 10, pp. 1826–1836, 2006, doi: 10.1109/JPROC.2006.883715.

[45] T. Miller, T. Beer, T. Grant, D. Batten, D. Lamb, and D. Trimm, "Methanol as an alternative transport fuel," *Proc. 14th Int. Union Air Pollut. Prev. Environ. Prot. Assoc. World Congr. 2007, 18th Clean Air Soc. Aust. New Zeal. Conf.*, no. 4000096701, 2007.

[46] L. Bromberg and D. Cohn, "Alcohol fueled heavy duty vehicles using clean, high efficiency engines," *SAE Tech. Pap.*, 2010, doi: 10.4271/2010-01-2199.

[47] "Heavy Duty Vehicles Using Clean, High Efficiency Alcohol Engines," 2010.

[48] S. Gupta and D. N. Shrivastava, "Emission Evaluation of Diesel Engine with Carbureted Methanol," *Int. J. Contemp. Res. Rev.*, no. June, pp. 2–7, 2017, doi: 10.15520/ijcrr/2017/8/07/284.

[49] T. A. Semelsberger, R. L. Borup, and H. L. Greene, "Dimethyl ether (DME) as an alternative fuel," *J. Power Sources*, vol. 156, no. 2, pp. 497–511, 2006, doi: 10.1016/j.jpowsour.2005.05.082.

[50] C. Arcoumanis, C. Bae, R. Crookes, and E. Kinoshita, "The potential of di-methyl ether (DME) as an alternative fuel for compression-ignition engines: A review," *Fuel*, vol. 87, no. 7, pp. 1014–1030, 2008, doi: 10.1016/j.fuel.2007.06.007.

[51] GE, "Feasibility of Methanol as Gas Turbine Fuel," *GE position Pap.*, no. 2, pp. 2–5, 2001.

[52] D. LIEDERMAN, S. YURCHAK, J. C. W. KUO, and W. LEE, "Mobil Methanol-To-Gasoline Process.," *J Energy*, vol. V 6, no. N 5, pp. 340–341, 1982, doi:

10.2514/3.62614.

[53] "The Methanol Industry|Methanol Institute|www.methanol.org." https://www.methanol.org/the-methanol-industry/ (accessed Aug. 03, 2021).

[54] "Renewable Methanol | METHANOL INSTITUTE." https://www.methanol.org/renewable/ (accessed Aug. 03, 2021).

[55] "Haru Oni Hydrogen Project - fuel from wind and water | Hydrogen Solutions | Siemens Energy Global." https://www.siemens-energy.com/global/en/offerings/renewable-energy/hydrogen-solutions/haru-oni.html (accessed Aug. 04, 2021).

[56] "BMWi - Federal Ministry for Economic Affairs and Energy - 'Haru Oni' PtX project Minister Altmaier hands over first approval notice for international green hydrogen project." https://www.bmwi.de/Redaktion/EN/Pressemitteilungen/2020/12/20201202-haru-oni-ptx-project-minister-altmaier-hands-over-first-approval-notice-for-international-green-hydrogen-project.html (accessed Aug. 04, 2021).

[57] G. H. Graaf, E. J. Stamhuis, and A. A. C. M. Beenackers, "Kinetics of low-pressure methanol synthesis," *Chem. Eng. Sci.*, vol. 43, no. 12, pp. 3185–3195, 1988, doi: 10.1016/0009-2509(88)85127-3.

[58] K. M. Vanden Bussche and G. F. Froment, "A steady-state kinetic model for methanol synthesis and the water gas shift reaction on a commercial Cu/ZnO/Al2O3 catalyst," *J. Catal.*, vol. 161, no. 1, pp. 1–10, 1996, doi: 10.1006/jcat.1996.0156.

[59] P. Villa, P. Forzattl, G. Buzzl-Ferrarls, G. Garone, and I. Pasquon, "Synthesis of Alcohols from Carbon Oxides and Hydrogen. 1. Kinetics of the Low-Pressure Methanol Synthesis," *Ind. Eng. Chem. Process Des. Dev.*, vol. 24, no. 1, pp. 12–19, 1985, doi: 10.1021/i200028a003.

[60] C. Seidel, A. Jörke, B. Vollbrecht, A. Seidel-Morgenstern, and A. Kienle, "Kinetic modeling of methanol synthesis from renewable resources," *Chem. Eng. Sci.*, vol. 175, pp. 130–138, 2018, doi: 10.1016/j.ces.2017.09.043.

[61] J. J. Meyer, P. Tan, A. Apfelbacher, R. Daschner, and A. Hornung, "Modeling of a Methanol Synthesis Reactor for Storage of Renewable Energy and Conversion of CO2 - Comparison of Two Kinetic Models," *Chem. Eng. Technol.*, vol. 39, no. 2, pp. 233–245, 2016, doi: 10.1002/ceat.201500084.

[62] M. A. McNeil, C. J. Schack, and R. G. Rinker, "Methanol synthesis from hydrogen, carbon monoxide and carbon dioxide over a CuO/ZnO/Al2O3 catalyst. II. Development of a phenomenological rate expression," *Appl. Catal.*, vol. 50, no. 1, pp. 265–285, 1989, doi: 10.1016/S0166-9834(00)80841-6.

[63] T. A. Henkel, "Modellierung von Reaktion und Stofftransport in geformten Katalysatoren am Beispiel der Methanolsynthese," p. 210, 2011.

[64] M. Takagawa and M. Ohsugi, "Study on reaction rates for methanol synthesis from carbon monoxide, carbon dioxide, and hydrogen," *J. Catal.*, vol. 107, no. 1, pp. 161–172, 1987, doi: 10.1016/0021-9517(87)90281-8.

[65] Y. Slotboom *et al.*, "ºCritical assessment of steady-state kinetic models for the synthesis of methanol over an industrial Cu/ZnO/Al2O3 catalyst," *Chem. Eng. J.*, vol. 389, no. January, p. 124181, 2020, doi: 10.1016/j.cej.2020.124181.

[66] K. Klier, V. Chatikavanij, R. G. Herman, and G. W. Simmons, "Catalytic synthesis of methanol from CO H2. IV. The effects of carbon dioxide," *J. Catal.*, vol. 74, no. 2, pp. 343–360, 1982, doi: 10.1016/0021-9517(82)90040-9.

[67] J. Skrzypek, M. Lachowska, and H. Moroz, "Kinetics of methanol synthesis over commercial copper/zinc oxide/alumina catalysts," *Chem. Eng. Sci.*, vol. 46, no. 11, pp. 2809–2813, 1991, doi: 10.1016/0009-2509(91)85150-V.

[68] "Asgard Model.pdf." .

[69] T. Kubota *et al.*, "Kinetic study of methanol synthesis from carbon dioxide and hydrogen," *Appl. Organomet. Chem.*, vol. 15, no. 2, pp. 121–126, 2001, doi: 10.1002/1099-0739(200102)15:2<121::aid-aoc106>3.0.co;2-3.

[70] G. H. Graaf, H. Scholtens, E. J. Stamhuis, and A. A. C. M. Beenackers, "Intra-particle diffusion limitations in low-pressure methanol synthesis," *Chem. Eng. Sci.*, vol. 45, no. 4, pp. 773–783, 1990, doi: 10.1016/0009-2509(90)85001-T.

[71] C. V. Miguel, M. A. Soria, A. Mendes, and L. M. Madeira, "Direct CO2 hydrogenation to methane or methanol from post-combustion exhaust streams - A thermodynamic study," *J. Nat. Gas Sci. Eng.*, vol. 22, pp. 1–8, 2015, doi: 10.1016/j.jngse.2014.11.010.

[72] J. Atkins, Peter W. / de Paula, *Atkins: Physikalische Chemie*. Wiley-VCH, 2013.

[73] T. Swaddle, *Inorganic Chemistry: An Industrial and Environmental Perspective*, no. 1. University of Calgary, Alberta, Canada: Press, Academic, 1997.

[74] "The Reaction Quotient - Chemistry LibreTexts." https://chem.libretexts.org/Bookshelves/Physical_and_Theoretical_Chemistry_Textbook_Maps/Supplemental_Modules_(Physical_and_Theoretical_Chemistry)/Equilibria/Chemical_Equilibria/The_Reaction_Quotient (accessed Aug. 16, 2021).

[75] J. Terreni, A. Borgschulte, M. Hillestad, and B. D. Patterson, "Understanding catalysis—a simplified simulation of catalytic reactors for CO2 reduction," *ChemEngineering*, vol. 4, no. 4, pp. 1–16, 2020, doi: 10.3390/chemengineering4040062.

[76] K. Stangeland, H. Li, and Z. Yu, *Thermodynamic Analysis of Chemical and Phase Equilibria in CO2 Hydrogenation to Methanol, Dimethyl Ether, and Higher Alcohols*, vol. 57, no. 11. 2018.

[77] J. Skrzypek, M. Lachowska, and D. Serafin, "Methanol synthesis from CO2 and H2: dependence of equilibrium conversions and exit equilibrium concentrations of components on the main process variables," *Chem. Eng. Sci.*, vol. 45, no. 1, pp. 89–96, 1990, doi: 10.1016/0009-2509(90)87083-5.

[78] R. Haubrichs and P. L. Zaffalon, *Johnson Matthey Technology Review: Methanol Production – A Technical History*, vol. 61, no. 3. 2017.

[79] F. Gallucci, *Inorganic Membrane Reactors for Methanol Synthesis*. Elsevier B.V., 2018.

[80] "German Patent 565,309_Verfahren Zur Darstellung von Methanol und Seinen Homologen. .pdf." .

[81] P. J. A. Tijm, F. J. Waller, and D. M. Brown, "Methanol technology developments for the new millennium," *Appl. Catal. A Gen.*, vol. 221, no. 1–2, pp. 275–282, 2001, doi: 10.1016/S0926-860X(01)00805-5.

[82] G. Liu, D. Willcox, M. Garland, and H. H. Kung, "The role of CO2 in methanol synthesis on CuZn oxide: An isotope labeling study," *J. Catal.*, vol. 96, no. 1, pp. 251–260, 1985, doi: 10.1016/0021-9517(85)90378-1.

[83] M. W. dorn * R.P.W.J. Struis, S. Stucki, "A membrane re actor for me thanol synthesis," 1996.

[84] M. A. Llosa Tanco, D. A. Pacheco Tanaka, and A. Mendes, "Composite-alumina-carbon molecular sieve membranes prepared from novolac resin and boehmite. Part II: Effect of the carbonization temperature on the gas permeation properties," *Int. J. Hydrogen Energy*, vol. 40, no. 8, pp. 3485–3496, 2015, doi: 10.1016/j.ijhydene.2014.11.025.

[85] B. Zhang, D. Zhao, Y. Wu, H. Liu, T. Wang, and J. Qiu, "Fabrication and application of catalytic carbon membranes for hydrogen production from methanol steam

reforming," *Ind. Eng. Chem. Res.*, vol. 54, no. 2, pp. 623–632, 2015, doi: 10.1021/ie503094r.

[86] S. Tanaka, T. Yasuda, Y. Katayama, and Y. Miyake, "Pervaporation dehydration performance of microporous carbon membranes prepared from resorcinol/formaldehyde polymer," *J. Memb. Sci.*, vol. 379, no. 1–2, pp. 52–59, 2011, doi: 10.1016/j.memsci.2011.05.046.

[87] "Carbon membranes - Fraunhofer IKTS." https://www.ikts.fraunhofer.de/en/departments/environmental_process_engineering/nanoporous_membranes/zeolite_carbon_membranes/carbon_membranes_new.html (accessed Jul. 03, 2021).

[88] "Increased Product yield through the use of membrane reactors." https://www.ikts.fraunhofer.de/content/dam/ikts/downloads/annual_reports/jb2017/34_Increased_product_yield_through_the_use_of_membrane_reactors.pdf (accessed Jul. 03, 2021).

[89] Dr. rer. nat. Adrian Simon, "Increased product yield through the use of membrane reactors - Fraunhofer IKTS." https://www.ikts.fraunhofer.de/en/departments/environmental_process_engineering/nanoporous_membranes/zeolite_carbon_membranes/increased_product_yield_membrane_reactors.html (accessed May 02, 2021).

[90] K. I. Sawamura, T. Shirai, M. Takada, Y. Sekine, E. Kikuchi, and M. Matsukata, "Selective permeation and separation of steam from water-methanol-hydrogen gas mixtures through mordenite membrane," *Catal. Today*, vol. 132, no. 1–4, pp. 182–187, 2008, doi: 10.1016/j.cattod.2007.12.005.

[91] G. Chen and Q. Yuan, "Methanol synthesis from CO2 using a silicone rubber/ceramic composite membrane reactor," *Sep. Purif. Technol.*, vol. 34, no. 1–3, pp. 227–237, 2004, doi: 10.1016/S1383-5866(03)00195-3.

[92] J. Gorbe *et al.*, "Preliminary study on the feasibility of using a zeolite A membrane in a membrane reactor for methanol production," *Sep. Purif. Technol.*, vol. 200, pp. 164–168, 2018, doi: 10.1016/j.seppur.2018.02.036.

[93] F. Gallucci, L. Paturzo, and A. Basile, "An experimental study of CO2 hydrogenation into methanol involving a zeolite membrane reactor," *Chem. Eng. Process. Process Intensif.*, vol. 43, no. 8, pp. 1029–1036, 2004, doi: 10.1016/j.cep.2003.10.005.

[94] L. G. J. Van Der Ham, H. Van Den Berg, A. Benneker, G. Simmelink, J. Timmer, and S. Van Weerden, "Hydrogenation of carbon dioxide for methanol production," *Chem. Eng. Trans.*, vol. 29, no. 3, pp. 181–186, 2012, doi: 10.3303/CET1229031.

[95] G. Leonzio, E. Zondervan, and P. U. Foscolo, "Methanol production by CO2 hydrogenation: Analysis and simulation of reactor performance," *Int. J. Hydrogen Energy*, vol. 44, no. 16, pp. 7915–7933, 2019, doi: 10.1016/j.ijhydene.2019.02.056.

[96] L. Yu, C. Zeng, C. Wang, and L. Zhang, "In situ impregnation−gelation−hydrothermal crystallization synthesis of hollow fiber zeolite NaA membrane," *Microporous Mesoporous Mater.*, vol. 244, pp. 278–283, 2017, doi: 10.1016/j.micromeso.2016.10.047.

[97] M. Danesh-Khorasgani and A. Nezamzadeh-Ejhieh, "PVC-zeolite nanoparticle-surfactant anion exchanger membrane: preparation, characterization, and its application in development of ion-selective electrode for detection of sulfate," *J. Solid State Electrochem.*, vol. 20, no. 10, pp. 2827–2833, 2016, doi: 10.1007/s10008-016-3265-9.

[98] C. Pagis, A. R. Morgado Prates, D. Farrusseng, N. Bats, and A. Tuel, "Hollow Zeolite Structures: An Overview of Synthesis Methods," *Chem. Mater.*, vol. 28, no. 15, pp. 5205–5223, 2016, doi: 10.1021/acs.chemmater.6b02172.

[99] R. Dragomirova and S. Wohlrab, "Zeolite membranes in catalysis—From separate units to particle coatings," *Catalysts*, vol. 5, no. 4, pp. 2161–2222, 2015, doi:

10.3390/catal5042161.

[100] S. Daer, J. Kharraz, A. Giwa, and S. W. Hasan, "Recent applications of nanomaterials in water desalination: A critical review and future opportunities," *Desalination*, vol. 367, pp. 37–48, 2015, doi: 10.1016/j.desal.2015.03.030.

[101] J. Caro, *Supported Zeolite and MOF Molecular Sieve Membranes: Preparation, Characterization, Application*. Elsevier B.V., 2016.

[102] A. Tavolaro and P. Tavolaro, "The preparation of transition metal-containing mordenite catalytic tubular composite membranes," *Catal. Commun.*, vol. 10, no. 5, pp. 586–591, 2009, doi: 10.1016/j.catcom.2008.10.041.

[103] Z. A. E. P. Vroon, K. Keizer, A. J. Burggraaf, and H. Verweij, "Preparation and characterization of thin zeolite MFI membranes on porous supports," *J. Memb. Sci.*, vol. 144, no. 1–2, pp. 65–76, 1998, doi: 10.1016/S0376-7388(98)00035-0.

[104] S. J. Kim *et al.*, "One-Step Synthesis of Zeolite Membranes Containing Catalytic Metal Nanoclusters," *ACS Appl. Mater. Interfaces*, vol. 8, no. 37, pp. 24671–24681, 2016, doi: 10.1021/acsami.6b06576.

[105] "Fausto Gallucci." https://www.tue.nl/en/research/researchers/fausto-gallucci/ (accessed Aug. 12, 2021).

[106] "Fundamental Concepts in Heterogeneous Catalysis - Jens K. Nørskov, Felix Studt, Frank Abild-Pedersen, Thomas Bligaard - Google Libros." https://books.google.de/books?hl=es&lr=&id=BiZeBAAAQBAJ&oi=fnd&pg=PT22&dq=Nørskov,+J.K.%3B+Studt,+F.%3B+Abild-Pedersen,+F.%3B+Bligaard,+T.+Fundamental+Concepts+in+Heterogeneous+Catalysis%3B+John+Wiley+%26+Sons,+Inc.:+Hoboken,+NJ,+USA,+2014&ots=UgDeSSrskO&sig=LNIe5C28UuG0zJ9c3YG8VNlZc9E&redir_esc=y#v=onepage&q&f=false (accessed Aug. 04, 2021).

[107] S. R. Logan, "The origin and status of the arrhenius equation," *J. Chem. Educ.*, vol. 59, no. 4, pp. 279–281, 1982, doi: 10.1021/ed059p279.

[108] G. Saville, "GIBBS-DALTON LAW," *A-to-Z Guid. to Thermodyn. Heat Mass Transf. Fluids Eng.*, Jul. 2008, doi: 10.1615/ATOZ.G.GIBBS-DALTON_LAW.

[109] J. Gillespie, "THE GIBBS-DALTON LAKV OF PARTIAL PRESSURES," vol. 36, no. 242, 1930.

[110] "Plug Flow Reactor | Vapourtec Ltd." https://www.vapourtec.com/flow-chemistry/plug-flow-reactor/ (accessed Aug. 06, 2021).

[111] D. Constales, G. S. Yablonsky, D. R. D'hooge, J. W. Thybaut, and G. B. Marin, *Complex Reactions: Kinetics and Mechanisms – Ordinary Differential Equations – Graph Theory*. 2017.

[112] J. Wu, M. Saito, M. Takeuchi, and T. Watanabe, "The stability of Cu/ZnO-based catalysts in methanol synthesis from a CO2-rich feed and from a CO-rich feed," *Appl. Catal. A Gen.*, vol. 218, no. 1–2, pp. 235–240, 2001, doi: 10.1016/S0926-860X(01)00650-0.

[113] B. T. Carvill, J. R. Hufton, M. Anand, and S. Sircar, "Sorption-Enhanced Reaction Process," *AIChE J.*, vol. 42, no. 10, pp. 2765–2772, 1996, doi: 10.1002/aic.690421008.

[114] "Applications for Python | Python.org." https://www.python.org/about/apps/ (accessed Aug. 09, 2021).

[115] "Solve Differential Equations with ODEINT." https://apmonitor.com/pdc/index.php/Main/SolveDifferentialEquations (accessed Aug. 09, 2021).

[116] "scipy.integrate.odeint — SciPy v1.7.1 Manual." https://docs.scipy.org/doc/scipy/reference/generated/scipy.integrate.odeint.html

(accessed Aug. 09, 2021).

[117] É. S. Van-Dal and C. Bouallou, "Design and simulation of a methanol production plant from CO2 hydrogenation," *J. Clean. Prod.*, vol. 57, pp. 38–45, 2013, doi: 10.1016/j.jclepro.2013.06.008.

[118] J. Toyir *et al.*, "Sustainable process for the production of methanol from CO2 and H2 using Cu/ZnO-based multicomponent catalyst," *Phys. Procedia*, vol. 2, no. 3, pp. 1075–1079, 2009, doi: 10.1016/j.phpro.2009.11.065.

[119] R. Gaikwad, A. Bansode, and A. Urakawa, "High-pressure advantages in stoichiometric hydrogenation of carbon dioxide to methanol," *J. Catal.*, vol. 343, pp. 127–132, 2016, doi: 10.1016/j.jcat.2016.02.005.

[120] A. Zachopoulos and E. Heracleous, "Overcoming the equilibrium barriers of CO2 hydrogenation to methanol via water sorption: A thermodynamic analysis," *J. CO2 Util.*, vol. 21, no. August, pp. 360–367, 2017, doi: 10.1016/j.jcou.2017.06.007.

APPENDIX A

```
#!/usr/bin/env python3
# -*- coding: utf-8 -*-
"""
V1
Created on Tue Jul  6 12:14:29 2021

@author: ignaciolaizquereda
"""

# -*- coding: utf-8 -*-
"""
Plug Flow Reactor (PFR)  based on the Graaf Kinetic Model -> Results based on
Position [m]

Set Up
"""
# Packages import
import math
from sympy import integrate, init_printing
init_printing(use_latex="mathjax")
from sympy import pi
import numpy as np
import matplotlib.pyplot as plt
from scipy.integrate import odeint
from matplotlib import cm
from matplotlib.ticker import LinearLocator, FormatStrFormatter
import pandas as pd
pd.plotting.register_matplotlib_converters()
import matplotlib.pyplot as plt
import seaborn as sns
print("Setup Complete")

#Reactor Type: Plug Flow Reactor (PFR)

ro_catalyst = 1000 #kg/m^3
number_tubes = 10000
diameter_reactor = 0.02 #meter
A_tubes= (np.pi*(diameter_reactor/2)**2)*number_tubes #m2
length = 30 #meter
T = 230 + 273 #K
P = 40 #bar
Pa = P* 100000
R = 8.314462618 #J/mol.K

print("Reactor Specifications Complete")
```

```
# ------------------------------------------------------------------------------
------------------------------------------------------------#
# Definition of the differential equations
def dy(y,x):

    # y' is in this case the array in which all data are stored
    NCO2 = y[0]
    NH2 = y[1]
    NCH3OH = y[2]
    NH2O = y[3]
    NCO = y[4]

    Ntotal = NCO2 + NH2 + NCH3OH + NH2O + NCO


    # Error messages are bypassed here, because in some reaction rates the root
must be taken. This avoids negative numbers.
    if NCO2 < 0:
        NCO2 = 0
    if NH2 < 0:
        NH2 = 0
    if NCH3OH < 0:
        NCH3OH = 0
    if NH2O < 0:
        NH2O = 0
    if NCO < 0:
        NCO = 0

    # Error messages are bypassed here, because in some reaction rates the
pressure can be infinite
    if NCO2 == 0:
        PCO2 = 0
    else:
        PCO2 = (NCO2/Ntotal)*P

    if NH2 == 0:
        PH2 = 0
    else:
        PH2 = (NH2/Ntotal)*P

    if NCH3OH == 0:
        PCH3OH = 0
    else:
        PCH3OH = (NCH3OH/Ntotal)*P

    if NH2O == 0:
        PH2O = 0
    else:
        PH2O = (NH2O/Ntotal)*P


    if NCO == 0:
        PCO = 0
```

```
    else:
        PCO = (NCO/Ntotal)*P

    # Arrhenius parameters for the temperature-dependent factors in the model of
the kinetics of methanol production according to Graaf
    K1eq = 2.39*10**(-13)*np.exp((9.84*10**4)/(R*T))
    K2eq = 1.07*10**(2)*np.exp((-3.91*10**4)/(R*T))
    K3eq = 2.56*10**(-11)*np.exp((5.87*10**4)/(R*T))
    k1 = 4.89*10**(7)*np.exp((-1.13*10**5)/(R*T))
    k2 = 9.64*10**(11)*np.exp((-1.53*10**5)/(R*T))
    k3 = 1.09*10**(5)*np.exp((-0.875*10**5)/(R*T))
    KCO = 2.16*10**(-5)*np.exp((0.468*10**5)/(R*T))
    KCO2 = 7.05*10**(-7)*np.exp((0.617*10**5)/(R*T))
    KH2O_KH2_05 = 6.37*10**(-9)*np.exp((0.840*10**5)/(R*T))


    # kinetics of the reduction of CO2 to methanol over a Cu/ZnO/Al2O3 catalyst
modeled by Graaf

    denom = (1 + KCO*PCO+KCO2*PCO2)*(PH2**(1/2)+(KH2O_KH2_05)*PH2O)

    r1 = k1*KCO*(PCO*PH2**(3/2)-(PCH3OH*PH2O)/(PH2**(1/2)*K1eq))/denom
    r2 = k2*KCO2*(PCO2*PH2-(PH2O*PCO)/K2eq)/denom
    r3 = k3*KCO2*(PCO2*PH2**(3/2)-(PCH3OH*PH2O)/(PH2**(3/2)*K3eq))/denom

    # Definition of the ODEs in the order in which the y-array was defined
    dNCO2dx = ro_catalyst*A_tubes*(-r2-r3)
    dNH2dx = ro_catalyst*A_tubes*(-2*r1-r2-3*r3)
    dNCH3OHdx = ro_catalyst*A_tubes*(r1+r3)
    dNH2Odx = ro_catalyst*A_tubes*(r2+r3)
    dNCOdx = ro_catalyst*A_tubes*(-r1+r2) #(P/P0_CO)*(Ntotal/NCO)
    #dNtotaldx = dNCO2dx + dNH2dx + dNCH3OHdx + dNH2Odx + dNCOdx


    return [dNCO2dx, dNH2dx, dNCH3OHdx, dNH2Odx, dNCOdx]

# Initial Conditions
y0H2 = 200
y0CO2 = 50
y0 = [y0CO2,y0H2,0,0,0]

# Creation of the x interval within the reactor
x = np.linspace(0,length,1000)

# ODEs are integrated by means of odeint, the initial values must be placed in
the square brackets in the correct order as they are for y.
y = odeint(dy,y0,x,mxstep=50000,full_output=0)

#Creating a DataFrame with the results
Results = pd.DataFrame(y)
Results.insert(0,"Position [m]", x, True)
#Renaming the columns of the dataframe
Results = Results.rename(columns={0:'NCO2',1:'NH2',2:'NCH3OH',3:'NH2O',4:'NCO'})
```

```
Results = Results.set_index('Position [m]')
#Showing the Results in a table and saving the data in arrays
print(Results)

NCO2 = Results['NCO2'].values
NH2 = Results['NH2'].values
NCH3OH = Results['NCH3OH'].values
NH2O = Results['NH2O'].values
NCO = Results['NCO'].values

#Plotting the data - Line Chart showing the moles streams trough the reactor
position (x)

# Set the width and height of the figure
plt.figure(figsize=(14,6))
plt.yscale("log")
plt.xscale("log")
#plt.xlim(0.01, 100)
# Add title
plt.title("Position-dependent component molar flow rates in a plug flow reactor")

sns.lineplot(data=Results)
```

APPENDIX B

```
#!/usr/bin/env python3
# -*- coding: utf-8 -*-
"""
Created on Tue Jul 6 12:14:29 2021

@author: ignaciolaizquereda
"""
# -*- coding: utf-8 -*-
"""
Membrane Plug Flow Reactor (PFR)  based on the Graaf Kinetic Model -> Results
based on Position [m]

Set Up
"""
# Packages import
import math
from sympy import integrate, init_printing
init_printing(use_latex="mathjax")
from sympy import pi
import numpy as np
import matplotlib.pyplot as plt
from scipy.integrate import odeint
from matplotlib import cm
from matplotlib.ticker import LinearLocator, FormatStrFormatter
import pandas as pd
pd.plotting.register_matplotlib_converters()
import matplotlib.pyplot as plt
import seaborn as sns
print("Setup Complete")


#Reactor Specifications - Reactor Type: Plug Flow Reactor (PFR)
ro_catalyst = 1000 #kg/m^3
number_tubes = 10000
diameter_reactor = 0.02 #meter
A_tubes= (np.pi*(diameter_reactor/2)**2)*number_tubes #m2
length = 3 #meter
T = 259.19 + 273 #K
P = 60 #bar
Pa = P* 100000
R = 8.314462618 #J/mol.K

print("Reactor Specifications Complete")

# ------------------------------------------------------------------------
------------------------------------------------------------#
```

```
# Definition of the differential equations
def dy(y,x):

    # y' is in this case the array in which all data are stored
    N1CO2 = y[0]
    N1H2 = y[1]
    N1CH3OH = y[2]
    N1H2O = y[3]
    N1CO = y[4]
    N2CH3OH = y[5]
    N2H2O = y[6]


    N1total = N1CO2 + N1H2 + N1CH3OH + N1H2O + N1CO
    N2total = N2CH3OH + N2H2O
    Ntotal = N1total + N2total


    # Error messages are bypassed here, because in some reaction rates the root
must be taken. This avoids negative numbers.
    if N1CO2 < 0:
        N1CO2 = 0
    if N1H2 < 0:
        N1H2 = 0
    if N1CH3OH < 0:
        N1CH3OH = 0
    if N1H2O < 0:
        N1H2O = 0
    if N1CO < 0:
        N1CO = 0

    # Error messages are bypassed here, because in some reaction rates the
pressure can be infinite
    if N1CO2 == 0:
        PCO2 = 0
    else:
        PCO2 = (N1CO2/N1total)*P
    if N1H2 == 0:
        PH2 = 0
    else:
        PH2 = (N1H2/N1total)*P
    if N1CH3OH == 0:
        PCH3OH = 0
    else:
        PCH3OH = (N1CH3OH/N1total)*P
    if N1H2O == 0:
        PH2O = 0
    else:
        PH2O = (N1H2O/N1total)*P
    if N1CO == 0:
        PCO = 0
    else:
        PCO = (N1CO/N1total)*P
```

```
    # Arrhenius parameters for the temperature-dependent factors in the model of
the kinetics of methanol production according to Graaf
    K1eq = 2.39*10**(-13)*np.exp((9.84*10**4)/(R*T))
    K2eq = 1.07*10**(2)*np.exp((-3.91*10**4)/(R*T))
    K3eq = 2.56*10**(-11)*np.exp((5.87*10**4)/(R*T))
    k1 = 4.89*10**(7)*np.exp((-1.13*10**5)/(R*T))
    k2 = 9.64*10**(11)*np.exp((-1.53*10**5)/(R*T))
    k3 = 1.09*10**(5)*np.exp((-0.875*10**5)/(R*T))
    KCO = 2.16*10**(-5)*np.exp((0.468*10**5)/(R*T))
    KCO2 = 7.05*10**(-7)*np.exp((0.617*10**5)/(R*T))
    KH2O_KH2_05 = 6.37*10**(-9)*np.exp((0.840*10**5)/(R*T))


    # kinetics of the reduction of CO2 to methanol over a Cu/ZnO/Al2O3 catalyst
modeled by Graaf

    denom = (1 + KCO*PCO+KCO2*PCO2)*(PH2**(1/2)+(KH2O_KH2_05)*PH2O)

    r1 = k1*KCO*(PCO*PH2**(3/2)-(PCH3OH*PH2O)/(PH2**(1/2)*K1eq))/denom
    r2 = k2*KCO2*(PCO2*PH2-(PH2O*PCO)/K2eq)/denom
    r3 = k3*KCO2*(PCO2*PH2**(3/2)-(PCH3OH*PH2O)/(PH2**(3/2)*K3eq))/denom


    # Definition of the ODEs in the order in which the y-array was defined
    dN1CO2dx = ro_catalyst*A_tubes*(-r2-r3)
    dN1H2dx = ro_catalyst*A_tubes*(-2*r1-r2-3*r3)
    dN1CH3OHdx = (ro_catalyst*A_tubes*(r1+r3)-
kronecker_delta_CH3OH*landa_CH3OH*N1CH3OH)
    dN1H2Odx = (ro_catalyst*A_tubes*(r2+r3)-kronecker_delta_H2O*landa_H2O*N1H2O)
    dN1COdx = ro_catalyst*A_tubes*(-r1+r2) #(P/P0_CO)*(Ntotal/NCO)
    dN2CH3OHdx = kronecker_delta_CH3OH*landa_CH3OH*N1CH3OH
    dN2H2Odx = kronecker_delta_H2O*landa_H2O*N1H2O
    #dNtotaldx = dNCO2dx + dNH2dx + dNCH3OHdx + dNH2Odx + dNCOdx


    return [dN1CO2dx, dN1H2dx, dN1CH3OHdx, dN1H2Odx, dN1COdx, dN2CH3OHdx,
dN2H2Odx]

# Initial Conditions
y0H2 = 200
y0CO2 = 50
y0 = [y0CO2,y0H2,0,0,0,0,0]
kronecker_delta_CH3OH = 1
kronecker_delta_H2O = 1
landa_CH3OH = 2
landa_H2O = 2

# Creation of the x interval within the reactor
x = np.linspace(0,length,100)

# ODEs are integrated by means of odeint, the initial values must be placed in
the square brackets in the correct order as they are for y..,mn
```

```
y = odeint(dy,y0,x,mxstep=0,full_output=0)

#Creating a DataFrame with the results
Results = pd.DataFrame(y)
Results.insert(0,"Position [m]", x, True)
#Renaming the columns of the dataframe
Results =
Results.rename(columns={0:'N1CO2',1:'N1H2',2:'N1CH3OH',3:'N1H2O',4:'N1CO',
5:'N2CH3OH',6:'N2H2O'})
Results = Results.set_index('Position [m]')
#Showing the Results in a table and saving the data in arrays
print("Temperature-dependent component molar flow rates Results at the end of the
Reactor - Two streams")
print(Results)

NCO2 = Results['N1CO2'].values
NH2 = Results['N1H2'].values
NCH3OH = Results['N1CH3OH'].values + Results['N2CH3OH'].values
NH2O = Results['N1H2O'].values + Results['N2H2O'].values
NCO = Results['N1CO'].values

#Plotting the data - Line Chart showing the moles streams trough the reactor
position (x)

# Set the width and height of the figure
plt.figure(figsize=(14,6))
plt.yscale("log")
# Add title
plt.title("Position-dependent component molar flow rates in a Plug Flow Reactor")

plt.xlim(0, 3)
plt.ylim(0.1, 250)
sns.lineplot(data=Results,dashes=False)

#Plotting the Total Molar Flow
Results_total = pd.DataFrame({'NCO2_total': NCO2, 'NH2_total': NH2,
'NCH3OH_total' : NCH3OH, 'NH2O_total' : NH2O, 'NCO_total' : NCO})
Results_total.insert(0,"Position [m]", x, True)
Results_total = Results_total.set_index('Position [m]')
print("Temperature-dependent component molar flow rates Results at the end of the
Reactor - Total Molar Flow trough the Reactor")
print(Results_total)

plt.figure(figsize=(14,6))
plt.yscale("log")
#plt.xscale("log")
#Add title
plt.title("Position-dependent total component molar flow rates in the the Plug
Flow Reactor - Total Molar Flow trough the Reactor")

plt.xlim(0.1, 3)
plt.ylim(0.1, 250)
sns.lineplot(data=Results_total,dashes=False)
```

APPENDIX C

```
#!/usr/bin/env python3
# -*- coding: utf-8 -*-

#!/usr/bin/env python3
# -*- coding: utf-8 -*-
"""
Created on Fri Jul 16 11:44:17 2021

@author: ignaciolaizquereda

Membrane Plug Flow Reactor (PFR)  based on the Graaf Kinetic Model -> Results
based on Temperature [°C]]

Set Up
"""
# Packages import
import math
from sympy import integrate, init_printing
init_printing(use_latex="mathjax")
from sympy import pi
import numpy as np
import matplotlib.pyplot as plt
from scipy.integrate import odeint
from matplotlib import cm
from matplotlib.ticker import LinearLocator, FormatStrFormatter
import pandas as pd
pd.plotting.register_matplotlib_converters()
import matplotlib.pyplot as plt
import seaborn as sns
print("Setup Complete")

#Reactor Type: Plug Flow Reactor (PFR) with in-situ product removal

ro_catalyst = 1000 #kg/m^3
number_tubes = 10000
diameter_reactor = 0.02 #meter
A_tubes= (np.pi*(diameter_reactor/2)**2)*number_tubes #m2
length = 3 #meter
R = 8.314462618 #J/mol.K


print("Reactor Specifications Complete")
```

```
# Definition of the List obeject in which the respective results are stored for
mole fraction and substance flow.
Ntotalf = []
y1CO2f = []
y1H2f = []
y1CH3OHf = []
y1H2Of = []
y1COf = []
y2CH3OHf = []
y2H2Of = []
NCO2ein = []
NH2ein = []

print("Final arrays ready for saving the parameters")

# Definition and initiation of the iteration variable
i = 0
j = 0

# ------------------------------------------------------------------------------
----------------------------------------------------------------#
# Definition of the differential equations
def dy(y,x):

    # y' is in this case the array in which all data are stored
    N1CO2 = y[0]
    N1H2 = y[1]
    N1CH3OH = y[2]
    N1H2O = y[3]
    N1CO = y[4]

    N1total = N1CO2 + N1H2 + N1CH3OH + N1H2O + N1CO

    # Error messages are bypassed here, because in some reaction rates the root
must be taken. This avoids negative numbers.
    if N1CO2 < 0:
        N1CO2 = 0
    if N1H2 < 0:
        N1H2 = 0
    if N1CH3OH < 0:
        N1CH3OH = 0
    if N1H2O < 0:
        N1H2O = 0
    if N1CO < 0:
        N1CO = 0

    # Error messages are bypassed here, because in some reaction rates the
pressure can be infinite
    if N1CO2 == 0:
        PCO2 = 0
    else:
        PCO2 = (N1CO2/N1total)*P
        #PCO2 = (P/P0)*(Ntotal/NCO2)
```

```
    if N1H2 == 0:
        PH2 = 0
    else:
        PH2 = (N1H2/N1total)*P
        #PH2 = (P/P0)*(Ntotal/NH2)

    if N1CH3OH == 0:
        PCH3OH = 0
    else:
        PCH3OH = (N1CH3OH/N1total)*P
        #print(PCH3OH)
        #PCH3OH = (P/P0)*(Ntotal/NCH3OH)

    if N1H2O == 0:
        PH2O = 0
    else:
        PH2O = (N1H2O/N1total)*P
        #PH2O = (P/P0)*(Ntotal/NH2O)

    if N1CO == 0:
        PCO = 0
    else:
        PCO = (N1CO/N1total)*P
        #PCO = (P/P0)*(Ntotal/NCO)

    # Arrhenius parameters for the temperature-dependent factors in the model of
the kinetics of methanol production according to Graaf
    K1eq = 2.39*10**(-13)*np.exp((9.84*10**4)/(R*T))
    K2eq = 1.07*10**(2)*np.exp((-3.91*10**4)/(R*T))
    K3eq = 2.56*10**(-11)*np.exp((5.87*10**4)/(R*T))
    k1 = 4.89*10**(7)*np.exp((-1.13*10**5)/(R*T))
    k2 = 9.64*10**(11)*np.exp((-1.53*10**5)/(R*T))
    k3 = 1.09*10**(5)*np.exp((-0.875*10**5)/(R*T))
    KCO = 2.16*10**(-5)*np.exp((0.468*10**5)/(R*T))
    KCO2 = 7.05*10**(-7)*np.exp((0.617*10**5)/(R*T))
    KH2O_KH2_05 = 6.37*10**(-9)*np.exp((0.840*10**5)/(R*T))


    # kinetics of the reduction of CO2 to methanol over a Cu/ZnO/Al2O3 catalyst
modeled by Graaf

    denom = (1 + KCO*PCO+KCO2*PCO2)*(PH2**(1/2)+(KH2O_KH2_05)*PH2O)

    r1 = k1*KCO*(PCO*PH2**(3/2)-(PCH3OH*PH2O)/(PH2**(1/2)*K1eq))/denom
    r2 = k2*KCO2*(PCO2*PH2-(PH2O*PCO)/K2eq)/denom
    r3 = k3*KCO2*(PCO2*PH2**(3/2)-(PCH3OH*PH2O)/(PH2**(3/2)*K3eq))/denom




    # Definition of the ODEs in the order in which the y-array was defined
```

```
    dN1CO2dx = ro_catalyst*A_tubes*(-r2-r3)
    dN1H2dx = ro_catalyst*A_tubes*(-2*r1-r2-3*r3)
    dN1CH3OHdx = ro_catalyst*A_tubes*(r1+r3)-
kronecker_delta_CH3OH*landa_CH3OH*N1CH3OH
    dN1H2Odx = ro_catalyst*A_tubes*(r2+r3)-kronecker_delta_H2O*landa_H2O*N1H2O
    dN1COdx = ro_catalyst*A_tubes*(-r1+r2) #(P/P0_CO)*(Ntotal/NCO)
    dN2CH3OHdx = kronecker_delta_CH3OH*landa_CH3OH*N1CH3OH
    dN2H2Odx = kronecker_delta_H2O*landa_H2O*N1H2O



    return [dN1CO2dx, dN1H2dx, dN1CH3OHdx, dN1H2Odx, dN1COdx, dN2CH3OHdx,
dN2H2Odx]

# Creation of the Temperature interval for the sensitivity analysis
temp = np.linspace(180, 340, 100)
pressure = np.linspace(20,60,3)
# Creation of the x interval within the reactor
x = np.linspace(0,length,10000)
# Initial Conditions
y0CO2 = 50
y0H2 = 200
y0 = [y0CO2,y0H2,0,0,0,0,0]
kronecker_delta_CH3OH = 1
kronecker_delta_H2O = 1
landa_CH3OH = 0.4
landa_H2O = 0

for P in pressure:
    j+=1

    #Plotting the data - Line Chart showing the moles streams and CO2 - MeOH
conversion for the given temperature range [°C]] and Pressures [20,40,60] bar

    if P == 20:
        for T in temp:
            i +=1
            T = T + 273
            # ODEs are integrated by means of odeint, the initial values must be
placed in the square brackets
            # in the correct order as they are for y.
            y = odeint(dy,y0,x,mxstep=50000,full_output=0)

            # Here the last value, which corresponds to the output component, is
added to the corresponding array.
            #For the input arrays, the input concentrations must be entered
accordingly.
            #Ntotalf.append(y[-1,0])
            y1CO2f.append(y[-1,0])
            y1H2f.append(y[-1,1])
            y1CH3OHf.append(y[-1,2])
            y1H2Of.append(y[-1,3])
            y1COf.append(y[-1,4])
```

```
            y2CH3OHf.append(y[-1,5])
            y2H2Of.append(y[-1,6])
            NCO2ein.append(50)
            NH2ein.append(150)

        #Creating the Numpy Array with the results. Note Results this time are
number of moles at the end of the reactor for different temperatures
        array =
np.array([temp,y1CO2f,y1H2f,y1CH3OHf,y1H2Of,y1COf,y2CH3OHf,y2H2Of]).T
        #Creating a DataFrame with the results
        Results_P_20bar = pd.DataFrame(array)
        #Renaming the columns of the dataframe
        Results_P_20bar = Results_P_20bar.rename(columns={0:'Temperature
[°C]',1:'N1CO2',2:'N1H2',3:'N1CH3OH',4:'N1H2O',5:'N1CO',6:'N2CH3OH',7:'N2H2O'})
        Results_P_20bar = Results_P_20bar.set_index('Temperature [°C]')

        print("Temperature-dependent component molar flow rates Results at the
end of the Reactor at P = 20 bar")
        print(Results_P_20bar)

        NCO2 = Results_P_20bar['N1CO2'].values
        NH2 = Results_P_20bar['N1H2'].values
        NCH3OH = Results_P_20bar['N1CH3OH'].values +
Results_P_20bar['N2CH3OH'].values
        NH2O = Results_P_20bar['N1H2O'].values + Results_P_20bar['N2H2O'].values
        NCO = Results_P_20bar['N1CO'].values

        Results_total_P_20bar = pd.DataFrame({'Temperature [°C]':
temp,'NCO2_total': NCO2, 'NH2_total': NH2, 'NCH3OH_total' : NCH3OH, 'NH2O_total'
: NH2O, 'NCO_total' : NCO})
        Results_total_P_20bar = Results_total_P_20bar.set_index('Temperature
[°C]')
        print("Temperature-dependent total component molar flow rates Results at
the end of the Reactor at P = 20 bar")
        print(Results_total_P_20bar)
        # Set the width and height of the figure
        #plt.figure(figsize=(14,6))
        #plt.yscale("log")
        # Add title
        #plt.title("Temperature-dependent component molar flow rates at the end
of the Plug Flow Reactor at P = 20 bar")

        #sns.lineplot(data=Results_total_P_20bar)

       #Calculating and Plotting the MeOH yield (also kown as Methanol to CO2
conversion) for the given temperature range and pressure
        yNCO2f = Results_total_P_20bar.NCO2_total
        yNH2f = Results_total_P_20bar.NH2_total
        yNCH3OHf = Results_total_P_20bar.NCH3OH_total
        yNH2Of = Results_total_P_20bar.NH2O_total
        yNCOf = Results_total_P_20bar.NCO_total

        conversion_total = ((y0CO2 + y0H2)-(yNCO2f+yNH2f))/(y0CO2 + y0H2)
```

```
        MeOH_yield_20bar = (yNCH3OHf.values/y0CO2)*100
        array_MeOH_yield_20bar = np.array([temp,MeOH_yield_20bar]).T
        dfMeOH_yield_20bar = pd.DataFrame(array_MeOH_yield_20bar)
        dfMeOH_yield_20bar = dfMeOH_yield_20bar.rename(columns={0:'Temperature
[°C]',1:'P = 20 bar | λCH3OH = 0.4 m-1'})
        dfMeOH_yield_20bar = dfMeOH_yield_20bar.set_index('Temperature [°C]')


        plt.figure(figsize=(14,6))
        plt.title("Temperature-dependent Methanol yield [%] at the end of the
Plug Flow Reactor for pressure 20 bar and given landas")
        plt.ylabel('MeOH yield [%]')
        plt.xlabel('Temperature [°C]')

        plt.xlim(180,340)
        sns.lineplot(data=dfMeOH_yield_20bar)

        #Reset the array for the next loop
        Ntotalf = []
        y1CO2f = []
        y1H2f = []
        y1CH3OHf = []
        y1H2Of = []
        y1COf = []
        y2CH3OHf = []
        y2H2Of = []
        NCO2ein = []
        NH2ein = []

    if P == 40:
        for T in temp:
            i +=1
            T = T + 273
            # ODEs are integrated by means of odeint, the initial values must be
placed in the square brackets
            # in the correct order as they are for y.
            y = odeint(dy,y0,x,mxstep=50000,full_output=0)

            # Here the last value, which corresponds to the output component, is
added to the corresponding array.
            #For the input arrays, the input concentrations must be entered
accordingly.
            y1CO2f.append(y[-1,0])
            y1H2f.append(y[-1,1])
            y1CH3OHf.append(y[-1,2])
            y1H2Of.append(y[-1,3])
            y1COf.append(y[-1,4])
            y2CH3OHf.append(y[-1,5])
            y2H2Of.append(y[-1,6])
            NCO2ein.append(50)
            NH2ein.append(150)
```

```
        #Creating the Numpy Array with the results. Note Results this time are
number of moles at the end of the reactor for different temperatures
        array =
np.array([temp,y1CO2f,y1H2f,y1CH3OHf,y1H2Of,y1COf,y2CH3OHf,y2H2Of]).T
        #Creating a DataFrame with the results
        Results_P_40bar = pd.DataFrame(array)
        #Renaming the columns of the dataframe
        Results_P_40bar = Results_P_40bar.rename(columns={0:'Temperature
[°C]',1:'N1CO2',2:'N1H2',3:'N1CH3OH',4:'N1H2O',5:'N1CO',6:'N2CH3OH',7:'N2H2O'})
        Results_P_40bar = Results_P_40bar.set_index('Temperature [°C]')

        print("Temperature-dependent component molar flow rates Results at the
end of the Reactor at P = 40 bar")
        print(Results_P_40bar)

        NCO2 = Results_P_40bar['N1CO2'].values
        NH2 = Results_P_40bar['N1H2'].values
        NCH3OH = Results_P_40bar['N1CH3OH'].values +
Results_P_40bar['N2CH3OH'].values
        NH2O = Results_P_40bar['N1H2O'].values + Results_P_40bar['N2H2O'].values
        NCO = Results_P_40bar['N1CO'].values

        Results_total_P_40bar = pd.DataFrame({'Temperature [°C]':
temp,'NCO2_total': NCO2, 'NH2_total': NH2, 'NCH3OH_total' : NCH3OH, 'NH2O_total'
: NH2O, 'NCO_total' : NCO})
        Results_total_P_40bar = Results_total_P_40bar.set_index('Temperature
[°C]')
        print("Temperature-dependent total component molar flow rates Results at
the end of the Reactor at P = 40 bar")
        print(Results_total_P_40bar)
        # Set the width and height of the figure
        #plt.figure(figsize=(14,6))
        #plt.yscale("log")
        # Add title
        #plt.title("Temperature-dependent component molar flow rates at the end
of the Plug Flow Reactor at P = 40 bar")

        #sns.lineplot(data=Results_total_P_40bar)

       #Calculating and Plotting the MeOH yield (also kown as Methanol to CO2
conversion) for the given temperature range and pressure
        yNCO2f = Results_total_P_40bar.NCO2_total
        yNH2f = Results_total_P_40bar.NH2_total
        yNCH3OHf = Results_total_P_40bar.NCH3OH_total
        yNH2Of = Results_total_P_40bar.NH2O_total
        yNCOf = Results_total_P_40bar.NCO_total

        conversion_total = ((y0CO2 + y0H2)-(yNCO2f+yNH2f))/(y0CO2 + y0H2)

        MeOH_yield_40bar = (yNCH3OHf.values/y0CO2)*100
        array_MeOH_yield_40bar = np.array([temp,MeOH_yield_40bar]).T
        dfMeOH_yield_40bar = pd.DataFrame(array_MeOH_yield_40bar)
```

```
        dfMeOH_yield_40bar = dfMeOH_yield_40bar.rename(columns={0:'Temperature
[°C]',1:'P = 40 bar | λCH3OH = 0.4 m-1'})
        dfMeOH_yield_40bar = dfMeOH_yield_40bar.set_index('Temperature [°C]')

        plt.figure(figsize=(14,6))
        plt.title("Temperature-dependent Methanol yield [%] at the end of the
Plug Flow Reactor for pressure 40 bar and given landas")
        plt.ylabel('MeOH yield [%]')
        plt.xlabel('Temperature [°C]')

        plt.xlim(180,340)
        sns.lineplot(data=dfMeOH_yield_40bar)

        #Reset the array for the next loop
        Ntotalf = []
        y1CO2f = []
        y1H2f = []
        y1CH3OHf = []
        y1H2Of = []
        y1COf = []
        y2CH3OHf = []
        y2H2Of = []
        NCO2ein = []
        NH2ein = []

    if P == 60:
        for T in temp:
            i +=1
            T = T + 273
            # ODEs are integrated by means of odeint, the initial values must be
placed in the square brackets
            # in the correct order as they are for y.
            y = odeint(dy,y0,x,mxstep=50000,full_output=0)

            # Here the last value, which corresponds to the output component, is
added to the corresponding array.
            #For the input arrays, the input concentrations must be entered
accordingly.

            y1CO2f.append(y[-1,0])
            y1H2f.append(y[-1,1])
            y1CH3OHf.append(y[-1,2])
            y1H2Of.append(y[-1,3])
            y1COf.append(y[-1,4])
            y2CH3OHf.append(y[-1,5])
            y2H2Of.append(y[-1,6])
            NCO2ein.append(50)
            NH2ein.append(150)

        #Creating the Numpy Array with the results. Note Results this time are
number of moles at the end of the reactor for different temperatures
        array =
np.array([temp,y1CO2f,y1H2f,y1CH3OHf,y1H2Of,y1COf,y2CH3OHf,y2H2Of]).T
```

```
        #Creating a DataFrame with the results
        Results_P_60bar = pd.DataFrame(array)
        #Renaming the columns of the dataframe
        Results_P_60bar = Results_P_60bar.rename(columns={0:'Temperature
[°C]',1:'N1CO2',2:'N1H2',3:'N1CH3OH',4:'N1H2O',5:'N1CO',6:'N2CH3OH',7:'N2H2O'})
        Results_P_60bar = Results_P_60bar.set_index('Temperature [°C]')

        print("Temperature-dependent component molar flow rates Results at the
end of the Reactor at P = 60 bar")
        print(Results_P_60bar)

        NCO2 = Results_P_60bar['N1CO2'].values
        NH2 = Results_P_60bar['N1H2'].values
        NCH3OH = Results_P_60bar['N1CH3OH'].values +
Results_P_60bar['N2CH3OH'].values
        NH2O = Results_P_60bar['N1H2O'].values + Results_P_60bar['N2H2O'].values
        NCO = Results_P_60bar['N1CO'].values

        Results_total_P_60bar = pd.DataFrame({'Temperature [°C]':
temp,'NCO2_total': NCO2, 'NH2_total': NH2, 'NCH3OH_total' : NCH3OH, 'NH2O_total'
: NH2O, 'NCO_total' : NCO})
        Results_total_P_60bar = Results_total_P_60bar.set_index('Temperature
[°C]')
        print("Temperature-dependent total component molar flow rates Results at
the end of the Reactor at P = 60 bar")
        print(Results_total_P_60bar)
        # Set the width and height of the figure
        #plt.figure(figsize=(14,6))
        #plt.yscale("log")
        # Add title
        #plt.title("Temperature-dependent component molar flow rates at the end
of the Plug Flow Reactor at P = 60 bar")

        #sns.lineplot(data=Results_total_P_60bar)

       #Calculating and Plotting the MeOH yield (also kown as Methanol to CO2
conversion) for the given temperature range and pressure
        yNCO2f = Results_total_P_60bar.NCO2_total
        yNH2f = Results_total_P_60bar.NH2_total
        yNCH3OHf = Results_total_P_60bar.NCH3OH_total
        yNH2Of = Results_total_P_60bar.NH2O_total
        yNCOf = Results_total_P_60bar.NCO_total

        conversion_total = ((y0CO2 + y0H2)-(yNCO2f+yNH2f))/(y0CO2 + y0H2)

        MeOH_yield_60bar = (yNCH3OHf.values/y0CO2)*100
        array_MeOH_yield_60bar = np.array([temp,MeOH_yield_60bar]).T
        dfMeOH_yield_60bar = pd.DataFrame(array_MeOH_yield_60bar)
        dfMeOH_yield_60bar = dfMeOH_yield_60bar.rename(columns={0:'Temperature
[°C]',1:'P = 60 bar | λCH3OH = 0.4 m-1'})
        dfMeOH_yield_60bar = dfMeOH_yield_60bar.set_index('Temperature [°C]')
```

```
        plt.figure(figsize=(14,6))
        plt.title("Temperature-dependent Methanol yield [%] at the end of the
Plug Flow Reactor for pressure 60 bar and given landas")
        plt.ylabel('MeOH yield [%]')
        plt.xlabel('Temperature [°C]')

        plt.xlim(180,340)
        #sns.lineplot(data=dfMeOH_yield_60bar)

        #Reset the array for the next loop
        Ntotalf = []
        y1CO2f = []
        y1H2f = []
        y1CH3OHf = []
        y1H2Of = []
        y1COf = []
        y2CH3OHf = []
        y2H2Of = []
        NCO2ein = []
        NH2ein = []


dfMeOHyield =
pd.concat([dfMeOH_yield_20bar,dfMeOH_yield_40bar,dfMeOH_yield_60bar], axis=1)
plt.title("Temperature-dependent CO2 -> MeOH conversion at the end of the Plug
Flow Reactor at P = 20, 40 and 60 bar")
sns.lineplot(data=dfMeOHyield)
```

APPENDIX D

Table 15. Temperature-dependent molar flow ratios. Operation Conditions: T = 180-340ºC, P = 20 bar, H_2/CO_2 = 4 (i.e. $N_{H2}^{in} = 200, N_{H2}^{in} = 50$) and given $\lambda_{H2O} = \lambda_{CH3OH} = 0$.

T [ºC]	N_{CO2}	N_{H2}	N_{CH3OH}	N_{H2O}	N_{CO}
180.00	48.960385	197.002347	0.979019	1.039615	0.060597
181.61	48.870430	196.750836	1.059797	1.129570	0.069772
183.23	48.773405	196.480694	1.146355	1.226595	0.080240
...	...	...	...	...	...
228.48	**42.129624**	**181.226814**	**5.451405**	**7.870376**	**2.418972**
...	...	...	...	...	...
336.76	32.801672	182.445811	0.177931	17.198328	17.020397
338.38	32.668856	182.330806	0.169025	17.331144	17.162119
340.00	32.536133	182.214957	0.160588	17.463867	17.303279

Table 16. Temperature-dependent molar flow ratios. Operation Conditions: T = 180-340ºC, P = 40 bar, H_2/CO_2 = 4 (i.e. $N_{H2}^{in} = 200, N_{H2}^{in} = 50$) and given $\lambda_{H2O} = \lambda_{CH3OH} = 0$.

T [ºC]	N_{CO2}	N_{H2}	N_{CH3OH}	N_{H2O}	N_{CO}
180.00	48.39853	195.329733	1.534402	1.601462	0.067059
181.61	48.261562	194.939089	1.661236	1.738438	0.077202
183.23	48.114005	194.519554	1.797225	1.885995	0.088770
...	...	...	...	...	...
231.71	**37.351428**	**168.443691**	**9.453868**	**12.648572**	**3.194704**
...	...	...	...	...	...
336.76	32.132478	181.346820	0.392829	17.867522	17.474692
338.38	32.017795	181.273442	0.372176	17.982205	17.610029
340.00	31.902734	181.197383	0.352676	18.097266	17.744590

Table 17. Temperature-dependent molar flow ratios. Operation Conditions: T = 180-340ºC, P = 60 bar, H_2/CO_2 = 4 (i.e. $N_{H2}^{in} = 200, N_{H2}^{in} = 50$) and given $\lambda_{H2O} = \lambda_{CH3OH} = 0$.

T [ºC]	N_{CO2}	N_{H2}	N_{CH3OH}	N_{H2O}	N_{CO}
180.00	48.028165	194.220258	1.903954	1.971835	0.067881
181.61	47.860680	193.738297	2.061191	2.139320	0.078129
183.23	47.680404	193.220835	2.229784	2.319596	0.089812
...	...	...	...	...	...
231.71	**34.422530**	**159.590151**	**12.416190**	**15.577470**	**3.161280**
...	...	...	...	...	...
336.76	31.653868	180.449782	0.602043	18.346132	17.744088
338.38	31.553544	180.413212	0.570166	18.446456	17.876290
340.00	31.452372	180.372221	**0.540076**	18.547628	**18.007552**

Table 18. Temperature-dependent molar flow ratios. Operation Conditions: T = 180-340ºC, P = 20 bar, H_2/CO_2 = 4 (i.e. $N_{H2}^{in} = 200, N_{H2}^{in} = 50$) and given $\lambda_{H2O} = \lambda_{CH3OH} = 0.4$.

T [ºC]	N_{CO2}	N_{H2}	N_{CH3OH}	N_{H2O}	N_{CO}
180.00	48.88877	196.795729	1.046524	1.111223	0.064699
181.61	48.792186	196.525581	1.133303	1.207814	0.074511
183.23	48.687921	196.235175	1.226373	1.312079	0.085706
...	...	...	...	...	...
238.12	**38.035123**	**172.799411**	**7.617856**	**11.964877**	**4.347021**
...	...	...	...	...	...
336.76	26.293584	174.814890	0.739347	23.706416	22.967070
338.38	26.117466	174.707631	0.704917	23.882534	23.177617
340.00	25.941976	174.597733	0.672122	24.058024	23.385902

Table 19. Temperature-dependent molar flow ratios. Operation Conditions: T = 180-340ºC, P = 40 bar, H_2/CO_2 = 4 (i.e. $N_{H2}^{in} = 200, N_{H2}^{in} = 50$) and given $\lambda_{H2O} = \lambda_{CH3OH} = 0.4$.

T [ºC]	N_{CO2}	N_{H2}	N_{CH3OH}	N_{H2O}	N_{CO}
180.00	48.225470	194.824804	1.700333	1.774530	0.074197
181.61	48.073091	194.390132	1.841480	1.926909	0.085430
183.23	47.908843	193.923010	1.9929	2.091157	0.098241
...	...	...	...	...	...
239.79	**31.717753**	**154.742785**	**13.487484**	**18.282247**	**4.794762**
...	...	...	...	...	...
336.76	25.172667	171.986524	1.593071	24.827333	23.234262
338.38	25.030884	171.997518	1.516683	24.969116	23.452432
340.00	24.888663	172.000655	1.444004	25.111337	23.667333

Table 20. Temperature-dependent molar flow ratios. Operation Conditions: T = 180-340ºC, P = 60 bar, H_2/CO_2 = 4 (i.e. $N_{H2}^{in} = 200, N_{H2}^{in} = 50$) and given $\lambda_{H2O} = \lambda_{CH3OH} = 0.4$.

T [ºC]	N_{CO2}	N_{H2}	N_{CH3OH}	N_{H2O}	N_{CO}
180.00	47.773984	193.474937	2.149523	2.226016	0.076493
181.61	47.584304	192.929000	2.327652	2.415696	0.088043
183.23	47.380045	192.342556	2.518745	2.619955	0.101210
...	...	...	...	...	...
241.41	**27.444965**	**141.873976**	**17.785494**	**22.555035**	**4.769540**
...	...	...	...	...	...
336.76	24.404123	169.625741	2.389191	25.595877	23.206686
338.38	24.288296	169.736244	2.276026	25.711704	23.435677
340.00	24.171104	169.834733	2.168185	25.828896	23.660711

Table 21. Temperature-dependent molar flow ratios. Operation Conditions: T = 180-340ºC, P = 20 bar, H_2/CO_2 = 4 (i.e. $N_{H2}^{in} = 200, N_{H2}^{in} = 50$) and given $\lambda_{H2O} = \lambda_{CH3OH} = 2$.

T [ºC]	N_{CO2}	N_{H2}	N_{CH3OH}	N_{H2O}	N_{CO}
180.00	48.752775	196.403358	1.174709	1.247225	0.072516
181.61	48.643494	196.097585	1.272954	1.356506	0.083552
183.23	48.525392	195.768479	1.378457	1.474608	0.096152
...	...	...	...	...	...
264.04	**22.928193**	**139.735956**	**16.596118**	**27.071807**	**10.475689**
...	...	...	...	...	...
336.76	13.287361	149.320584	6.983388	36.712639	29.729251
338.38	13.076059	149.559518	6.758270	36.923941	30.165670
340.00	12.865613	149.789433	6.538090	37.134387	30.596297

Table 22. Temperature-dependent molar flow ratios. Operation Conditions: T = 180-340ºC, P = 40 bar, H_2/CO_2 = 4 (i.e. $N_{H2}^{in} = 200, N_{H2}^{in} = 50$) and given $\lambda_{H2O} = \lambda_{CH3OH} = 2$.

T [ºC]	N_{CO2}	N_{H2}	N_{CH3OH}	N_{H2O}	N_{CO}
180.00	47.827463	193.663619	2.081922	2.172537	0.090615
181.61	47.639225	193.126431	2.256397	2.360775	0.104377
183.23	47.436087	192.548423	2.443832	2.563913	0.120082
...	...	...	...	...	...
262.42	**14.208337**	**105.256845**	**29.475746**	**35.791663**	**35.791663**
...	...	...	...	...	...
336.76	11.005822	135.056368	12.974727	38.994178	26.019451
338.38	10.874230	135.693117	12.590557	39.125770	26.535214
340.00	10.740987	136.314839	12.213074	39.259013	27.045939

Table 23. Temperature-dependent molar flow ratios. Operation Conditions: T = 180-340ºC, P = 60 bar, H_2/CO_2 = 4 (i.e. $N_{H2}^{in} = 200, N_{H2}^{in} = 50$) and given $\lambda_{H2O} = \lambda_{CH3OH} = 2$.

T [ºC]	N_{CO2}	N_{H2}	N_{CH3OH}	N_{H2O}	N_{CO}
180.00	47.128657	191.582621	2.773018	2.871343	0.098325
181.61	46.881987	190.872359	3.004814	3.118013	0.113199
183.23	46.616088	190.108575	3.253756	3.383912	0.130156
...	...	...	...	...	...
259.19	**9.178130**	**85.265900**	**36.956115**	**40.821870**	**3.865756**
...	...	...	...	...	...
336.76	9.573455	124.853255	17.360100	40.426545	23.066446
338.38	9.493303	125.701758	16.895773	40.506697	23.610924
340.00	9.409986	126.535057	16.437465	40.590014	24.152549

Table 24. Temperature-dependent molar flow ratios. Operation Conditions: T = 180-340ºC, P = 20 bar, H_2/CO_2 = 4 (i.e. $N_{H2}^{in} = 200, N_{H2}^{in} = 50$) and given $\lambda_{H2O} = 0.4$.

T [ºC]	N_{CO2}	N_{H2}	N_{CH3OH}	N_{H2O}	N_{CO}
180.00	48.889559	196.798059	1.045750	1.110441	0.064691
181.61	48.793145	196.528437	1.132354	1.206855	0.074501
183.23	48.689098	196.238686	1.225206	1.310902	0.085695
...	...	...	...	...	...
231.72	**40.321174**	**177.295759**	**6.512708**	**9.678826**	**3.166118**
...	...	...	...	...	...
336.76	26.373460	175.557805	0.407827	23.626540	23.218713
338.38	26.192696	175.415060	0.388818	23.807304	23.418487
340.00	26.012841	175.271399	0.370721	23.987159	23.616439

Table 25. Temperature-dependent molar flow ratios. Operation Conditions: T = 180-340ºC, P = 40 bar, H_2/CO_2 = 4 (i.e. $N_{H2}^{in} = 200, N_{H2}^{in} = 50$) and given $\lambda_{H2O} = 0.4$.

T [ºC]	N_{CO2}	N_{H2}	N_{CH3OH}	N_{H2O}	N_{CO}
180.00	48.226924	194.829157	1.698883	1.773076	0.074192
181.61	48.074840	194.395369	1.839735	1.925160	0.085425
183.23	47.910948	193.929320	1.990814	2.089052	0.098238
...	...	...	...	...	...
234.95	**34.322582**	**161.425200**	**11.448691**	**15.677418**	**4.228728**
...	...	...	...	...	...
336.76	25.333365	173.549568	0.891898	24.666635	23.774737
338.38	25.18223	173.485380	0.848427	24.817765	23.969338
340.00	25.031226	173.416917	0.807154	24.968774	24.161620

Table 26. Temperature-dependent molar flow ratios. Operation Conditions: T = 180-340ºC, P = 60 bar, H_2/CO_2 = 4 (i.e. $N_{H2}^{in} = 200, N_{H2}^{in} = 50$) and given $\lambda_{H2O} = 0.4$.

T [ºC]	N_{CO2}	N_{H2}	N_{CH3OH}	N_{H2O}	N_{CO}
180.00	47.775942	193.480814	2.147564	2.224058	0.076494
181.61	47.586639	192.936010	2.325315	2.413361	0.088046
183.23	47.382830	192.350924	2.515953	2.617170	0.101217
...	...	...	...	...	...
234.95	**30.707241**	**150.524645**	**15.091298**	**19.292759**	**4.201461**
...	...	...	...	...	...
336.76	24.636395	171.928572	1.353912	25.363605	24.009693
338.38	24.507359	171.931390	1.287985	25.492641	24.204657
340.00	24.377719	171.927005	1.225357	25.622281	24.396924

Table 27. Temperature-dependent molar flow ratios. Operation Conditions: T = 180-340ºC, P = 20 bar, H_2/CO_2 = 4 (i.e. $N_{H2}^{in} = 200, N_{H2}^{in} = 50$) and given $\lambda_{H2O} = 2$.

T [ºC]	N_{CO2}	N_{H2}	N_{CH3OH}	N_{H2O}	N_{CO}
180.00	48.754885	196.409599	1.172643	1.245115	0.072472
181.61	48.646023	196.105063	1.270480	1.353977	0.083497
183.23	48.528426	195.777448	1.375489	1.471574	0.096084
...	...	...	...	...	...
241.41	**34.190318**	**164.658930**	**9.765694**	**15.809682**	**6.043987**
...	...	...	...	...	...
336.76	13.989379	159.496636	2.246372	36.010621	33.764249
338.38	13.736856	159.408875	2.163991	36.263144	34.099153
340.00	13.487402	159.318731	2.084335	36.512598	34.428263

Table 28. Temperature-dependent molar flow ratios. Operation Conditions: T = 180-340ºC, P = 40 bar, H_2/CO_2 = 4 (i.e. $N_{H2}^{in} = 200, N_{H2}^{in} = 50$) and given $\lambda_{H2O} = 2$.

T [ºC]	N_{CO2}	N_{H2}	N_{CH3OH}	N_{H2O}	N_{CO}
180.00	47.832759	193.679383	2.076688	2.167241	0.090554
181.61	47.645514	193.145151	2.250181	2.354486	0.104304
183.23	47.443555	192.570655	2.436450	2.556445	0.119995
...	...	...	...	...	...
243.03	**25.301687**	**140.184137**	**17.558775**	**24.698313**	**7.139538**
...	...	...	...	...	...
336.76	12.160110	153.006951	4.576579	37.839890	33.263311
338.38	11.963756	153.144676	4.409540	38.036244	33.626704
340.00	11.769014	153.273173	4.247920	38.230986	33.983066

Table 29. Temperature-dependent molar flow ratios. Operation Conditions: T = 180-340ºC, P = 60 bar, H_2/CO_2 = 4 (i.e. $N_{H2}^{in} = 200, N_{H2}^{in} = 50$) and given $\lambda_{H2O} = 2$.

T [ºC]	N_{CO2}	N_{H2}	N_{CH3OH}	N_{H2O}	N_{CO}
180.00	47.136825	191.607019	2.764903	2.863175	0.098272
181.61	46.891649	190.901224	2.995213	3.108351	0.113138
183.23	46.627512	190.142711	3.242401	3.372488	0.130087
...	...	...	...	...	...
244.65	**19.602222**	**123.324339**	**23.138942**	**30.397778**	**7.258836**
...	...	...	...	...	...
336.76	11.038922	147.949865	6.544528	38.961078	32.416550
338.38	10.880969	148.247161	6.316904	39.119031	32.802127
340.00	10.723476	148.531438	6.096019	39.276524	33.180505

Table 30. Temperature-dependent molar flow ratios. Operation Conditions: T = 180-340ºC, P = 20 bar, H_2/CO_2 = 4 (i.e. $N_{H2}^{in} = 200, N_{H2}^{in} = 50$) and given $\lambda_{CH3OH} = 0.4$.

T [ºC]	N_{CO2}	N_{H2}	N_{CH3OH}	N_{H2O}	N_{CO}
180.00	48.959636	197.000109	0.979763	1.040364	0.060601
181.61	48.869501	196.748055	1.060723	1.130499	0.069776
183.23	48.772247	196.477229	1.147509	1.227753	0.080244
...	...	...	...	...	...
234.95	**40.211528**	**177.408633**	**6.401448**	**9.788472**	**3.387024**
...	...	...	...	...	...
336.76	32.730990	181.950333	0.390328	17.269010	16.878681
338.38	32.602150	181.860404	0.370873	17.397850	17.026976
340.00	32.473169	181.768304	0.352433	17.526831	17.174398

Table 31. Temperature-dependent molar flow ratios. Operation Conditions: T = 180-340ºC, P = 40 bar, H_2/CO_2 = 4 (i.e. $N_{H2}^{in} = 200, N_{H2}^{in} = 50$) and given $\lambda_{CH3OH} = 0.4$.

T [ºC]	N_{CO2}	N_{H2}	N_{CH3OH}	N_{H2O}	N_{CO}
180.00	48.397332	195.326112	1.535610	1.602668	0.067059
181.61	48.260098	194.934692	1.662703	1.739902	0.077199
183.23	48.112225	194.514202	1.799011	1.887775	0.088763
...	...	...	...	...	...
236.57	**35.131033**	**162.831297**	**11.149868**	**14.868967**	**3.719100**
...	...	...	...	...	...
336.76	31.984390	180.287431	0.848480	18.015610	17.167131
338.38	31.878179	180.268778	0.804701	18.121821	17.317120
340.00	31.771086	180.244527	0.763279	18.228914	17.465635

Table 32. Temperature-dependent molar flow ratios. Operation Conditions: T = 180-340ºC, P = 60 bar, H_2/CO_2 = 4 (i.e. $N_{H2}^{in} = 200, N_{H2}^{in} = 50$) and given $\lambda_{CH3OH} = 0.4$.

T [ºC]	N_{CO2}	N_{H2}	N_{CH3OH}	N_{H2O}	N_{CO}
180.00	48.026637	194.215664	1.905487	1.973363	0.067876
181.61	47.858847	193.732780	2.063033	2.141153	0.078120
183.23	47.678202	193.214200	2.232001	2.321798	0.089797
...	...	...	...	...	...
238.18	**31.610265**	**152.349167**	**14.630549**	**18.389735**	**3.759187**
...	...	...	...	...	...
336.76	31.434230	178.862383	1.285923	18.565770	17.279847
338.38	31.346337	178.906771	1.219783	18.653663	17.433880
340.00	31.256870	178.942561	1.157154	18.743130	17.585976

Table 33. Temperature-dependent molar flow ratios. Operation Conditions: T = 180-340ºC, P = 20 bar, H_2/CO_2 = 4 (i.e. $N_{H2}^{in} = 200, N_{H2}^{in} = 50$) and given $\lambda_{CH3OH} = 2$.

T [ºC]	N_{CO2}	N_{H2}	N_{CH3OH}	N_{H2O}	N_{CO}
180.00	48.958656	196.997180	0.980738	1.041344	0.060607
181.61	48.868288	196.744428	1.061930	1.131712	0.069782
183.23	48.770742	196.472722	1.149010	1.229258	0.080249
...	...	...	...	...	...
247.88	**35.627048**	**166.749472**	**9.438788**	**14.372952**	**4.934163**
...	...	...	...	...	...
336.76	32.453865	180.034188	1.209839	17.546135	16.336296
338.38	32.340304	180.037859	1.151223	17.659696	16.508473
340.00	32.225735	180.034751	1.095492	17.774265	16.678774

Table 34. Temperature-dependent molar flow ratios. Operation Conditions: T = 180-340ºC, P = 40 bar, H_2/CO_2 = 4 (i.e. $N_{H2}^{in} = 200, N_{H2}^{in} = 50$) and given $\lambda_{CH3OH} = 2$.

T [ºC]	N_{CO2}	N_{H2}	N_{CH3OH}	N_{H2O}	N_{CO}
180.00	48.395760	195.321395	1.537183	1.604240	0.067057
181.61	48.258196	194.928978	1.664609	1.741804	0.077195
183.23	48.109920	194.507267	1.801326	1.890080	0.088754
...	...	...	...	...	...
251.11	**29.572104**	**146.495801**	**16.538151**	**20.427896**	**3.889745**
...	...	...	...	...	...
336.76	31.412898	176.316458	2.548220	18.587102	16.038882
338.38	31.338320	176.490166	2.424077	18.661680	16.237602
340.00	31.261083	176.649256	2.305914	18.738917	16.433003

Table 35. Temperature-dependent molar flow ratios. Operation Conditions: T = 180-340ºC, P = 60 bar, H_2/CO_2 = 4 (i.e. $N_{H2}^{in} = 200, N_{H2}^{in} = 50$) and given $\lambda_{CH3OH} = 2$

T [ºC]	N_{CO2}	N_{H2}	N_{CH3OH}	N_{H2O}	N_{CO}
180.000000	48.024660	194.209715	1.907473	1.975340	0.067867
181.616162	47.856479	193.725650	2.065415	2.143521	0.078106
183.232323	47.675364	193.205643	2.234861	2.324636	0.089775
...	...	...	...	...	...
252.73	**25.515186**	**132.673561**	**21.420812**	**24.484814**	**3.064002**
...	...	...	...	...	...
336.767677	30.598663	173.076241	3.761211	19.401337	15.640126
338.383838	30.555999	173.390353	3.582823	19.444001	15.861179
340.000000	30.509323	173.684259	3.412532	19.490677	16.078145

Table 36. Position-dependent molar flow rates through the plug flow reactor for P = 60 bar, T = 225.25ºC and H_2/CO_2 = 1 (i.e. $N_{H2}^{in} = 50, N_{H2}^{in} = 50$).

Position [m]	N_{CO2}	N_{H2}	N_{CH3OH}	N_{H2O}	N_{CO}
0.0000	50.000000	50.000000	0.000000	0.000000	0.000000
0.0003	49.997518	49.993447	0.002036	0.002482	0.000447
0.0006	49.995038	49.986901	0.004069	0.004962	0.000893
0.0009	49.992562	49.980363	0.006099	0.007438	0.001339
…	…	…	…	…	…
2.9991	44.376896	35.821177	4.277859	5.623104	1.345245
2.9994	44.376760	35.820913	4.277924	5.623240	1.345317
2.9997	44.376624	35.820649	4.277988	5.623376	1.345388
3.0000	**44.376488**	**35.820384**	**4.278052**	**5.623512**	**1.345460**

Table 37. Position-dependent molar flow rates through the plug flow reactor for P = 60 bar, T = 228.48ºC and H_2/CO_2 = 2 (i.e. $N_{H2}^{in} = 100, N_{H2}^{in} = 50$).

Position [m]	N_{CO2}	N_{H2}	N_{CH3OH}	N_{H2O}	N_{CO}
0.0000	50.000000	100.000000	0.000000	0.000000	0.000000
0.0003	49.996274	99.990117	0.003078	0.003726	0.000648
0.0006	49.992551	99.980243	0.006154	0.007449	0.001295
0.0009	49.988831	99.970378	0.009227	0.011169	0.001942
...	...	...	...	...	...
2.9991	40.238575	74.917402	7.660587	9.761425	2.100838
2.9994	40.238317	74.916842	7.660737	9.761683	2.100946
2.9997	40.238059	74.916283	7.660888	9.761941	2.101053
3.0000	**40.237801**	**74.915724**	**7.661038**	**9.762199**	**2.101161**

Table 38. Position-dependent molar flow rates through the plug flow reactor for P = 60 bar, T = 231.71 ºC and H_2/CO_2 = 3 (i.e. $N_{H2}^{in} = 150, N_{H2}^{in} = 50$)

Position [m]	N_{CO2}	N_{H2}	N_{CH3OH}	N_{H2O}	N_{CO}
0.0000	50.000000	150.000000	0.000000	0.000000	0.000000
0.0003	49.995227	149.987399	0.003914	0.004773	0.000859
0.0006	49.990458	149.974807	0.007825	0.009542	0.001717
0.0009	49.985692	149.962224	0.011734	0.014308	0.002575
...	...	...	...	...	...
2.9991	36.786474	116.207737	10.289368	13.213526	2.924158
2.9994	36.786160	116.207080	10.289540	13.213840	2.924300
2.9997	36.785847	116.206423	10.289712	13.214153	2.924441
3.0000	**36.785533**	**116.205766**	**10.289884**	**13.214467**	**2.924583**

Table 39. Position-dependent molar flow rates through the plug flow reactor for P = 60 bar, T = 231.71 ºC and H_2/CO_2 = 4 (i.e. $N_{H2}^{in} = 200, N_{H2}^{in} = 50$).

Position [m]	N_{CO2}	N_{H2}	N_{CH3OH}	N_{H2O}	N_{CO}
0.0000	50.000000	200.000000	0.000000	0.000000	0.00000
0.0003	49.994985	199.986711	0.004137	0.005015	0.000879
0.0006	49.989972	199.973431	0.008271	0.010028	0.001757
0.0009	49.984963	199.960158	0.012403	0.015037	0.002635
...	...	...	...	...	...
2.9991	34.423791	159.593009	12.415391	15.576209	3.160818
2.9994	34.423371	159.592056	12.415657	15.576629	3.160972
2.9997	34.422950	159.591103	12.415924	15.577050	3.161126
3.0000	**34.422530**	**159.590151**	**12.416190**	**15.577470**	**3.161280**

APPENDIX E

The 2030 Agenda for Sustainable Development, adopted by all United Nations Member States in 2015, aims to provide a shared blueprint for peace and prosperity for people and the planet, now and into the future. All United Nations Member States have together agreed to develop 17 Sustainable Development Goals (SDGs) to end poverty, improve health and education, reduce inequality, and spur economic growth – all while tackling climate change and preserving the oceans and forest (see Figure 45) [27].

Figure 45. Sustainable Development Goals (SDGs) [27].

The creation of this cooperation is not something new and it is built on decades of work by countries and the UN, including the UN Department of Economic and Social Affairs. Today the objective of the Division for Sustainable Development Goals (DSGS), division within the mentioned Department of Economic and Social Affairs (UNDESA), is to provide both support and capacity-building for the SDGs and their related thematic issues. Their focus is especially on water, energy, climate, oceans, urbanization, transport, science, and

technology. DSDG is at the core of the strategy of the UN 2030 Agenda, and they aim to facility the engagement between all the stakeholders to implement the global goals [27].

An interested reader is referred more information about the Sustainable Development Goals in the United Nations website [27]: https://sdgs.un.org/es/goals

According to the Times Higher Education ranking, the Universidad de Comillas is between the top 5 of universities with respect to the fulfillment of the SDGs. Comillas is the fourth university in the world in meeting SDG 7 (Affordable and Clean Energy), fifth worldwide in SDG 13 (Climate Action), and fifteenth in SDG 8 (Decent Work and Economic Growth).

The Times Impact ranking evaluates more than 1,100 universities worldwide in relation to their performance in achieving the United Nations Sustainable Development Goals (SDGs). It uses carefully calibrated indicators to provide comprehensive and balanced comparisons in three broad areas: research, outreach, and governance.

More information about this can be found in Comillas website: https://www.comillas.edu/noticias/17-comillas/2281-comillas-lider-mundial-en-cumplimiento-de-ods.

In this sense, this thesis aims to contribute to some Sustainable Development Goals (SDGs). The production of e-Methanol together with Power-to-X technologies can reduce the GHG emissions of the power, transport, and industrial sectors.

Thus, this thesis is aligned to the following Sustainable Development Goals (SDGs): *3. Good Health and Well-being, 7. Affordable and clean energy, 9. Industry, Innovation and Infrastructure, 11. Sustainable Cities and Communities, 12. Responsible Consumption and Production and 13. Climate Action* [27].

e-Methanol could decarbonize the transport system in a fast and affordable way. Therefore, this thesis is aligned to the sustainable development goals “Affordable and clean Energy” and “Sustainable Cities and Communities”.

Similarly, the aim of this thesis is to prove the use of membrane reactors to increase the yield and efficiency of the renewable methanol synthesis. Thus, this research is also aligned to the sustainable development goals "Industry, Innovation and Infrastructure", "Responsible Consumption and Production" and "Climate Action".

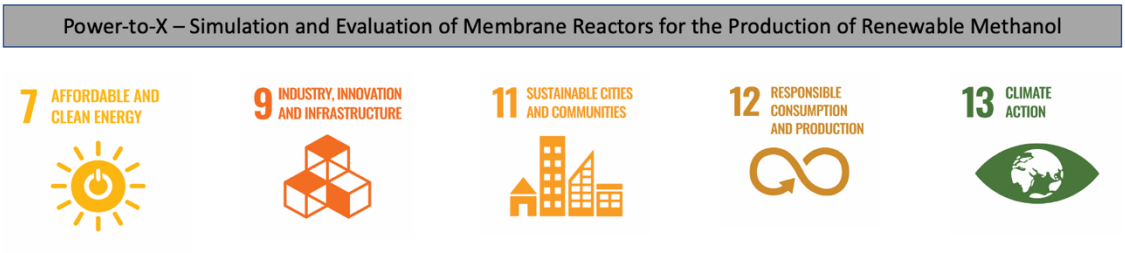

Figure 46. Alignment of the project with the Sustainable Development Goals (SDGs), own creation based on the Sustainable Development Goals (SDGs) taken from [27].